ON THE GAS VELOCITY MEASUREMENTS WITHIN THE GAS FIELD FORMED AROUND T GEOMETRIC POINT OF A FREE FALL TYPE GAS ATOMIZER

By

Bikas Mandal

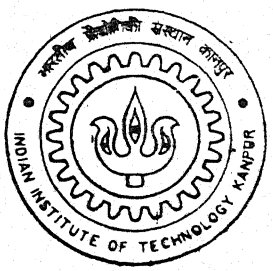

DEPARTMENT OF MATERIALS AND METALLURGICAL ENGINEERING

Indian Institute of Technology Kanpur

MAY, 2002

ON THE GAS VELOCITY MEASUREMENTS WITHIN THE GAS FIELD FORMED AROUND THE GEOMETRIC POINT OF A FREE FALL TYPE GAS ATOMIZER

A Thesis submitted
In Partial Fulfillment of the Requirements
For the degree of

MASTER OF TECHNOLOGY

By

BIKAS MANDAL

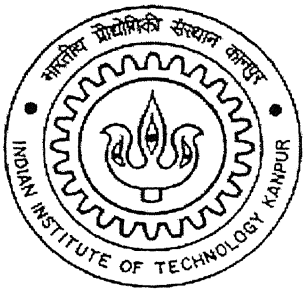

to the

DEPARTMENT OF MATERIALS AND METALLURGICAL ENGINEERING

INDIAN INSTITUTE OF TECHNOLOGY KANPUR

MAY, 2002

CERTIFICATE

This is to certify that the investigation on **'ON THE GAS VELOCITY MEASUREMENTS WITHIN THE GAS FIELD FORMED AROUND THE GEOMETRIC POINT OF A FREE FALL TYPE GAS ATOMIZER'** has been carried out by **Mr. BIKAS MANDAL** under our guidance and it has not been submitted elsewhere for a degree.

S.C. Koria
Professor & Head
Department of Materials
and Metallurgical Engineering
Indian Institute of Technology Kanpur

R.K.Dube
Professor
Department of Materials
and Metallurgical Engineering
Indian Institute of Technology Kanpur

ACKNOWLEDGEMENT

At the outset I would like to convey my deepest sense of gratitude to my thesis supervisors **Prof. R.K. Dube** and **Prof. S.C.Koria** without support, inspiration, prudence, able guidance it could never have been completed.

I would like to convey my sincere thanks to Mr. S.C.Soni for extending all possible and sincere help through the course of study.

Finally I would like to mention those integral part of my IIT life, my friends, who have made every moment of stay here at IITK to rejoice in future. The list is endless, still, the support, cooperation and help rendered by my laboratory partners Rajesh, Ramu, Shyam and my batch mate Debu, Tapas, Pinaki, Sagnik, Arnab, Subho can never be forgot.

Bikas Mandal

May, 2002

IIT Kanpur.

ABSTRACT

In the free fall gas atomization, a vertically falling molten metal stream is disintegrated by the energetic gas field formed around the geometric point. The gas field is created by passing gas through a converging type atomizer. The atomization mainly occurs around the geometric point, which is also called as impingement point. The resultant droplets formed after atomization solidifies during their flight in the gas stream. The size and size distribution of the droplets are controlled by the velocity of gas in the gas field of an atomizer. Therefore, knowledge of the spatial variation in the gas velocity of gas and shape of gas field is important for controlled atomization. In this present study, an attempt has been made to measure the pressure at different points within the gas field by moving pitot tube in X, Y and Z directions. From the values of pressure, velocity of gas is calculated.

From the experimental results, it has been found that the gas field created by an atomizer shows large variation in velocities around the geometric point. The velocity in the gas field around the geometric point shows spatial variation. The atomizing gas is found to be possesses maximum velocity at the geometric point and the velocity at the geometric point increases with increase in plenum pressure. Gas velocity decreases at any value of Y, with either increase in ± X or ± Z directions from the geometric point and vice versa. Due to different velocities of gas within the gas field, disintegration the molten metal stream results in different size of droplets and this leads to size distribution in a powder collective.

CONTENTS

LIST OF FIGURES

mm at plenum pressure of 1000 kPa.

Figure 4.3.22 Iso-velocity line for the velocity of 160 m/s on XY plane situated at Z=50 at plenum pressure of 1000 kPa.

Figure 4.4 Iso-velocity lines for the velocity of 120 m/s, 140 m/s and 160 m/s on XY plane situated at Z=0 at plenum pressure of 1000 kPa.

LIST OF TABLES

Chapter–1
INTRODUCTION

1. Atomization of Liquid Metals:

Atomization may be defined as the break up of liquid metals into fine droplets. This is the most widely used process for tonnage production of metal and alloy powders. It allows for the production of a broad range of alloy compositions with extensive control over resulting powder characteristics and properties. During atomization, energy is transferred from atomizing media, such as gas, a fluid or mechanical surface, to the molten metal. The energy that is required for atomization can be imparted onto the molten metal in a variety of ways. Depending on the mode in which the energy is supplied, liquid metal atomization processes can be classified into the following major categories [1-2]:

1. Twin fluid atomization,
2. Vacuum atomization,
3. Centrifugal atomization,
4. Mono-sized droplet atomization.

In twin fluid atomization process, the fluid being atomized is molten metal. A secondary fluid is used as the atomization media to break up the molten metal into droplets. The secondary fluid may be either gas, water or oil and the respective processes are known as gas, water or oil atomization.

In the process of vacuum atomization, the starting molten metal contains dissolved gases. During atomization, the molten metal is injected into a low pressure/vacuum environment. On exposure to the vacuum the entrapped gases expand and are released into the low-pressure atmosphere causing the deformation and disintegration of the molten metal [2].

In centrifugal atomization, the molten metal is formed directly or injected from a source onto a surface i.e. rotating at high speeds. The metal is stretched in to the

Mono-sized droplet atomization refers to the generation of uniformly sized droplets from liquid streams [2]. The principle of mono-sized droplet atomization is based on the Rayleigh mechanism of liquid column breakup.

Out of all the above-mentioned methods, twin-fluid atomization is the most widely used method for powder production. The present work is related to gas atomization, and hence it will be discussed in details as follows

Chapter –2
LITERATURE REVIEW

2.1 Gas Atomization Of Liquid Metals

2.1.1 Types of Gas Atomizer

The gas atomizers can be of two types according to the relative positions between the atomization gas jets and liquid metal steram. These are closed or confined type atomizers and open or free fall type atomizers. The respective atomization process is known as confined gas atomization and free fall gas atomization.

Figure 2.1 shows the schematic sketch of a confined type atomizer. In confined gas atomization, the gas jets hit the liquid metal stream as it leaves the liquid metal delivery tube. The gas jet is generally tangential to the edge of the liquid metal delivery tube.

In free fall gas atomization liquid metal is allowed to fall under the action of gravitational forces for a certain distance prior to interacting with the gas field formed by the various gas jets. Figure 2.2 shows the schematic sketch of an atomizer used in free fall gas atomization. The point of intersection of the axes of the nozzles is termed geometric point or focal point [3]. The angle of intersection of the axes of nozzles is defined as the apex angle or impingement angle [3,4].

The present study is on the free fall type gas atomization of liquid metals, and hence the subsequent survey of literature is concerned with this type of atomization.

2.1.2 Mechanism Of Gas Atomization:

Dombrowski and Jones first proposed the basic conceptual mechanism of droplet formation in gas atomization [2]. According to the schematic diagram shown in Figure 2.3 [3] three stages are responsible for the disintegration of a liquid sheet into droplets. These stages are

1. formation and growth of disturbance waves in the liquid,
2. fragmentation of liquid sheets, which forms ligaments,
3. breakdown of ligaments into droplets.

First, waves initiate on the liquid sheet as a result of the disturbances that are imposed by the ambient atmosphere or the atomization media. The variation of air pressure and the shear force generated by the relative velocity at the gas-liquid interface cause some

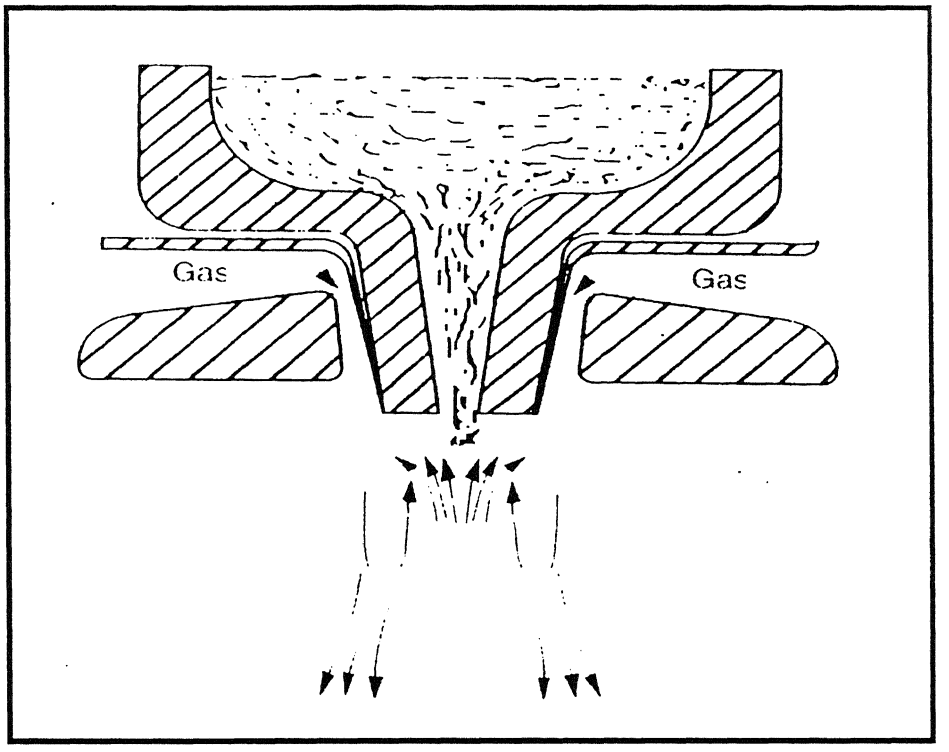

Figure 2.1 Schematic sketch of a confined type atomizer.

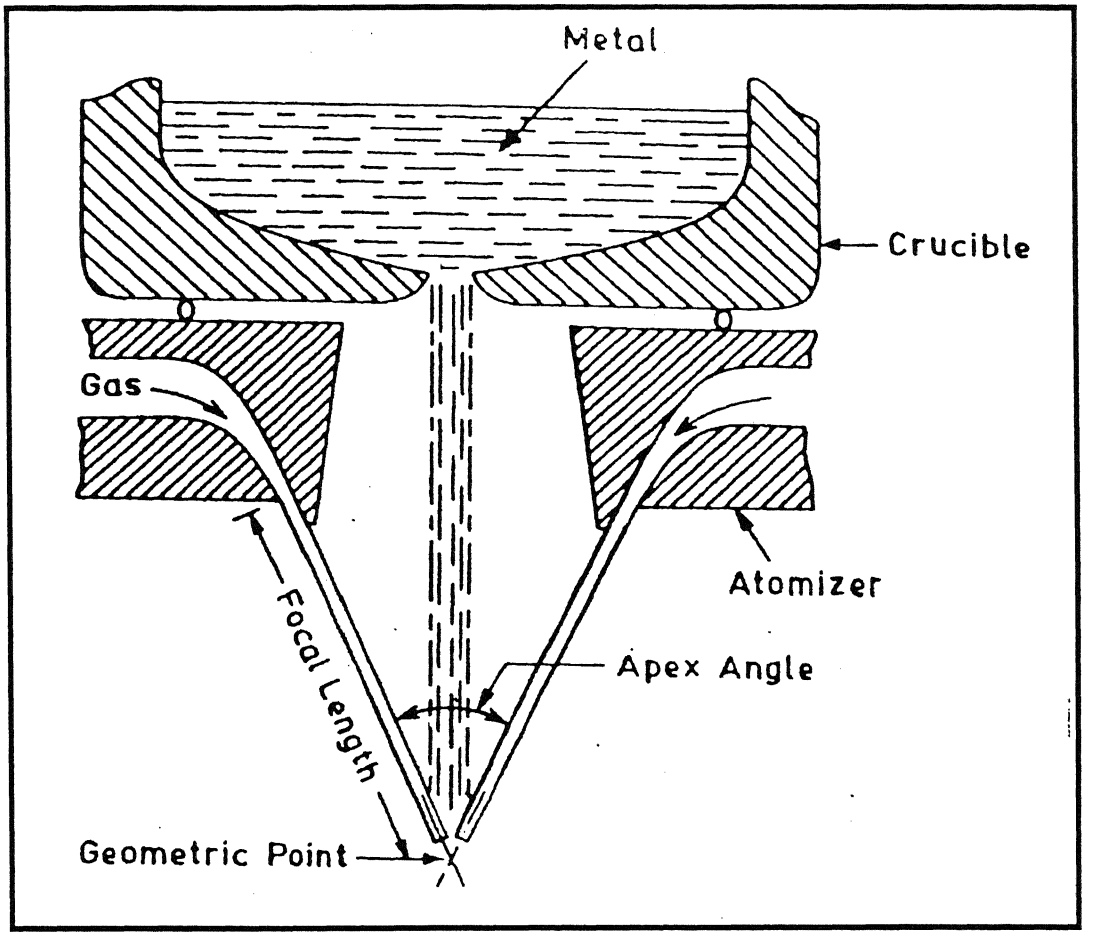

Figure 2.2 Schematic sketch of an atomizer used in free fall type gas atomization.

of these waves to grow in amplitude as a function growing waves reach some critical amplitude the sheet of liquid with ripples and protuberances becomes unstable. At this point, fragments are torn off from the liquid sheet at the crests and troughs. Third, liquid fragments become unstable under the aerodynamic and surface tension forces and further break down into ligaments. Finally, droplets are formed by the spheroidization of ligaments under the action of surface tension forces.

Recent results suggest that the twin fluid atomization of liquids may more complex than the model proposed by Dombrowski and Johns. To that effect, Klar and Fesko suggest that the conventional twin fluid atomization of a molten metal may consist of five distinct stages. These stages are illustrated schematically in Figure 2.4[3] and are described as follows:

(a) formation of waves from initial disturbances,

(b) formation of fragments from the liquid,

(c) formation of droplets by the disintegration of fragments,

(d) breakup of large droplets, and

(e) coalescence of droplets during collision.

In stage I, waves form in the liquid as a result of the initial disturbances that are present on the surface of the liquid. There are several proposed origins of the initial disturbances. For example, it has been suggested that the most important disturbances are generated inside of the delivery tube. Turbulence can be generated inside the delivery tube by flow separation at sharp corners, wall roughness, boundary layers and shear flow. In stage II, the amplitude of growing waves reaches a critical value. In this stage fragments with relatively large aspect ratios are torn off from the disturbed liquid. In stage III, the fragments that were torn off from the liquid during stage II become unstable and droplets are formed by the subsequent breakup and spheroidization of liquid fragments. Moreover, it has been proposed that the droplets formed during stage III may be subjected to further breakup when their size is greater than a certain critical value. Accordingly, for droplets that are large than the critical size, the aerodynamic forces that are generated due to relative velocity between gas and droplets may exceed the restoring force arising from surface tension. In stage IV, the droplets that are greater than a critical size experience further deformation, becoming first flat and then bowl

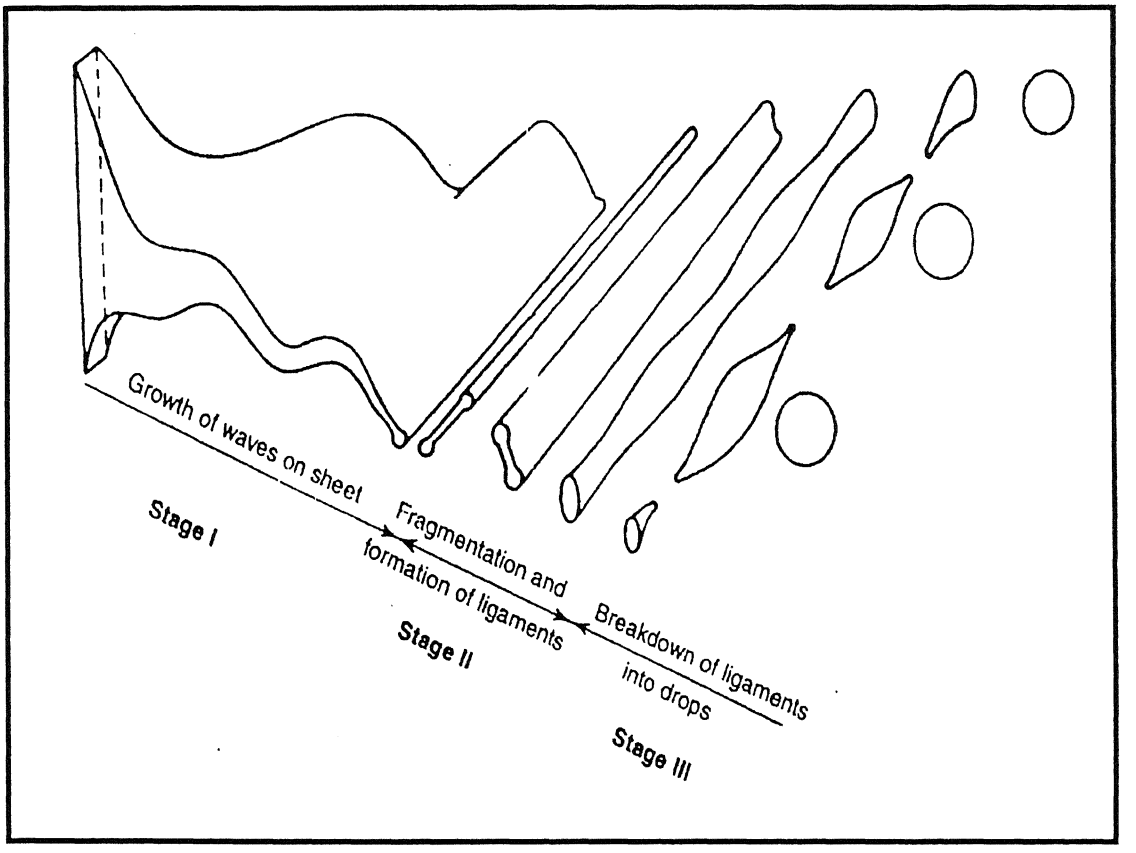

Figure 2.3 Mechanism of disintegration of a liquid sheet [3].

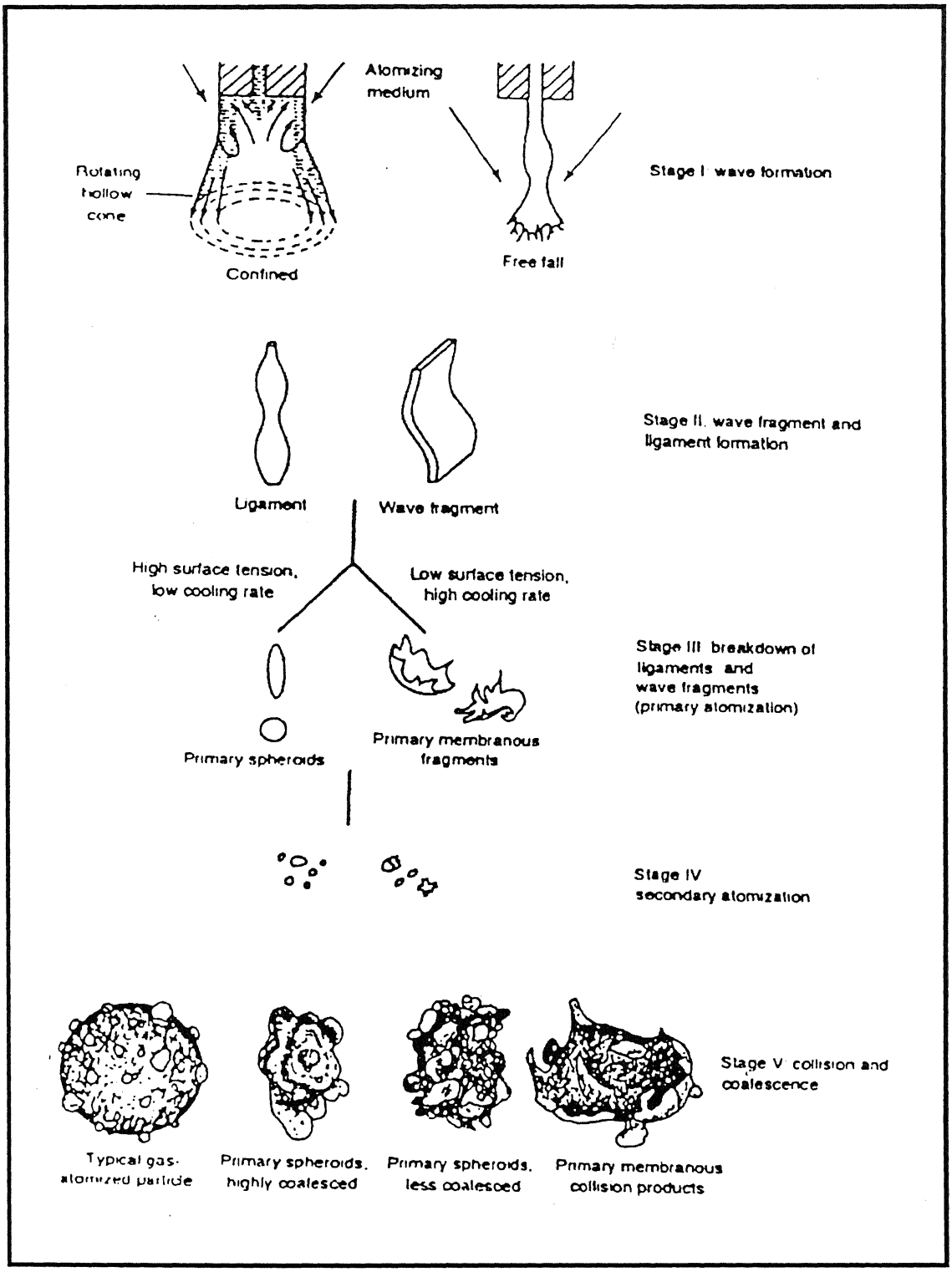

Figure 2.5 Droplet formation stage during twin fluid atomization [3].

shaped. The resultant liquid with a bowl-like geometry eventually bursts into droplets of smaller sizes. Since in this stage, new droplets are formed by the breakup of coarse droplets that were formed earlier, this particular stage is also referred to as secondary atomization. In stage V, collisions occur between droplets, which formed during the early stages, leading under certain conditions, to droplet coalescence.

2.1.3. Powder characteristics:

2.1.3.1.Size and size distribution:

The parameters affecting the particle size and size distribution can be broadly classified in the following three categories:

(1) Parameters related to atomizer,

(2) Parameters related to atomizing gas,

(3) Parameters related to metal being atomized.

A. Effect of parameters related to atomizer on the powder size and size distribution:

The parameters related to the atomizer are diameter of nozzle, number of nozzles, apex angle, and focal length. See and Johnston [4], See et al. [3] and Helmersion [5] studied the effect of some of them on powder characteristics. They reported that the increase in apex angle decreased the powder particle size. It was due to the decrease in focal length with that of apex angle. See and Johnston studied the influence of apex angle on the atomization behavior of lead and tin. They have shown that an increase in apex angle increases the mass median diameter of powder particle. Singh et al. studied the effect of apex angle on mass median size of powders by taking nozzle of different apex angle at different plenum pressure. The characteristics of different atomizers used by Singh et al. is shown in Table 2.1[13]. Figure 2.6 [13] gives the variation of relative mass median size (X_g/X_L) with relative plenum pressure (P/P_L) for different types of atomizers having the same apex angle as obtained by Singh et al. The results indicate that atomizer can produce powders of different mass median size by controlling the plenum pressure. Figure 2.7 [13] gives the variation of mass median size with focal length for atomizers a4 and A4 containing nozzles of 2 and 3 mm diameter, respectively at different plenum pressure. From this Figure it is clear that mass median size increases with increase in the focal length at all plenum pressure. Figure 2.8 [13] shows the mass median size as a function of the apex angle of atomizer

A212, A412 and A612 at different plenum pressure as observed by Singh et al. It can be seen that at each plenum pressure, the mass median size increases rapidly initially and then slowly with the increase in apex angle.

B. Effect of parameters related to atomizing gas on the powder size and size distribution:

The parameters related to atomizing gas are in general plenum pressure, mass flow rate and its type i.e. nitrogen, argon or air etc. it has been observed by numerous investigators that when the atomization pressure increases, with other variables being kept constant, the resultant mass median diameter of the powder decreases. Uslan et al. [11] studied the effect of gas type and gas pressure on mean powder size as shown in Figure 2.9. It is clear from the figure that mean powder size decreased as the atomization gas pressure increased. Singh et al. [13] studied the effect of plenum pressure on mass median size of powder particles. They have shown that each atomizer can produce powders of different mass median size by controlling the plenum pressure. Gas flow rate influences the distribution of droplet size.

C. Effect of parameters related to metal being atomized on powder size and size distribution:

Parameters related to the metal being atomized are superheat of the liquid metal, diameter of liquid metal delivery tube; mass flow rate of the metal, and the composition of metal. Helmersion et al. [10] studied the effect of metal superheat on powder particle size. They have shown that increasing the superheat of the melt results in a corresponding delay of solidification, and thus a longer flight distance in the liquid state. This means that growth of dendrites will start at a point with lower relative velocity, implying lower cooling rate during solidification and thus, a coarser dendrite microstructure. Lubanska reported that size of metal powder is a function of mass flow rate of liquid metal. As metal flow rate increases size of powder particles increases. The influence of liquid mass flow rate on the mass median size of droplets was studied by Kim & Marshall. They have shown that mass median diameter of droplets increases with increase in liquid mass flow rate. The mass median size of powder particles is independent of diameter of liquid metal delivery tube, as shown by Singh et al. [13].

Table 2.1 Characteristics of different atomizers [13].

Type of atomizers	Number of nozzles (N)	Diameter of nozzle(D), in mm.	Apex angle (α), in degree.	Focal length (F), in mm.	Limiting plenum pressure (P_L), kPa
a49	4	2	40	90	1500
A47	4	3	40	70	750
A49	4	3	40	90	1000
B49	6	3	40	90	1100
A212	4	3	20	120	ND
A412	4	3	40	120	ND
A612	4	3	60	120	1500

* ND is could not be determined.

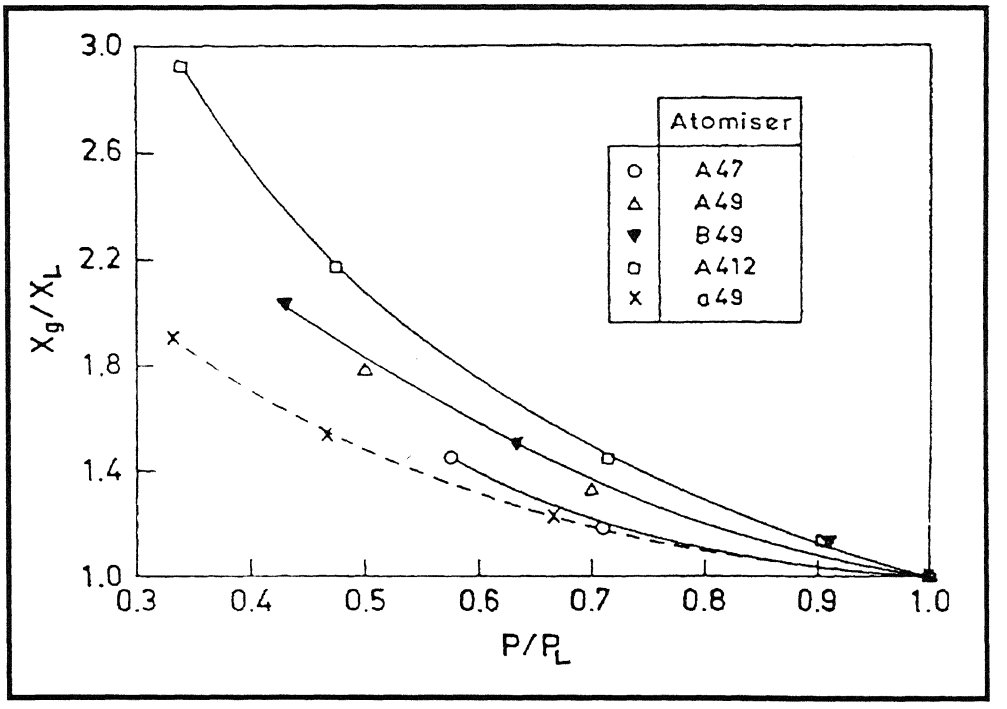

Figure 2.6 Variation of mass median size (X_g/X_L) with relative plenum pressure (P/P_L)[13].

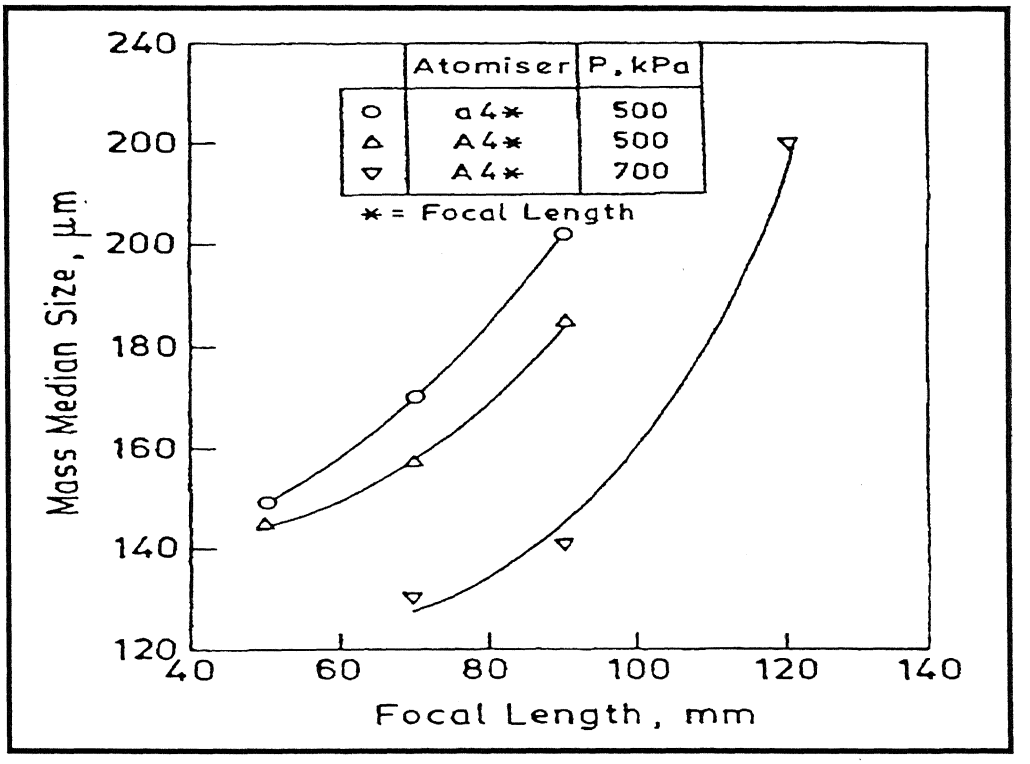

Figure 2.7 Variation of mass median size with focal length [3].

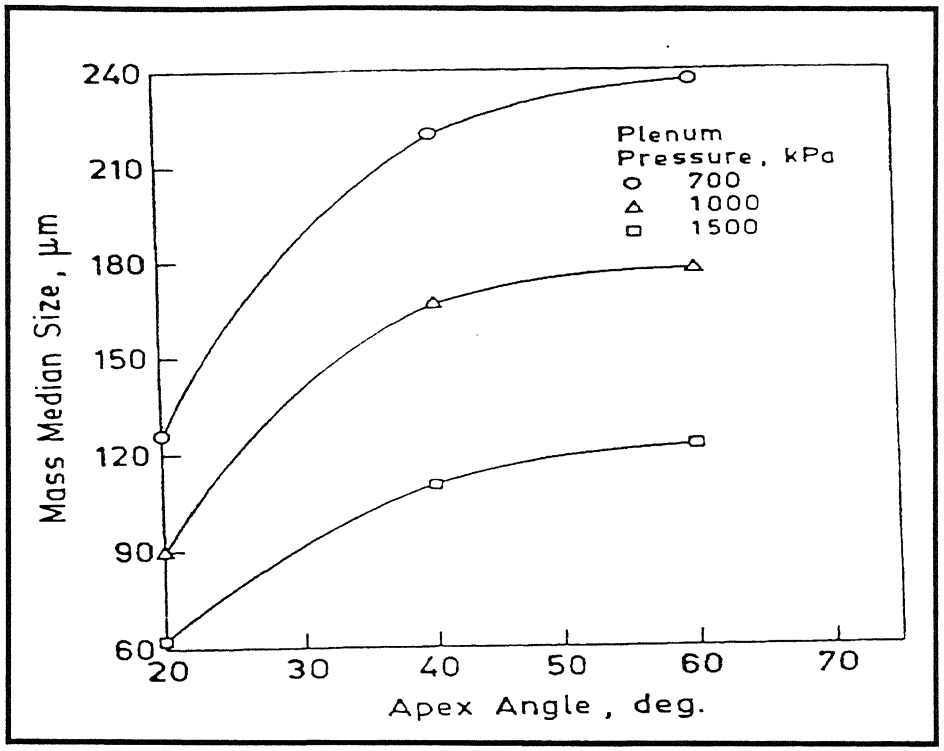

Figure 2.8 Variation of mass median size with apex angle of atomizers [13]

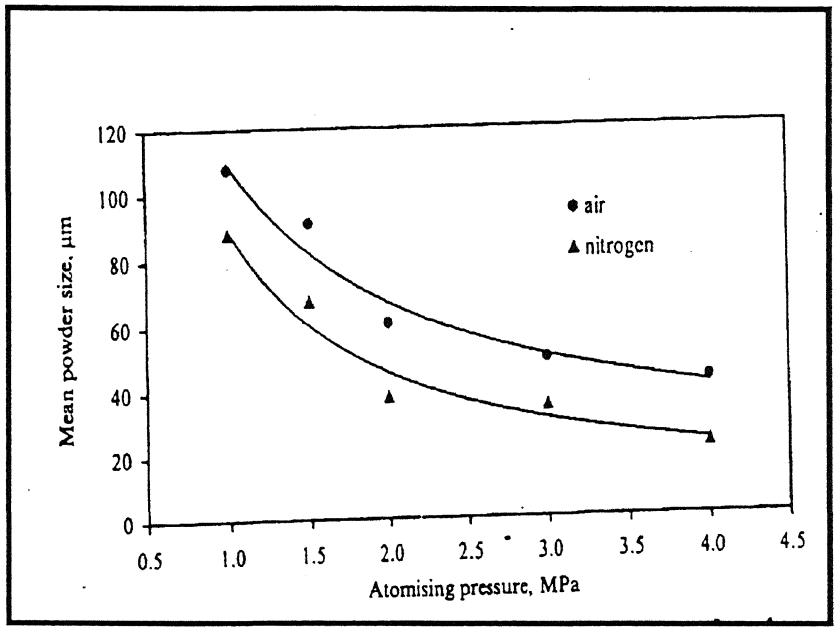

Figure 2.9 The effect of gas type and gas pressure on mean powder size [11].

Out of all the above-described factors, which affected the powder size, the gas atomization pressure is the single most critical processing parameter that affects the size distribution of droplets in a significant manner.

2.1.4 Particle Shape:

Particle shape depends on the spheroidization and solidification time. If solidification time is greater than that of spheroidization time, particle will be spherical. See and Johnston [4] calculated the spheroidization and solidification time of the atomized droplets. They found that the solidification time was greater than the spheroidization time. Therefore they argued that powder particles should have been spherical, but practically it was not the case. The reported reason was the oxidation of powder particles. Solidification time and spherodization time depends on cooling rate, atomizing gas type and gas pressure. The cooling rate of liquid droplets has a significant effect on powder particle shape. Uslan et al. studied the effect of atomizing gas type on particle shape. Figure 2.10 [11] shows effect of atomizing gas type on particle shape. It can be seen that nitrogen gas produces more spherical powder than air. This could be explained in terms of differences in oxide layer thickness. Nitrogen will produce a thinner oxide envelope and hinder spherodization while air will produce a thick oxide envelope that will interfere with spherodization. Gas pressure is the most important parameter that can affect greater extent on powder morphology i.e. powder particle shape. Figure 2.11[11] showing the effect of atomizing gas pressure on powder morphology. As the atomizing gas pressure increases, smaller droplets are produced and thus the resulting powders are spherical shape.

2.2 Gas field created by high-pressure gas jets:

The atomizing gas field is created by the impingement of gas jets produced by the nozzle of an atomizer. The atomization of liquid metals stream takes place in the gas field and atomized droplets fly in the gas field during their solidification. So the knowledge of gas field generated by gas atomizer is important for three reasons:

(1) Flow from the atomizer gas jets controls the size distribution of droplets created from the melt stream.

(2) The gas flow field controls the trajectory and motion of metal droplets formed during atomization.

(3) The gas flow field controls heat transfer from the particles during their flight within the gas field.

Figure 2.10 Micrographs showing the effect of gas type on powder morphology (a) nitrogen atomized (b) air atomized [11].

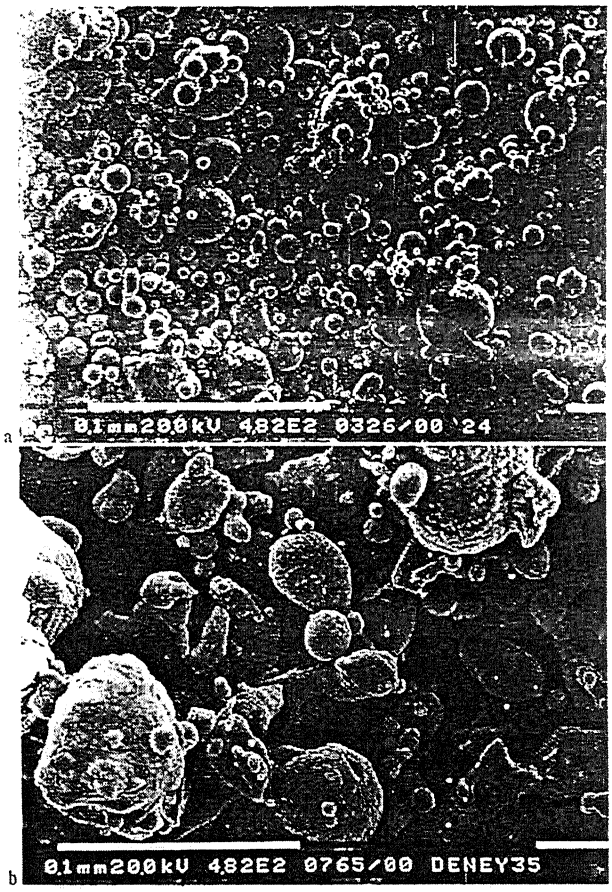

Figure 2.11 Micrographs showing the effect of atomizing gas pressure on powder Powder morphology (a) 4.0 MPa; (b) 1.0 MPa [11]

So the measurement of pressure within the gas field is important for controlled gas atomization. The experimental technique was employed to measure gas pressure is Pitot tube measurement. From pressure readings, gas velocity can be calculated. Some investigators studied the velocity in the gas field created by an atomizer of free fall type. Kim and Jones have measured the gas velocity associated with free fall type. Bewley and Cantor studied the gas velocity at different positions within the gas field of a confined type atomizer [7].

2.3 Effect of various parameters on the gas velocity:

Moir and Jones [8] and Moir et al. [9] investigated the velocity variation by changing simultaneously both focal length and apex angle of the atomizer. The gas velocity was measured at different plenum pressure and for different number of nozzles by both Pitot tube and hot wire anemometry and the results obtained were found to be in good agreement. It was reported that velocity increases with increasing the plenum pressure or decreasing the number of nozzles. Singh et al. studied the gas velocity at the geometric point of free fall type atomizers with different focal lengths, apex angles, and number and diameter of nozzles. Figure 2.12 shows the variation of velocity as a function of plenum pressure for atomizers of different focal lengths. The apex angle of the atomizer is 60^0 and there are four nozzles. The dashed lines are for 2 mm and solids lines for 3 mm nozzle diameters. It can be seen that the atomizers of smaller focal lengths produce higher velocities as compared with greater focal length at all plenum pressure. It was also observed that the gas velocity is lower for the 2 mm diameter as compared with that of the 3 mm nozzle at all plenum pressures for all type of atomizers of different focal length. In Figure 2.13 [12] the velocity is shown as a function of focal length for atomizers with 60^0 apex angle at various plenum pressures. There are four nozzles and the diameter of each nozzle is 3 mm. It can be seen that the velocity increases with decrease in focal length at all plenum pressures. Figure 2.14 shows the velocity of air as a function of apex angle of the atomizer containing four nozzles at various plenum pressures. The focal length of the atomizers 120 mm. The experimental results obtained by Singh et al. shows that the velocity is independent of apex angles. Figure 2.15 [12] shows the variation of air velocity as a function of number of nozzles at different plenum pressures for an atomizer of apex angle 40^0 and focal length 120

mm. It can be seen from the above Figure that velocity is independent of the number of nozzles at all plenum pressure and nozzle diameters.

Singh et al. [12] also studied the velocity around the geometric point i.e. both in horizontal and vertical distances. Figure 2.16 [12] shows the variation of air velocity as a function of horizontal distance (measured from geometric point) of atomizers of 2 mm and 3 mm nozzle diameter at different plenum pressures. It can be seen that the velocity remains constant up to distance of 2 to 5 mm for different plenum pressures and nozzle diameters. Beyond this distance the velocity decreases with increase in horizontal distance. Figure 2.17 [12] shows the variation in velocities along the central axis passing through the geometric point of atomizers of different focal lengths. It can be seen from the figure that the velocity remains constant up to about 10 to 12 mm both upstream and down stream of the geometric point. Beyond this distance the decrease in velocity is faster along upstream side and reach a very small value as compared with that downstream. The decrease in velocity with distance depends on velocity at the geometric point. Higher velocity at the geometric point results in more rapid decrease in velocity with distance on both sides of the geometric point.

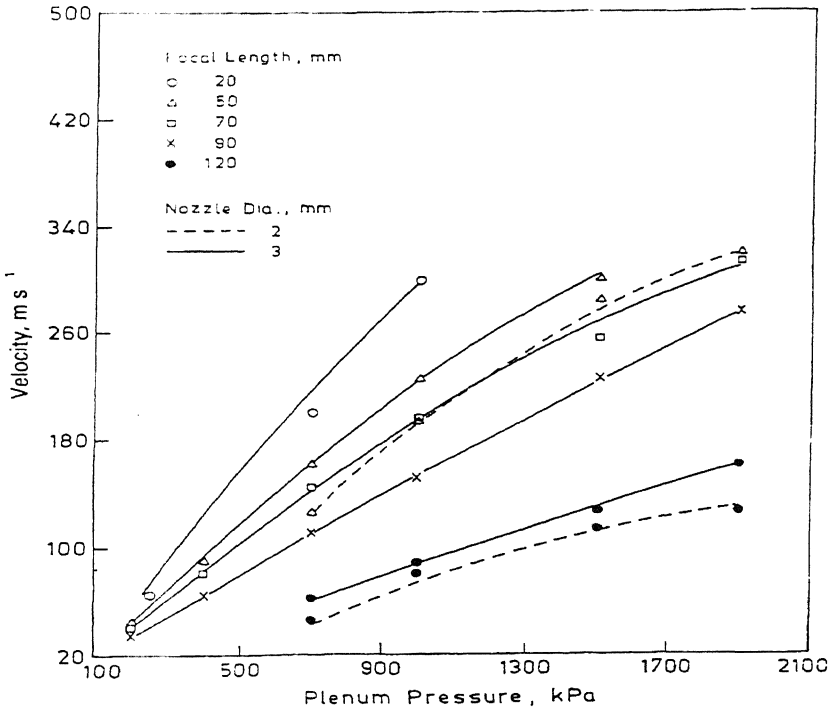

Figure 2.12 Variation of air velocity at geometric point as function of plenum pressure: $\alpha=60^0$, N=4 [12].

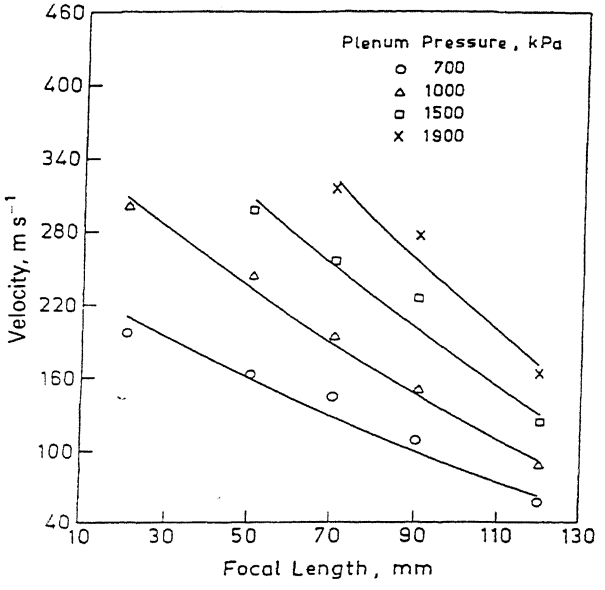

Figure 2.13 Variation of air velocity with focal length at geometric point: $\alpha=40^0$, N=4, D=3 mm [12].

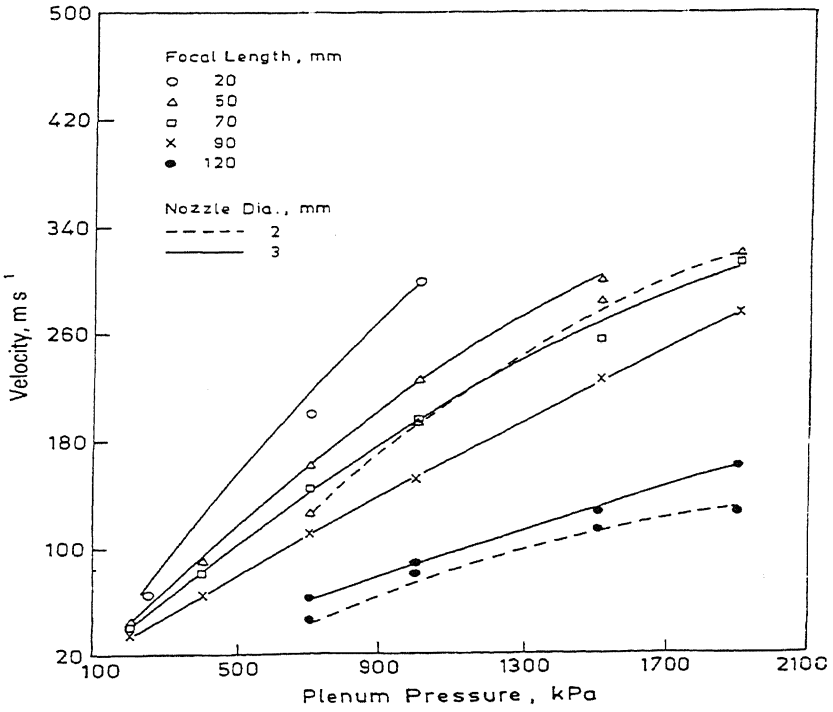

Figure 2.12 Variation of air velocity at geometric point as function of plenum pressure: $\alpha=60^0$, N=4 [12].

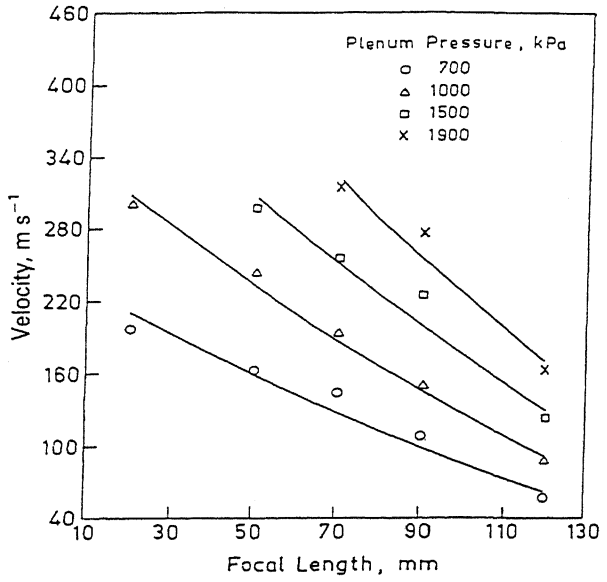

Figure 2.13 Variation of air velocity with focal length at geometric point: $\alpha=60^0$, N=4, D=3 mm [12].

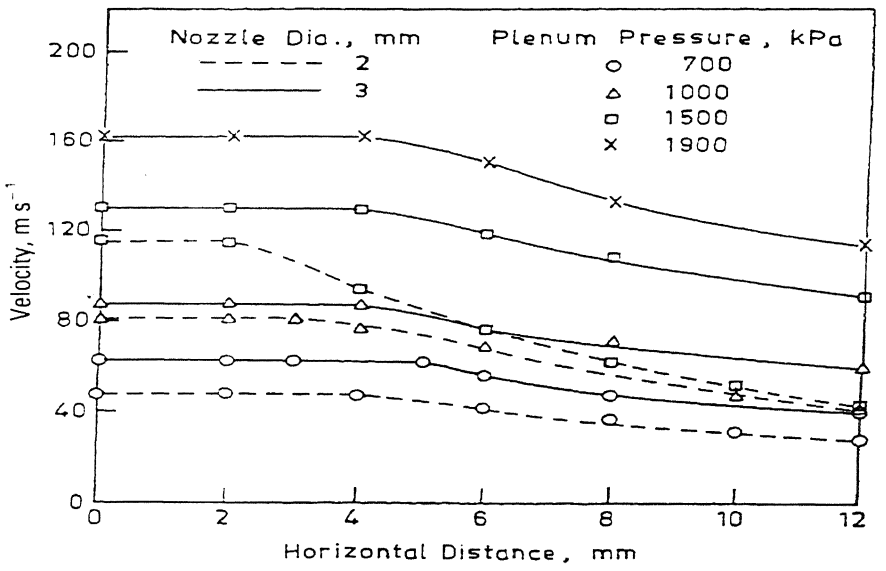

Figure 2.16 Air velocity as function of horizontal distance from geometric point: $\alpha=40^0$, F=120 mm, N=4 [12].

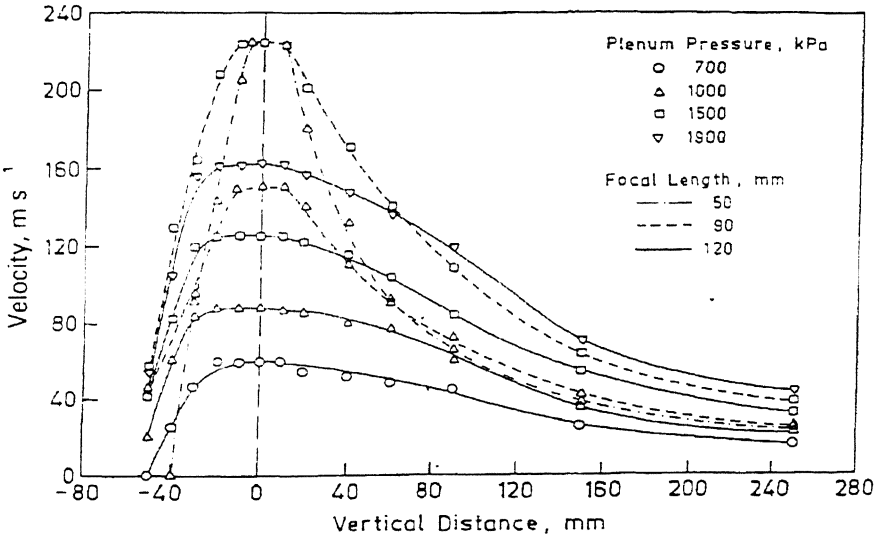

Figure 2.17 Air velocity as function of vertical distance measured from geometric point:$\alpha=40^0$, N=4, D=3 mm [12].

2.4 Objectives of the present study:

The objectives of the present work are as follows:

1. To study the atomizing gas field produced by atomizers of free fall type at different plenum pressure. This would be done by measuring pressure by pitot tube method at different points within the atomizing gas field, and subsequently calculating the corresponding gas velocity.
2. To study the spatial variation of gas velocity around the geometric point at different plenum pressure.

Chapter-3
EXPERIMENTAL SET UP AND PROCEDURE

This chapter describes the experimental set up and procedure to investigate the gas velocity within the impingement zone formed by gas atomizer of free fall type. Figure 3.1 is a schematic diagram of the experimental set up used in the present study. As seen from the figure, the main constituents of the set-up are the atomizer, atomizing nozzles, compressor, rotameter, pressure gauge, stop-valve and Pitot tube assembly connected to the mercury manometer.

3.1 Experimental Set Up

3.1.1 Atomizer

In atomizers of the present study nozzles were arranged concentric to the central axis of the atomizer. The atomizer consists of a manifold having a number of holes for fitting nozzles and gas supply arrangements as shown in Figure 3.2. The holes were designed to be positioned at equal circumferential distances and inclined conically making an apex angle such that the geometric point (it is the point of intersection of axes of holes) lies on the central axis of the manifold. In Figure 3.2, G refers to the geometric point of the atomizer while α gives the apex angle. The distance from the gas nozzles exit, N or N_1, to the geometric point G, is termed as focal length in the present study. The distance from the exit of central hole of the atomizer M, to the geometric point G, is the free fall distance of the atomizer and equal in dimensions to the focal length of the atomizer. The air was fed tangentially into the pressurizing manifold through three separate inlets, commonly connected to a compressor. The focal length of atomizer was varied by using nozzles of different length.

3.1.2. Pressure measuring system

The pressure of air upstream was measured by means of a calibrated pressure transducer and it is termed as 'plenum pressure' while the pressures in the air field around the geometric point were measured by a pitot tube connected to a water/mercury

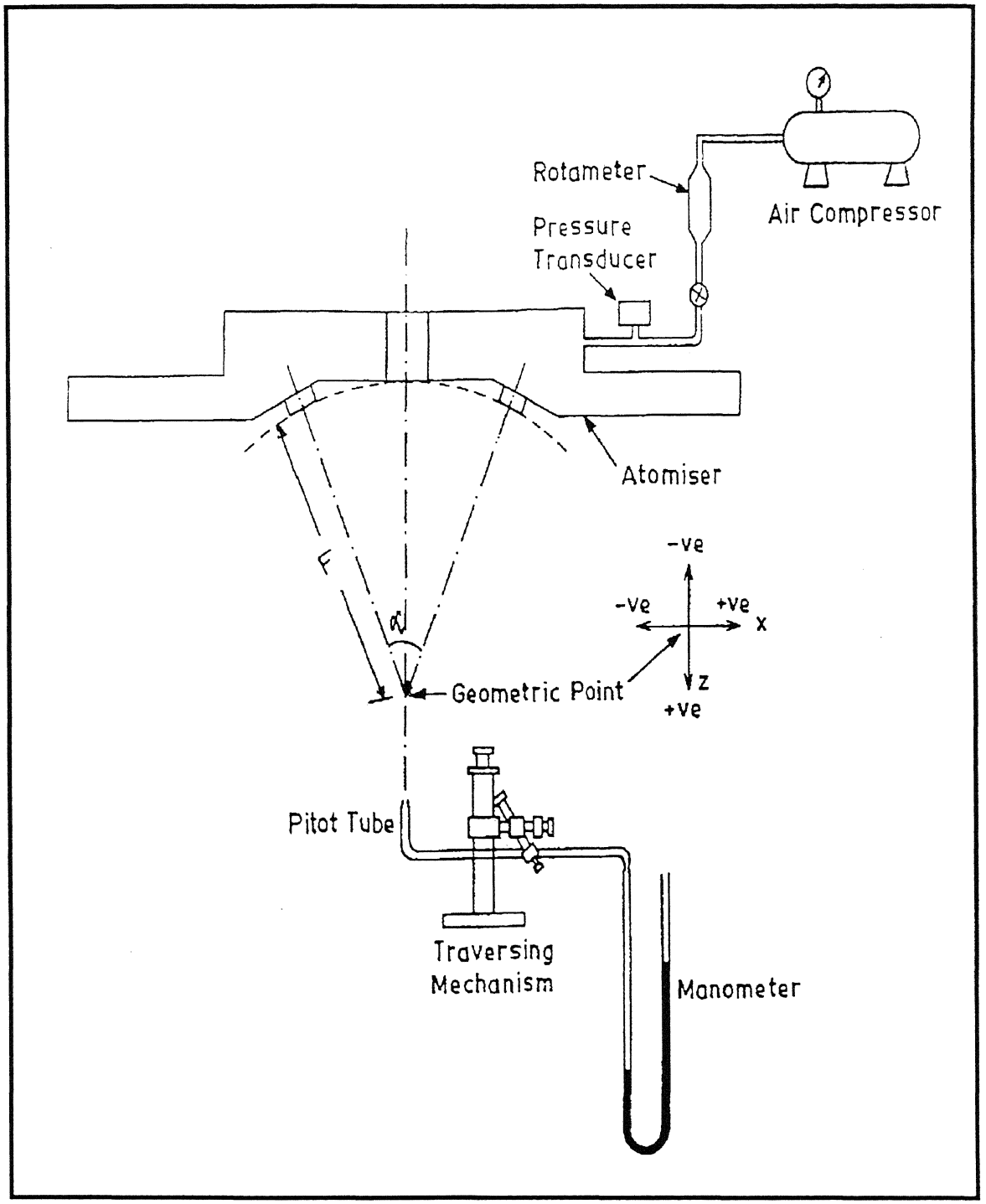

Figure 3.1 Schematic diagram of the experimental set up.

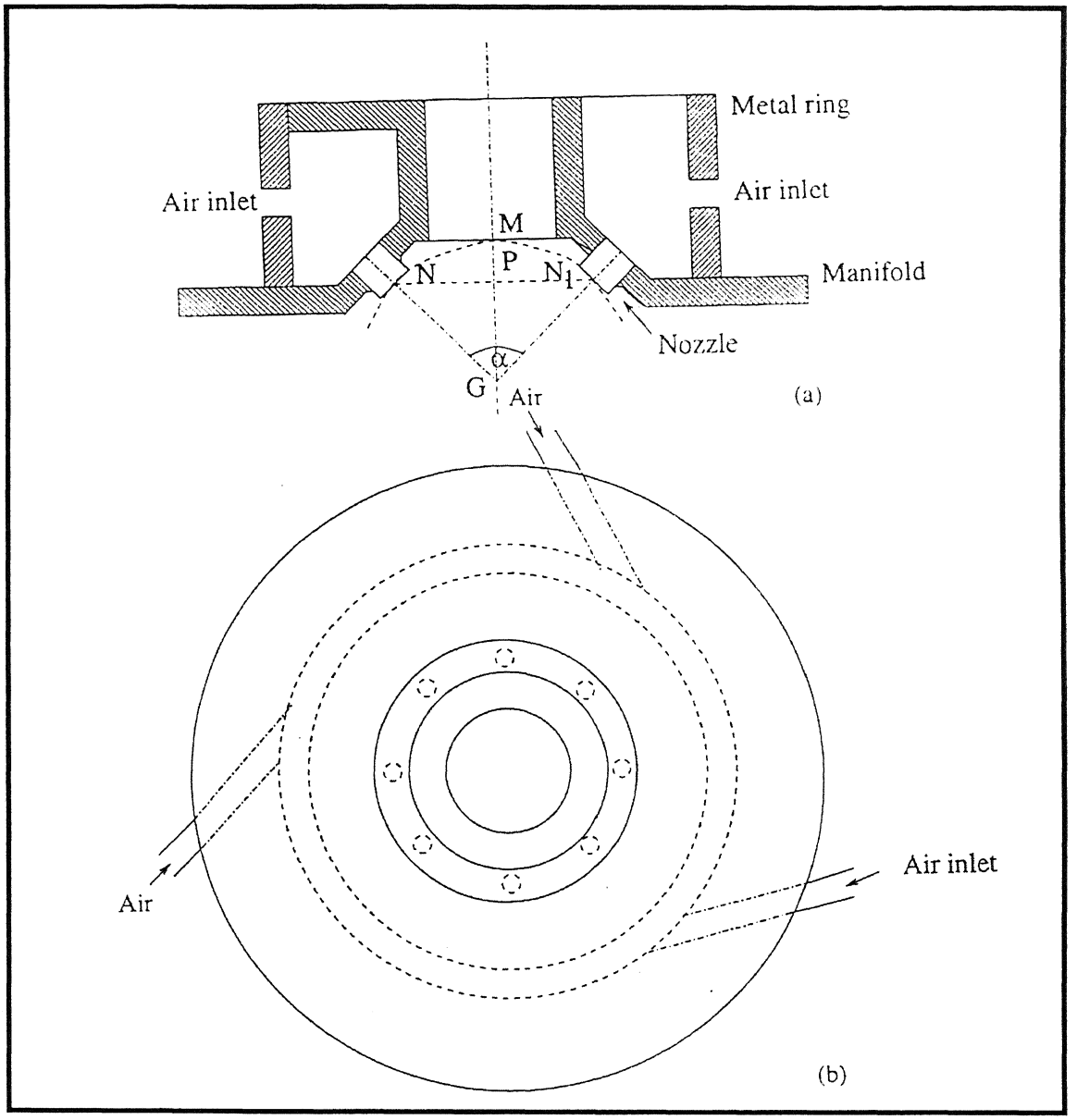

Figure 3.2 Schematic figure showing (a) sectional elevation and (b) plan of a free fall type atomization.

manometer. The Pitot tube made of stainless steel of 0.7 mm inner diameter × 1.3 mm outer diameter. The Pitot tube was fixed on a traversing mechanism as shown in the Figure 3.1. By means of knobs on the traversing mechanism, it was possible to move the tube spatially within the airfield. The accuracy of the movement of the tube was ± 0.1 mm.

3.2 Experimental procedure

The first step of the experiment was to determine the location of the geometric point of the atomizer. The geometric point was located such that the distance from the geometric point to each of the nozzles and exit hole of the atomizer was 50mm. At this geometric point the tip of the Pitot tube was kept so that tip always pointed opposite to the direction of airflow. The geometric point was considered as the co-ordinate origin and the movement of the Pitot tube was made accordingly. From this geometric point, the Pitot tube was moved in the plus X and minus X directions keeping Z fixed at a certain plenum pressure. Subsequently, from this geometric point the Pitot tube was moved in the plus Z and minus Z directions keeping X fixed and plus Y and minus Y directions by keeping X and Z fixed at a certain plenum pressure. Corresponding to each movement of the Pitot tube, in the X, Y or Z directions, and the pressure readings in the mercury manometer was taken. This procedure was repeated for atomizer of focal length 50 mm and apex angle 40^0 at three plenum pressures of 8 bar, 10 bar, 12 bar each. All measurements were taken one to three time(s) under identical conditions and mean was taken.

3.3 Velocity Measurement in the Gas Field

From the pressure readings, the air velocity was calculated. The relationship between pitot pressure and Mach number (M) of the jet is given by: [16]

$$\frac{P_0}{P} = (1 + \frac{\gamma - 1}{2} M^2)^{(\frac{\gamma}{\gamma - 1})} \qquad (3.1)$$

where P_0 = Stagnation pressure in kPa

= Pitot reading, in kPa + Atmospheric pressure, in kPa

P = Atmospheric pressure =101.3 kPa

$\gamma = C_p/C_v$

= 1.4 for air

From the experimental values of pitot readings, the values of Mach number (M) for each case can be calculated from the eq. (3.1). The Mach number and velocity are related as follows

$$M^2 = \frac{V^2 w}{\gamma RT} \tag{3.2}$$

where, V = velocity of air,

where, T is stagnation temperature

R = Universal gas constant

= 8.314 kJ (kg-mole)$^{-1}$K^{-1} and

= Molecular weight of air

= 0.029 kg (kg-mole)$^{-1}$

The stagnation temperature (T) is given by

$$T = \frac{T_0}{(1 + \frac{\gamma - 1}{2} M^2)} \tag{3.3}$$

where, T_0 is atmospheric temperature

= 298 K

Combining equations (3.2) and (3.3) gives

$$V = \left(\frac{\gamma RT_0}{w\left(\frac{1}{M^2} + \frac{\gamma - 1}{2}\right)}\right)^{\frac{1}{2}} \tag{3.4}$$

By equation (3.1), Mach number is calculated and putting the value of Mach number in equation (3.4), the velocity of air is calculated.

Chapter 4
RESULTS AND DISCUSSIONS

This chapter describes the experimental results of gas flow rate and the resulting gas velocity around the geometric point of a free fall type atomizer. In free fall atomization, velocity of atomization gas is widely used parameter rather than pitot pressure, although both of these parameters are interrelated. Therefore, all the pressure readings were converted into velocity by equation (3.4). Method for calculation of velocity was given in appendix-A. The values of velocities were reported in appendix-B. Table B.1 to B.12, B.13 to B.24 and B.25 to B.36 represent the velocity for the plenum pressures of 800 kPa, 1000kPa and 1200 kPa respectively. In the following, results on gas velocity and its variation within the gas field are presented for different plenum pressure of an atomizer of focal length 50 mm and apex angle 40^0.

4.1 Variation of velocity in the gas field produced at 800 kPa plenum pressure:

Figures 4.1.1 to 4.1.7 show the variation of velocity on the XZ planes of gas field situated at Y=0, ± 2 mm, ± 4 mm, ± 6 mm. In this representation velocity is plotted as a function of Z at different values of X varying in between – 6 mm and + 6 mm.

From all the above figures the following observations can be made:

1. Remembering that the geometric point of an atomizer is situated at X=0, Y=0 and Z=0, the velocity of gas on the XZ plane situated at any value of Y, decreases with either increase in Z while keeping X constant or increase in X while keeping Z constant, both in positive or negative directions (Figure 4.1.1 to 4.1.7).
2. However, for any given value of either X or Y, the decrease in velocity with increase in Z is faster when the value of Z is negative as compared when Z is positive (Figure 4.1.1b). The impingement of jets at the geometric point causes the downward flow of the gas at a rate faster than the upward flow. Thus the entrainment of the surrounding air into the downward flow of the gas occurs slowly as compared with into the upward flow of gas.

3. For any given value of Y and Z, increase in X either in positive or negative direction for all values of Z decreases the velocity of gas in the gas field (Figure 4.1a and 4.1.1b to 4.1.7a and 4.1.7b).
4. Increase in the value of Y both in positive or negative directions, decreases the velocities both in X and Z directions. The extent of decrease depends on the value of Y.

For example at Y=0 the velocity of gas at X=0 and Z=0 is 205 m/s, which is almost same at Y=2 mm but decreases to 156 m/s at Y= + 6 mm and to 152 m/s at Y= - 6 mm. Similar information can be obtained at other values of Y and different combinations of X and Z (Figure 4.1.1a, 4.1.2a, 4.1.3a, 4.1.4a, 4.1.5a, 4.1.6a and 4.1.7a).

Figures 4.1.8 to 4.1.15 show the variation of velocity on XY planes of gas field situated at Z= 0, ± 10 mm, 20 cm, 30 mm, 40 mm, 50 mm, 60 mm. In this representation velocity is plotted as a function of X at different values of Y varying in between – 6 mm and + 6 mm.

From Figures 4.1.8 to 4.1.15 the following observations have been made:

1. The velocity of gas on the XY plane, situated at any value of Z, decreases with either increase in X while keeping Y constant, or increase in Y while keeping X constant both in positive and negative directions (Figure 4.1.8 to 4.1.15).
2. For any given value of either Y or Z, the rate of decrease in velocity with increase in X is similar in both the positive and negative directions. It is further observed that the curve on either side is almost symmetrical to each other (Figure 4.1.8 –4.1.15).
3. For any given value of Z and X, an increase in Y, either in positive or negative direction, decreases the velocity of gas in the gas field. For example at Z=0 the velocity of gas at X=2 mm and Y=0 is 195 m/s, but decreases to 145 m/s at Y= + 6 mm and to 137 m/s at Y= - 6 mm (Figure 4.1.8a and 4.1.18b). Similar observation can be obtained at other combinations of X and Y.
4. The increase in value of Z both in positive or negative directions decreases the velocities both in Y and X directions.

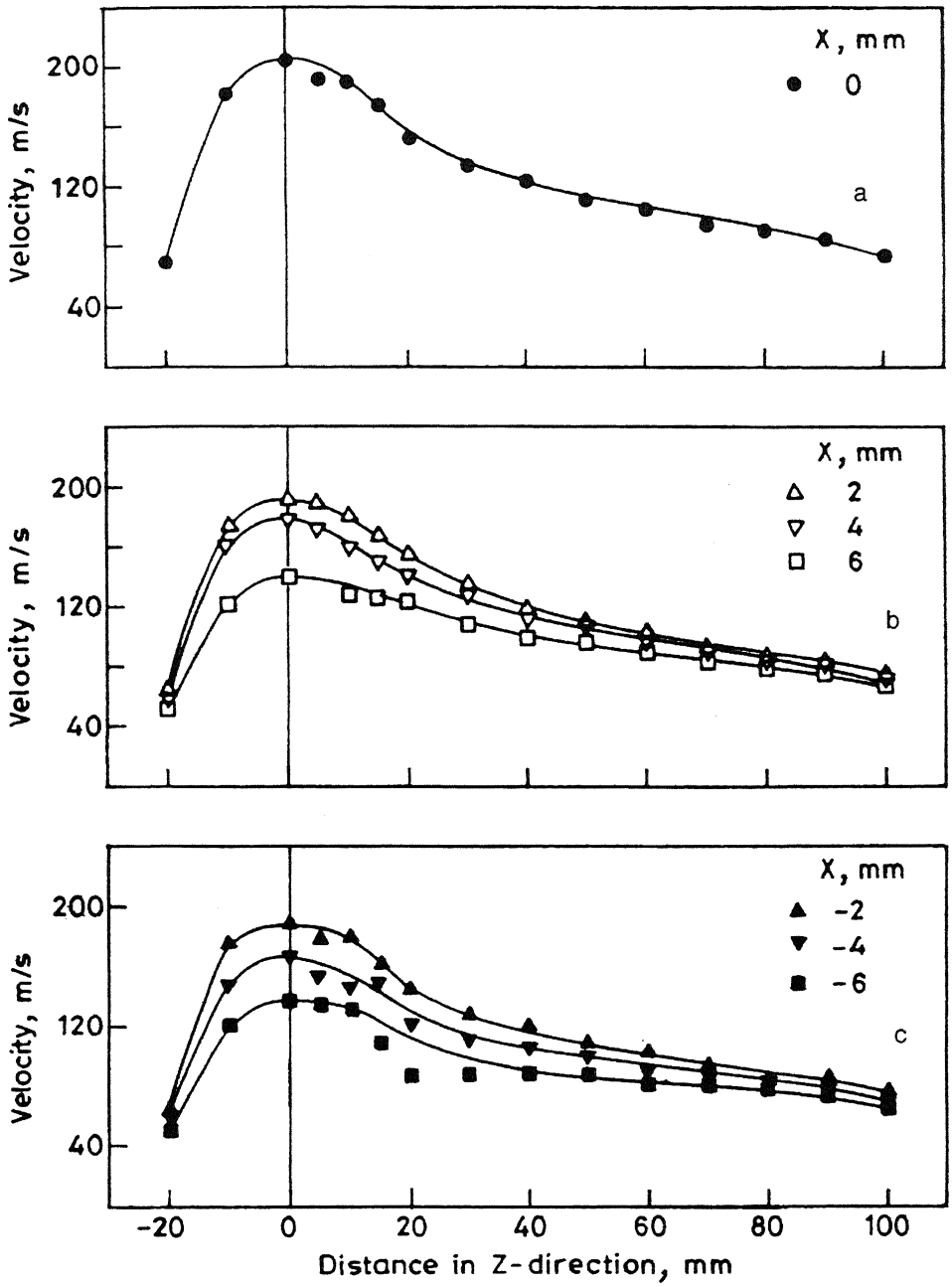

Figure 4.1.1 Variation of gas velocity on the XZ plane of gas field situated at Y=0.

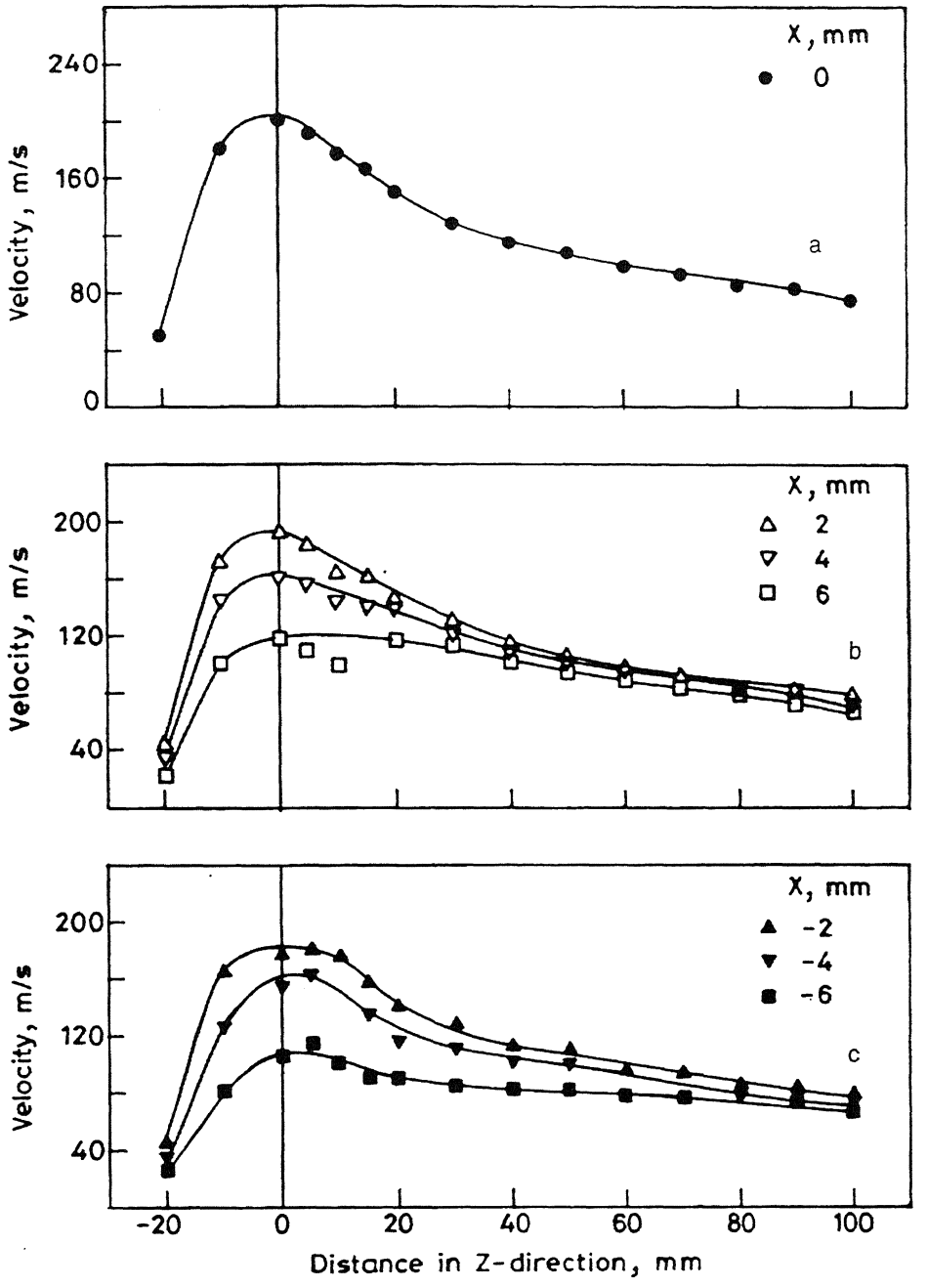

Figure 4.1.2 Variation of gas velocity on the XZ plane of gas field situated at Y = 2 mm.

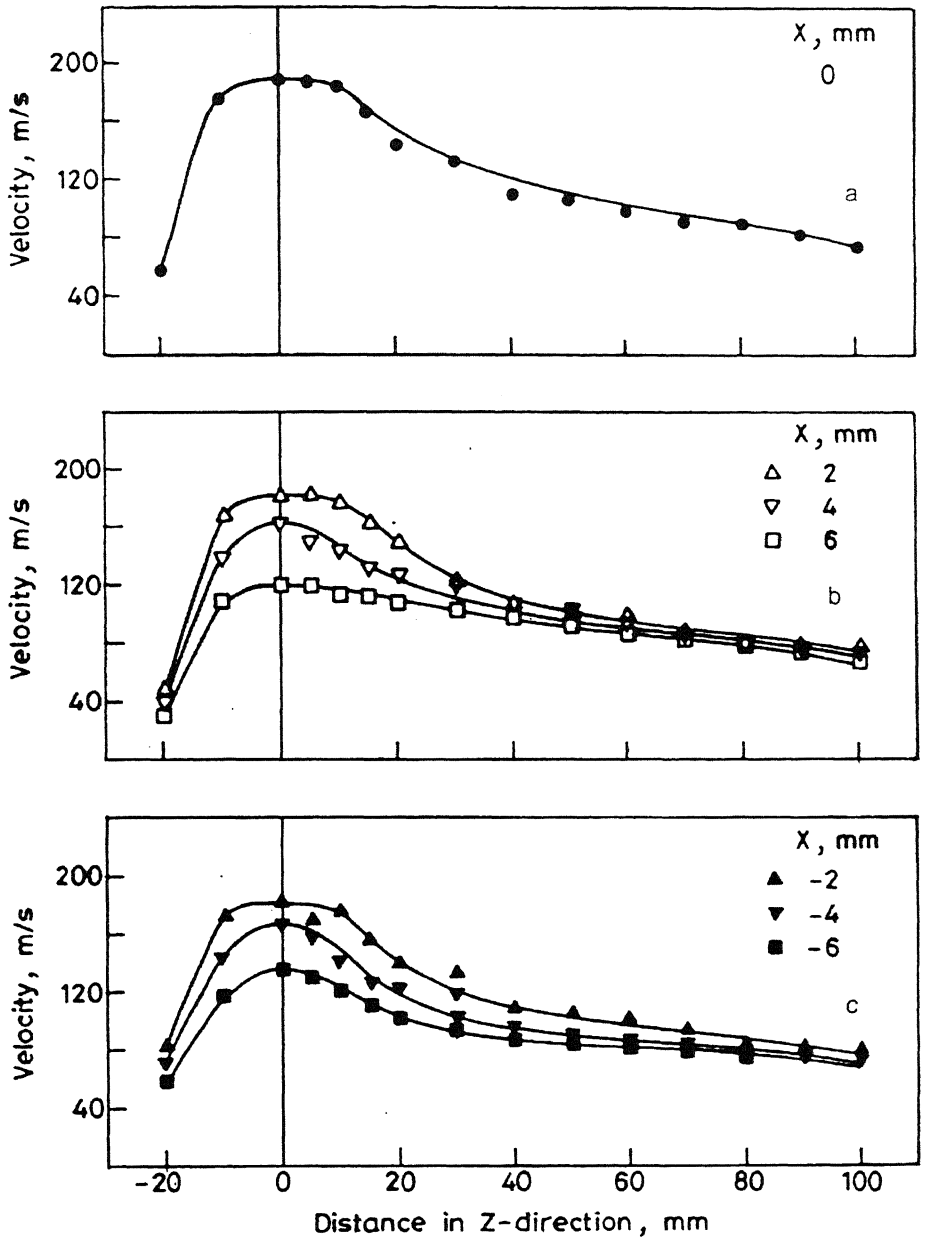

Figure 4.1.3 Variation of gas velocity on the XZ plane of gas field situated at Y = -2 mm.

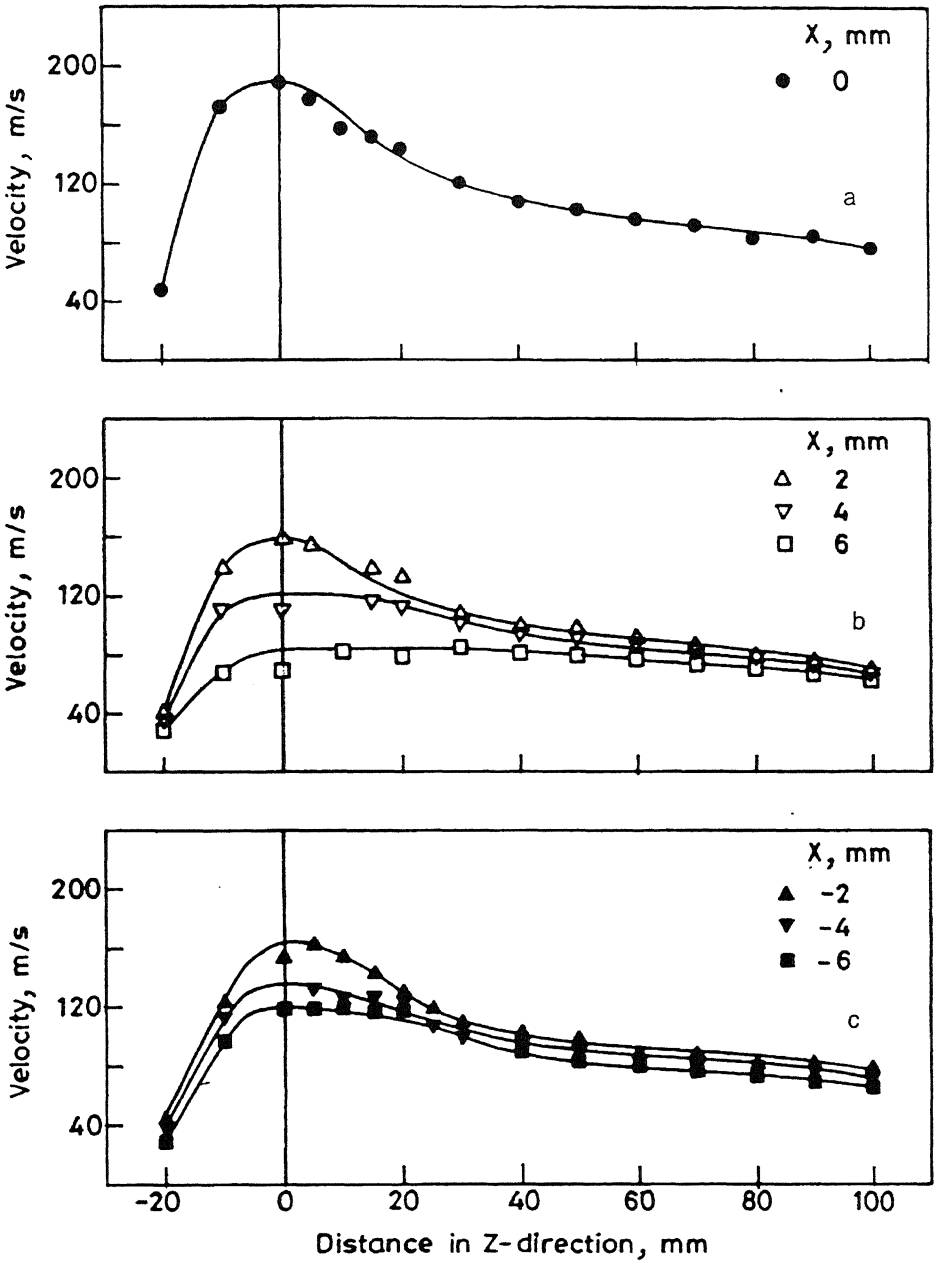

Figure 4.1.4 Variation of gas velocity on the XZ plane of gas field situated at Y = 4 mm.

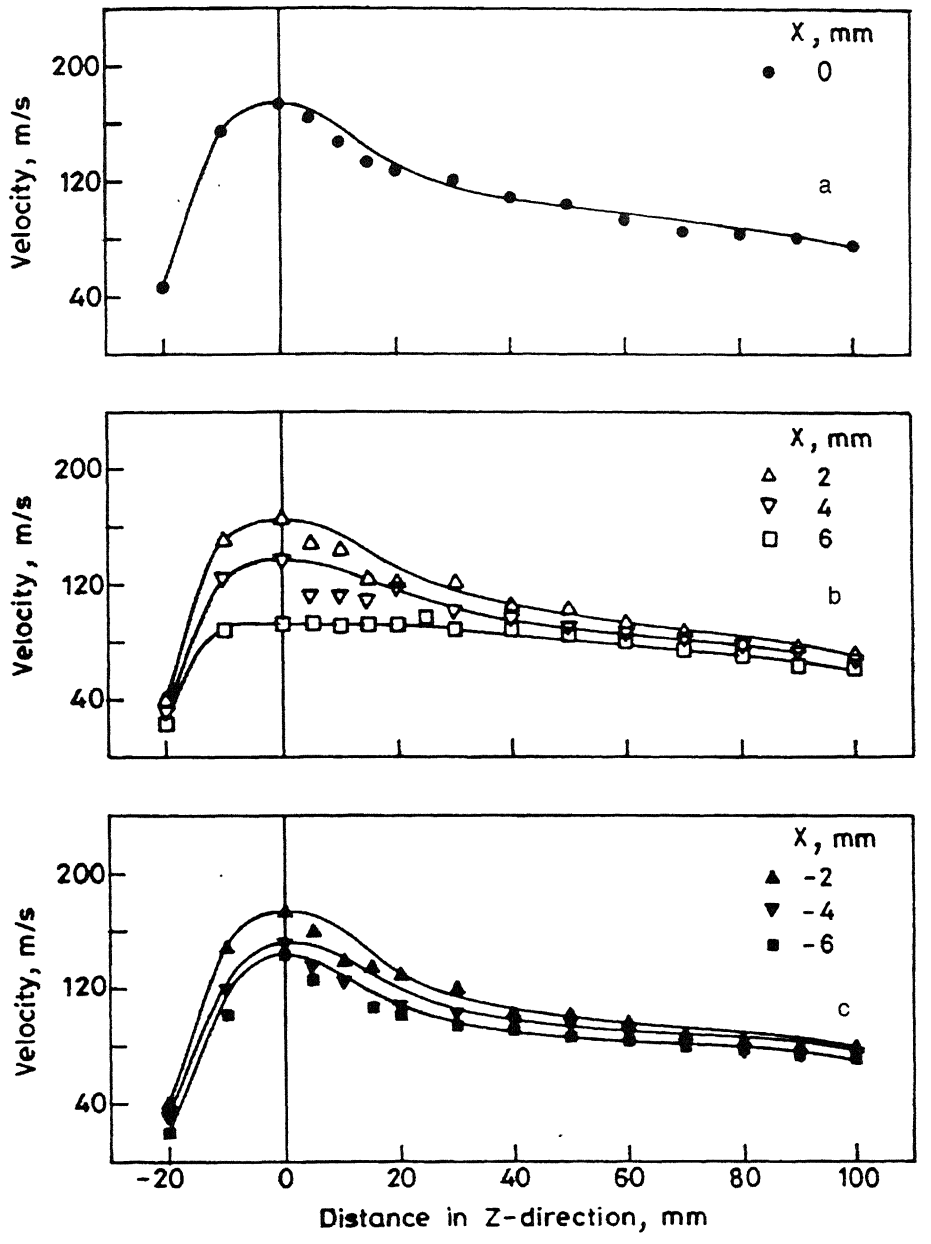

Figure 4.1.5 Variation of gas velocity on the XZ plane of gas field situated at Y= - 4 mm.

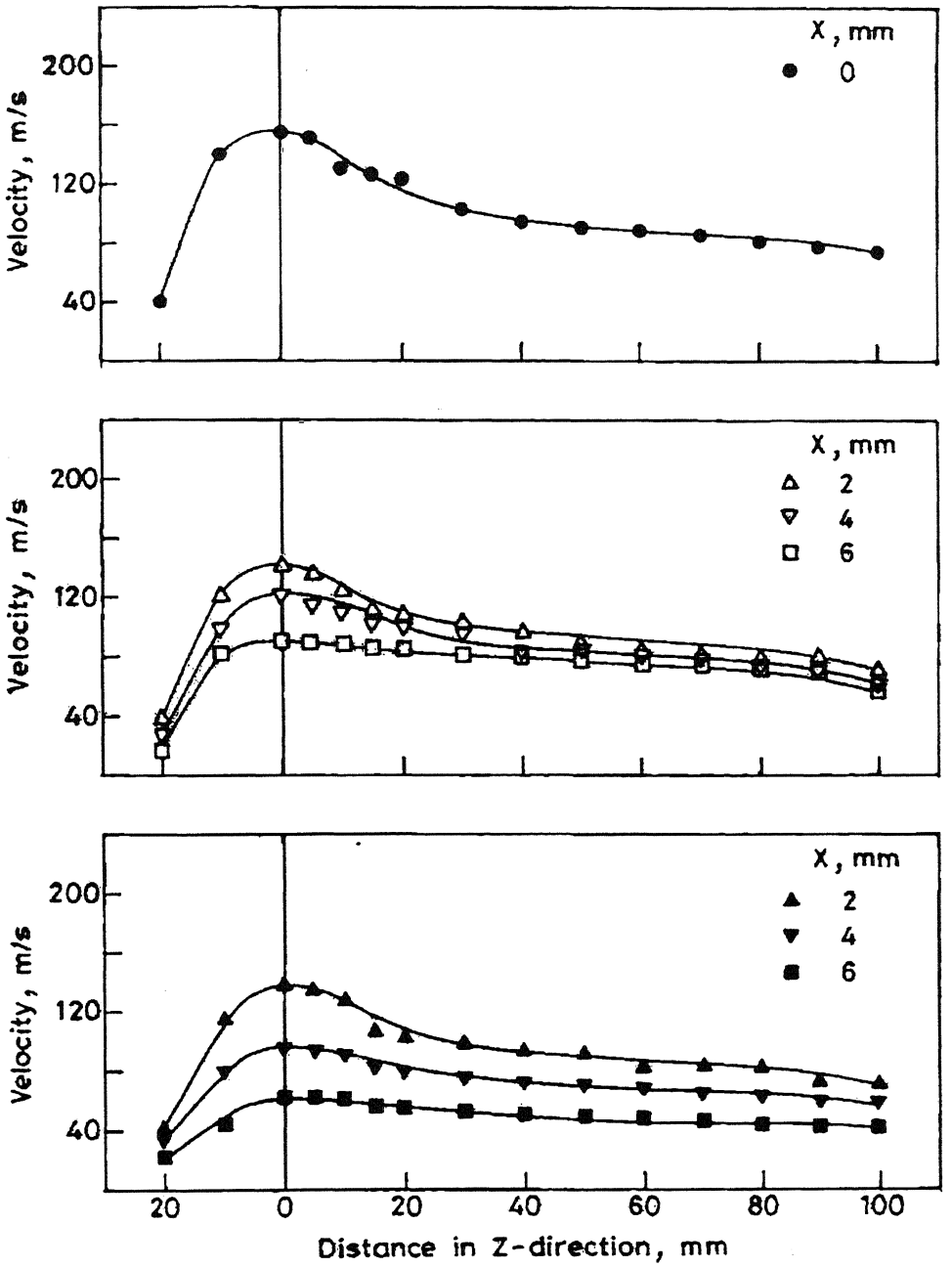

Figure 4.1.6 Variation of gas velocity on the XY plane of gas field situated at Y = 6 mm.

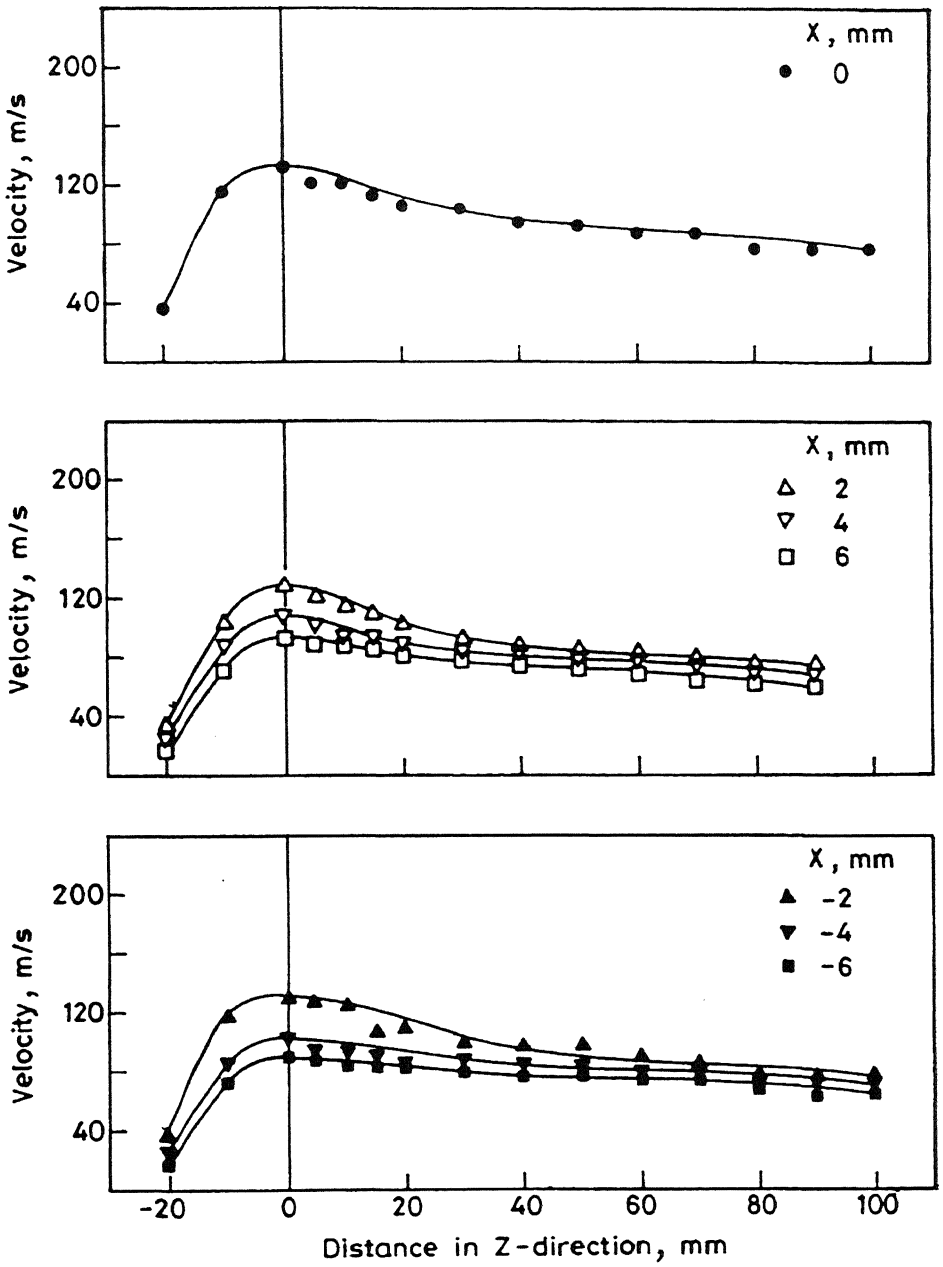

Figure 4.1.7 Variation of gas velocity on the XZ plane of gas field situated at Y= - 6 mm

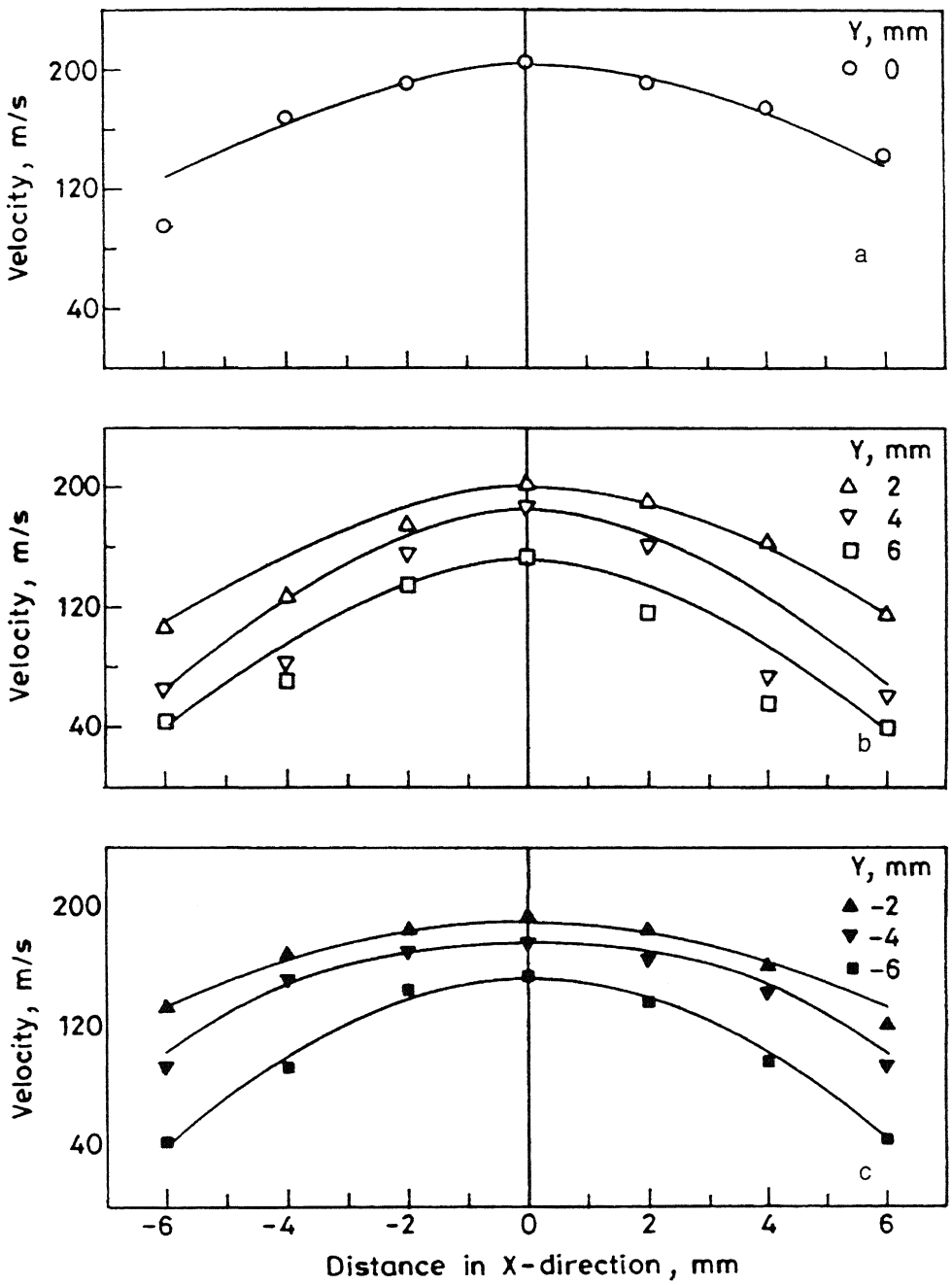

Figure 1.8 Variation of gas velocity on the XY plane of gas field situated at Z = 0.

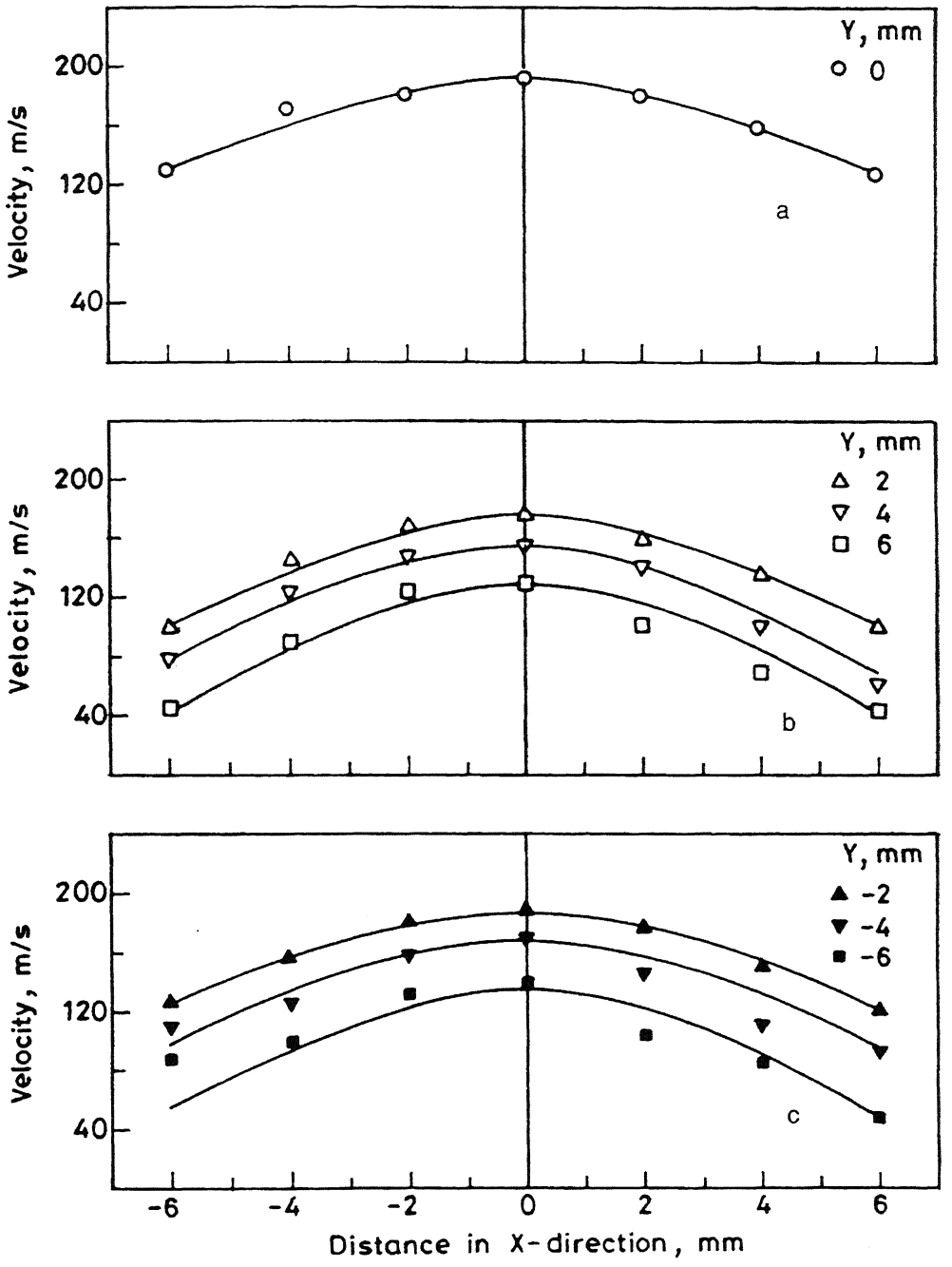

Figure 4.1.9 Variation of gas velocity on the XY plane of gas field situated at Z =10 mm.

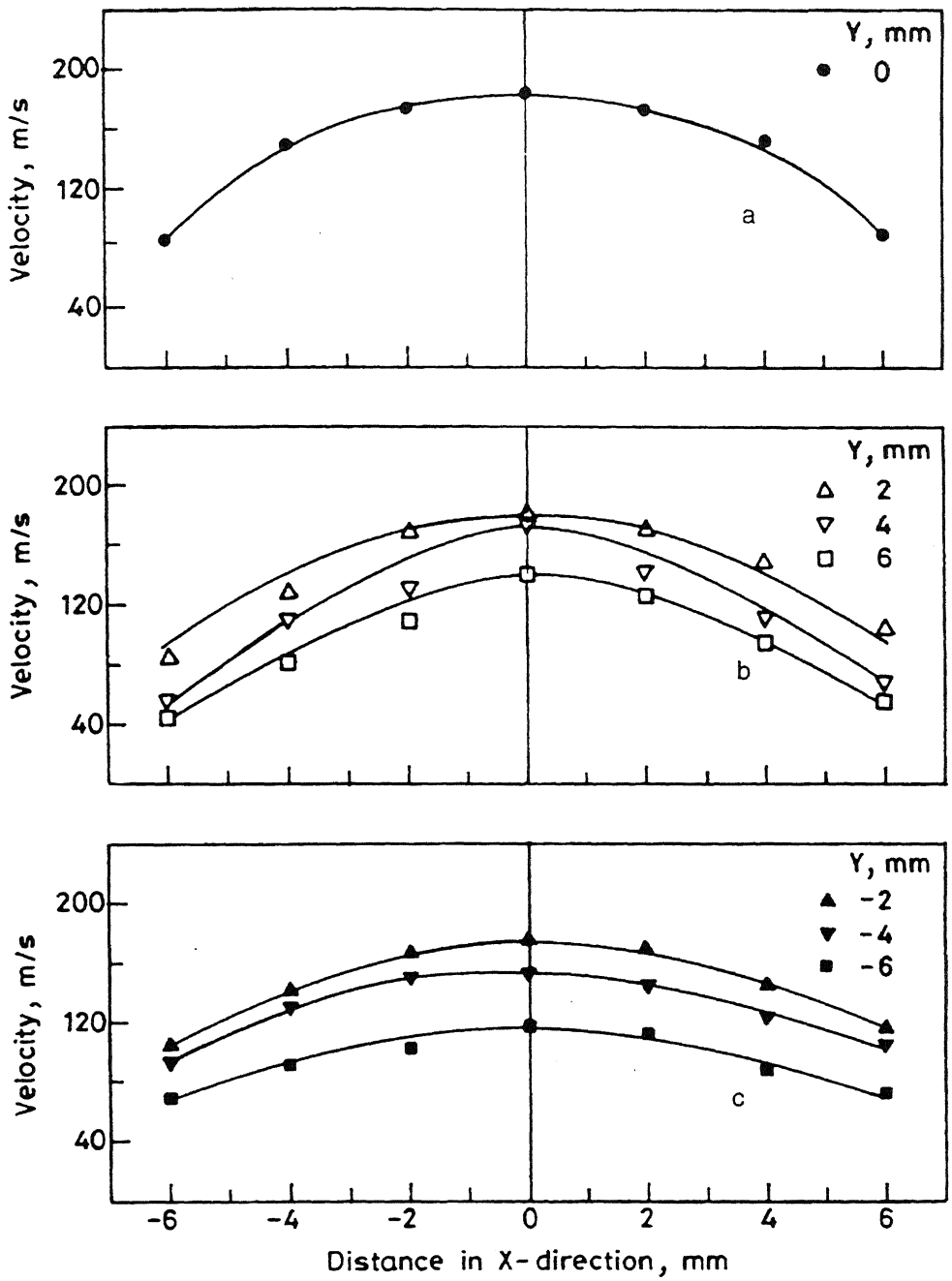

Figure 4.1.10 Variation of gas velocity on the XY plane of gas field situated at Z= - 10 mm.

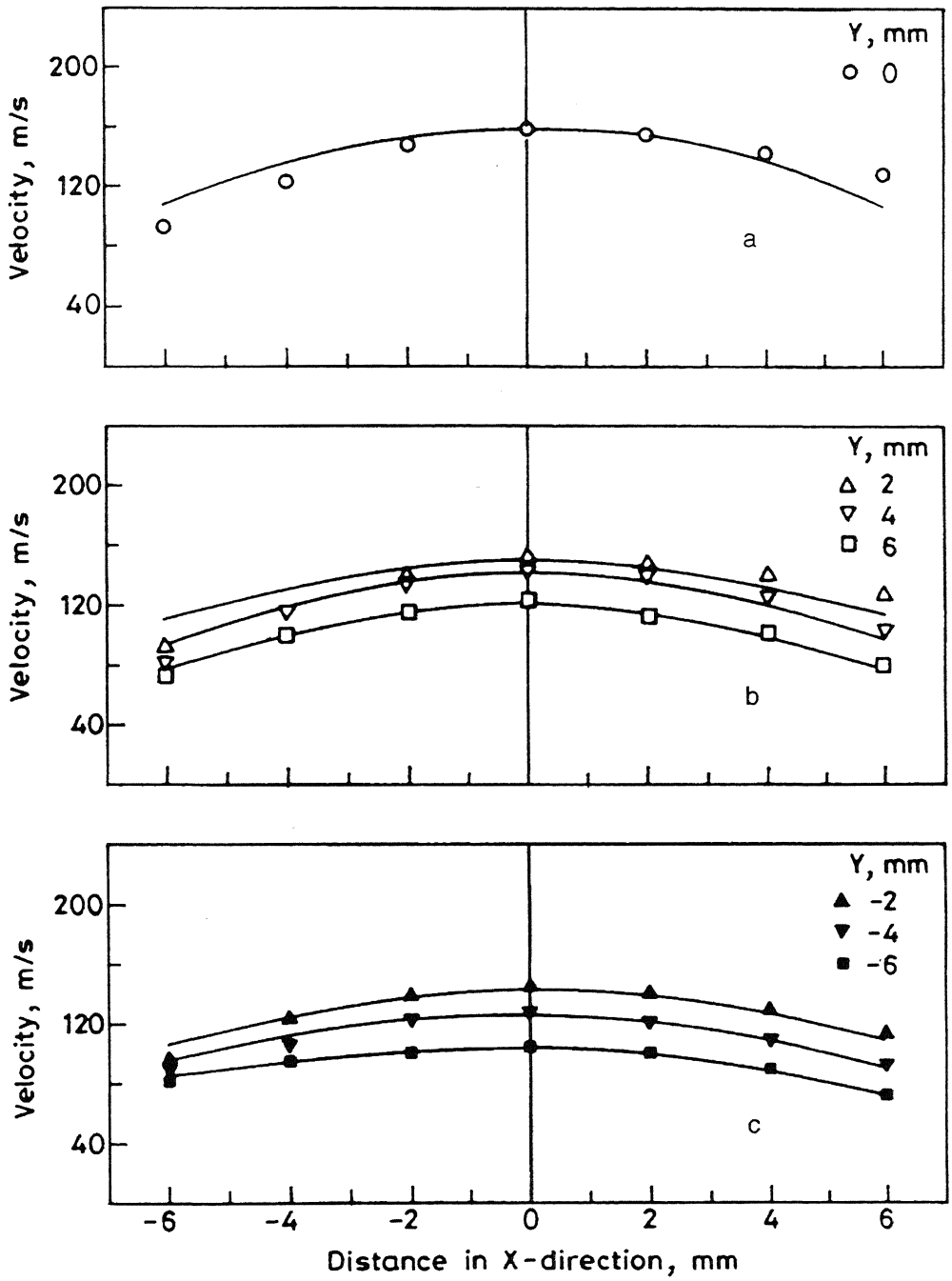

Figure 4.1.11 Variation of gas velocity on the XY plane of gas field situated at Z = 20 mm.

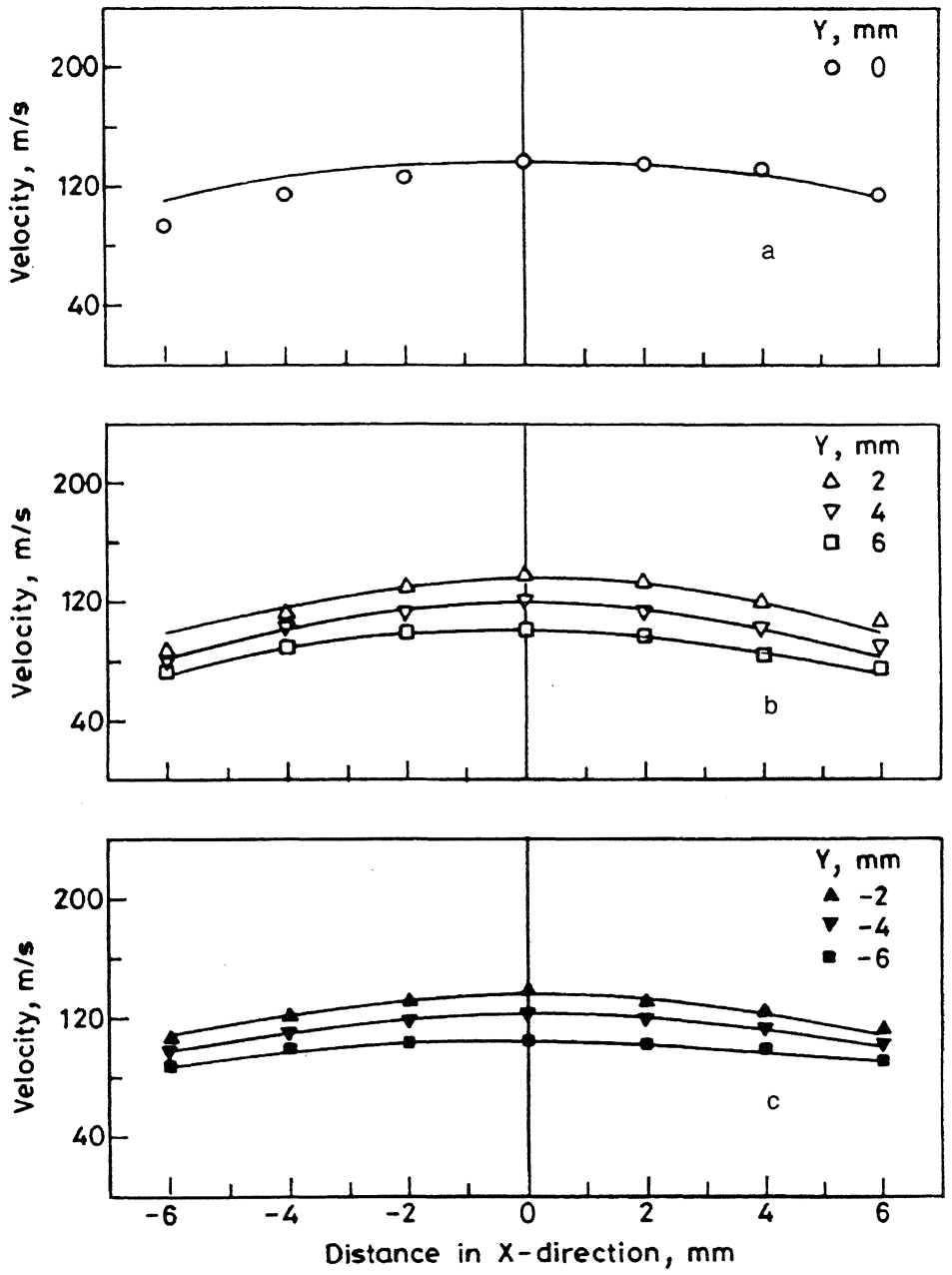

Figure 4.1.12 Variation of gas velocity on the XY plane of gas field situated at Z = 30 mm.

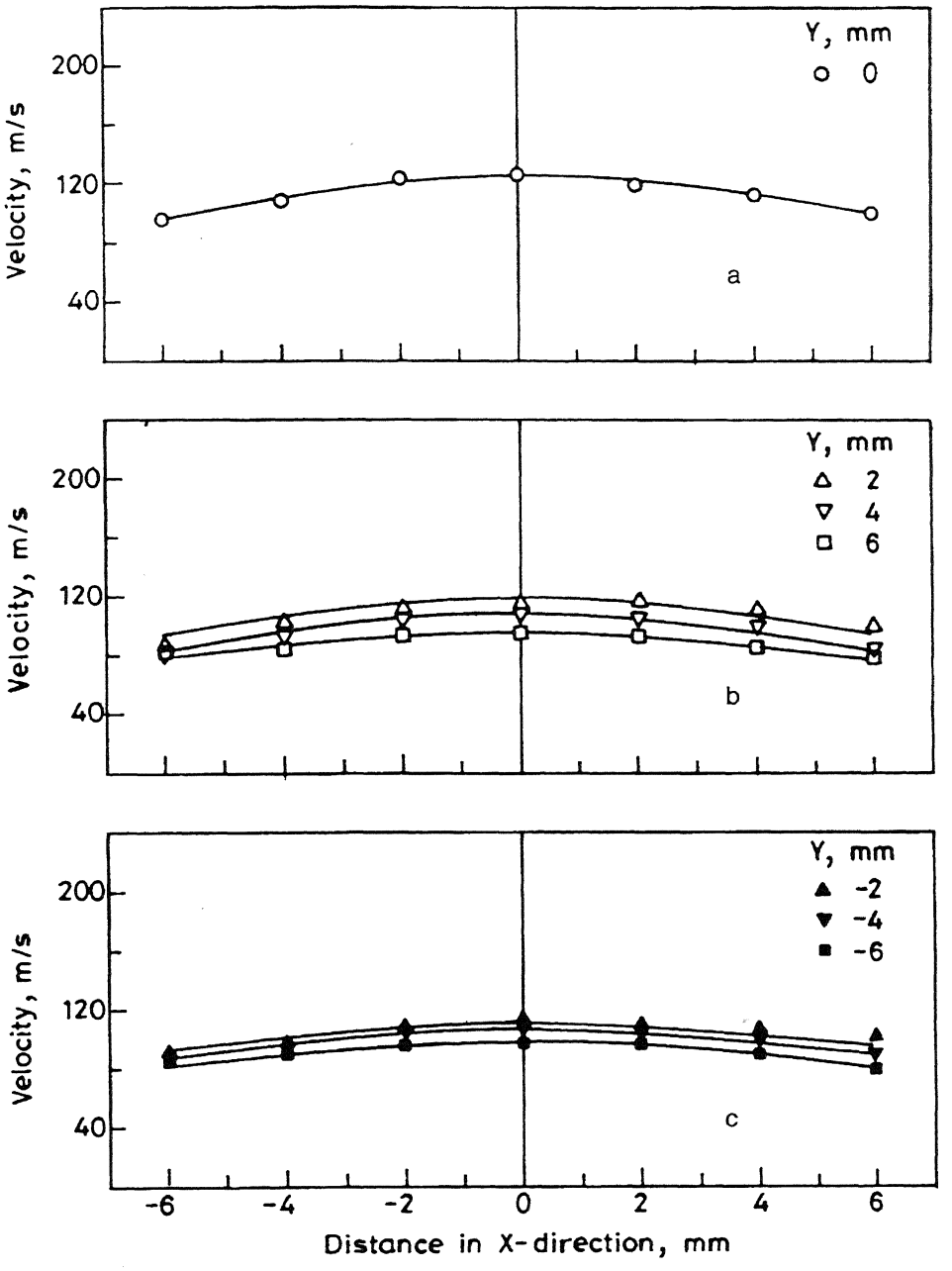

Figure 4.1.13 Variation of gas velocity on the XY plane of gas field situated at Z = 40 mm

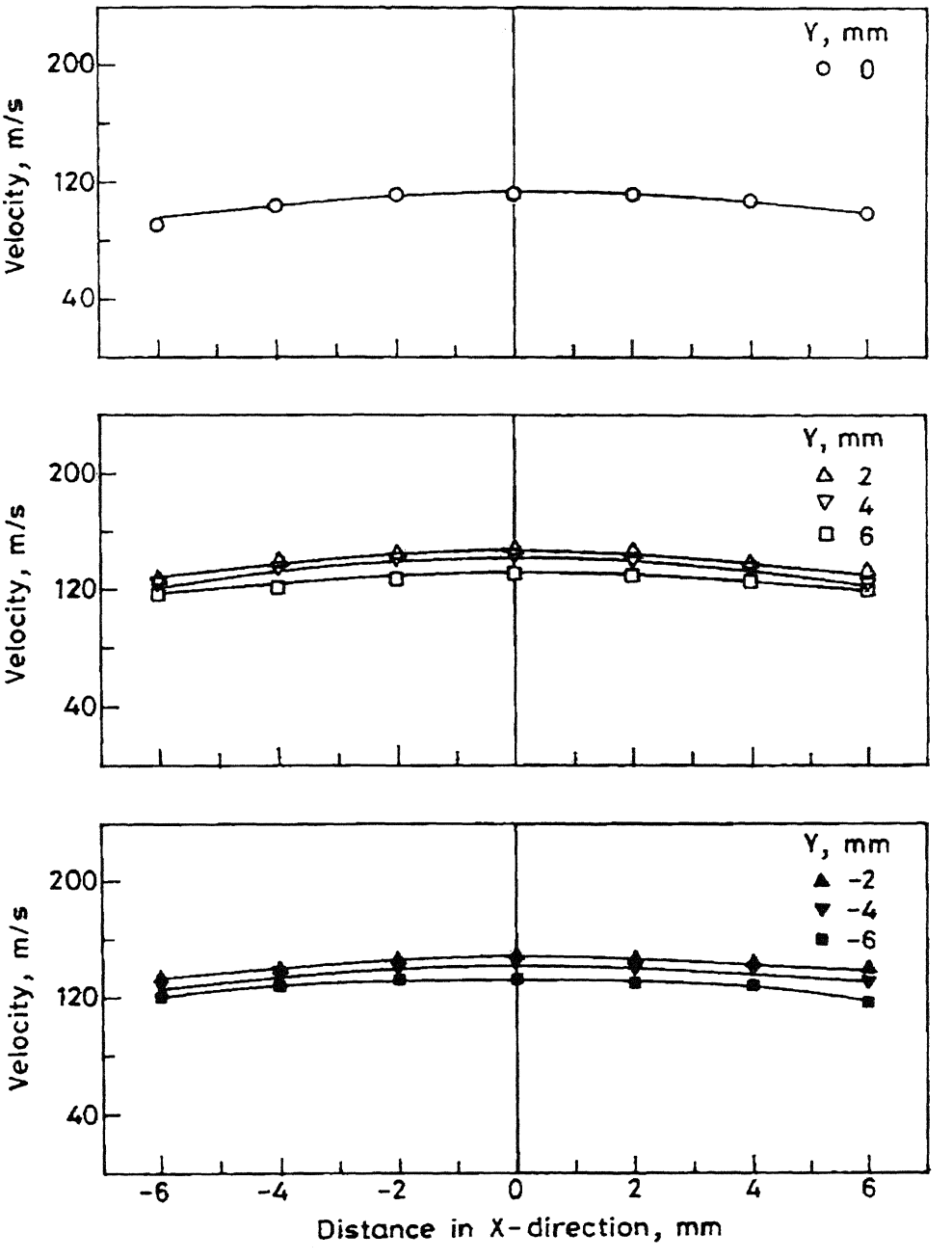

Figure 4.1.14 Variation of gas velocity on the XY plane of gas field situated at Z = 50 mm.

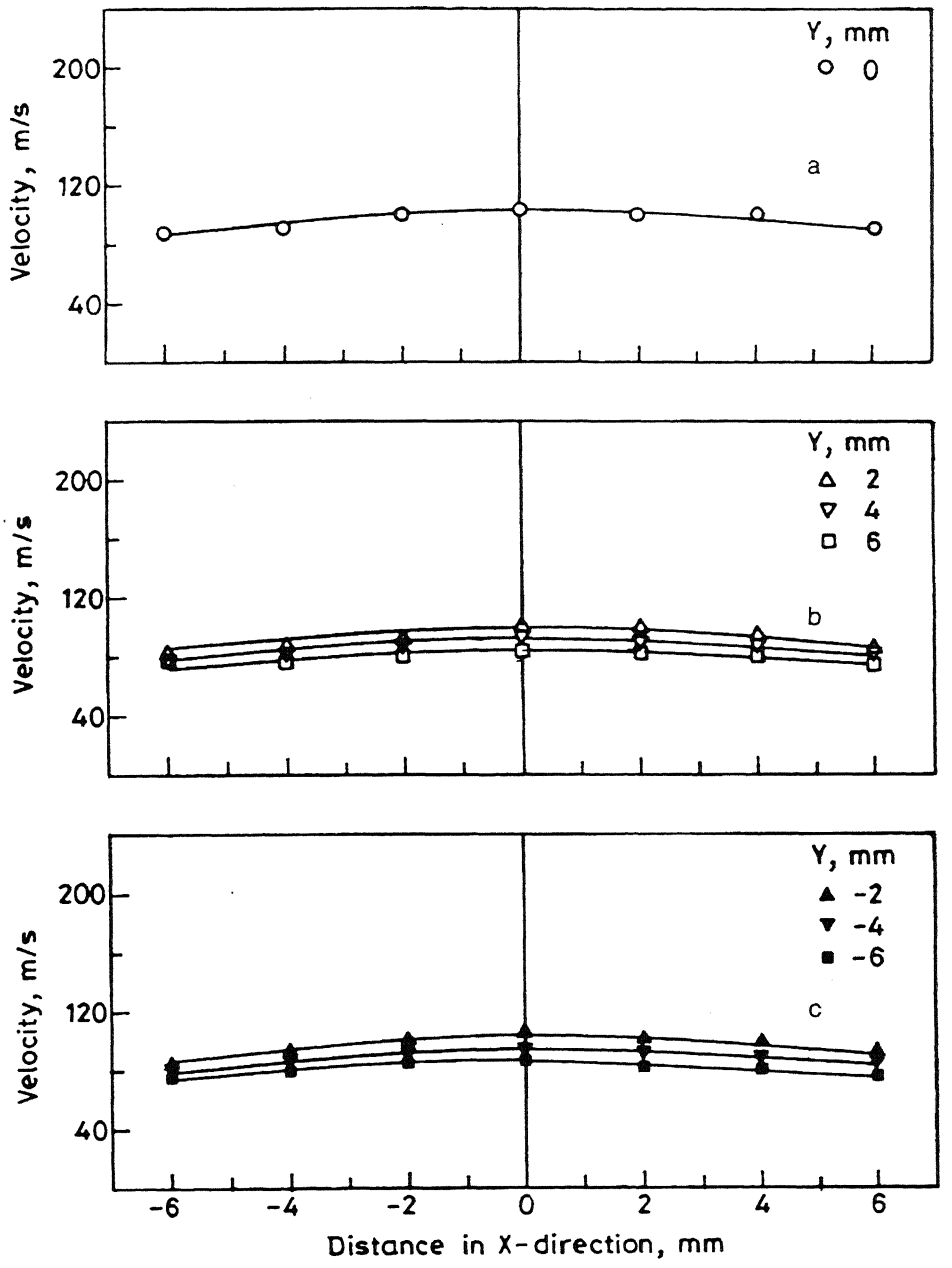

Figure 4.1.15 Variation of gas velocity on the XY plane of gas field situated at Z = 60 mm.

It can be seen that the velocity is different at different points on any given XY plane within the gas field. It would be interesting to know the position of iso-velocity lines for any given velocity value on these planes.

Figures 4.1.16 to 4.1.22 show the iso-velocity lines for velocity of 160 m/s on XY planes situated at Z = ± 10 mm, Z = ± 5 mm, Z = 0, Z = 15 mm. In this representation iso-velocity lines for the velocity of 160 m/s, have been shown.

From the above figures the following observations can be made:

1. The region up to which the gas velocity is 160 m/s is maximum for the XY plane situated at Z = 0, i.e. passing through the geometric point. The extent of this region decreases with increase in Z both in positive and negative directions.
2. The region up to which the gas velocity is 160 m/s was not found below Z = 15 mm.
3. The iso-velocity lines are in general symmetrical to the vertical line passing through the geometric point.

4.2 Variation of velocity in the gas field produced at 1000 kPa plenum pressure:

Figures 4.2.1 to 4.2.7 show the variation of velocity on the XZ planes of gas field situated at Y = 0, ± 2 mm, ± 4 mm, ± 6 mm. In this representation velocity is plotted as a function of Z at different values of X varying in between – 6 mm and + 6 mm.

From the above figures the following observations can be made:

1. The velocity of gas on the XZ plane situated at any value of Y, decreases with either increase in Z while keeping X constant or increase in X while keeping Z constant, both in positive or negative directions.
2. For any given value of either X or Y, the decrease in velocity with increase in Z is faster when the value of Z is negative as compared when Z is positive (Figure 4.21b). The impingement of jets at the geometric point causes the downward flow of the gas at a rate faster than the upward flow. Thus the entrainment of the surrounding air into the downward flow of the gas occurs slowly as compared with into the upward flow of gas.

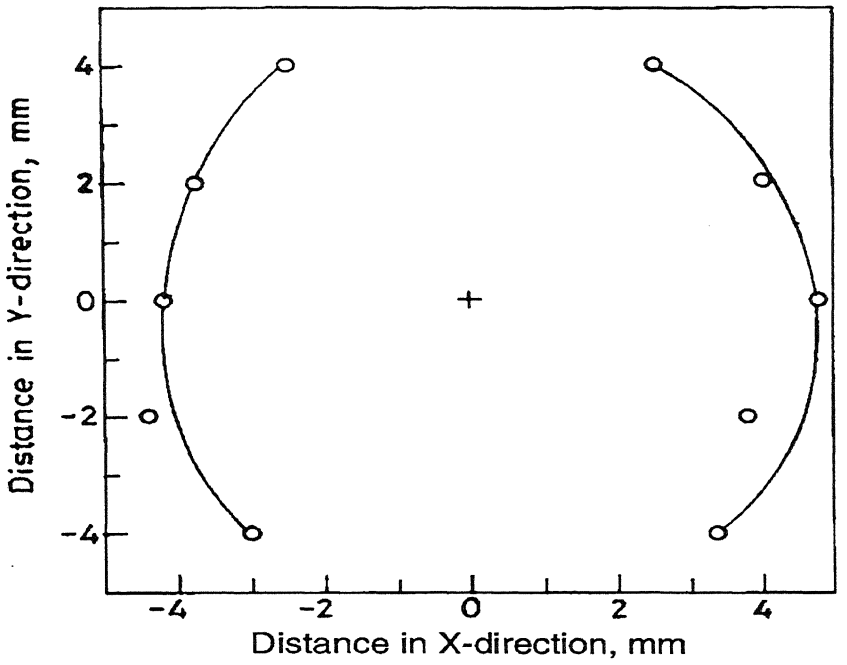

Figure 4.1.16 Iso-velocity line for velocity of 160 m/s on the XY plane situated at Z=0.

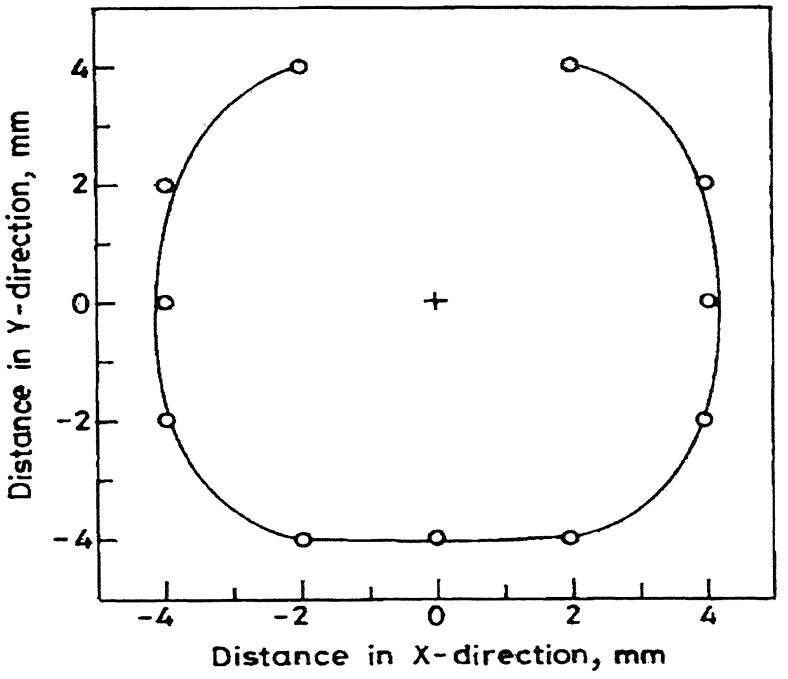

Figure 4.1.17 Iso-velocity line for the velocity of 160 m/s on the XY plane situated at Z=5 mm.

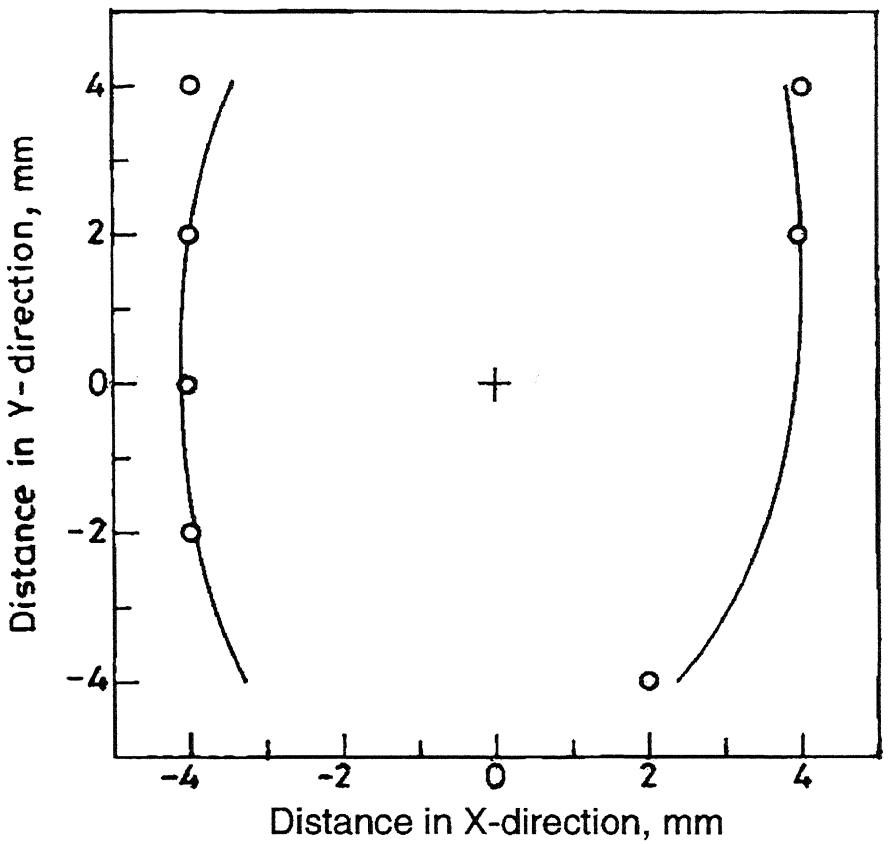

Figure 4.1.18 Iso-velocity line for the velocity of 160 m/s on the XY plane situated at Z= -5 mm.

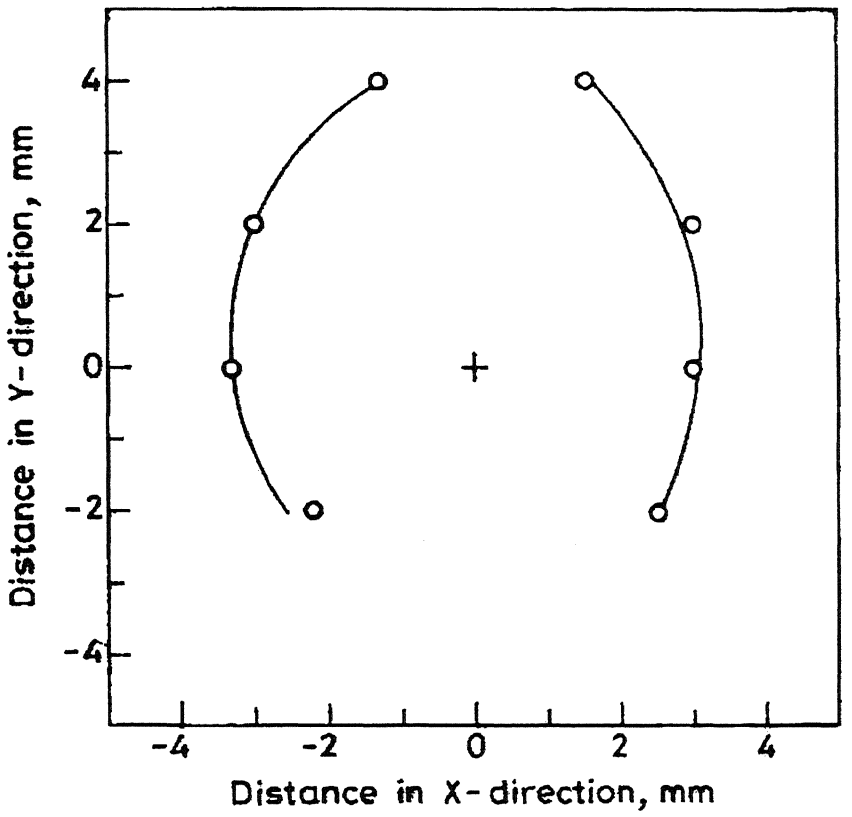

Figure 4.1.19 Iso-velocity line for the velocity of 160 m/s on the XY plane situated at Z=10 mm

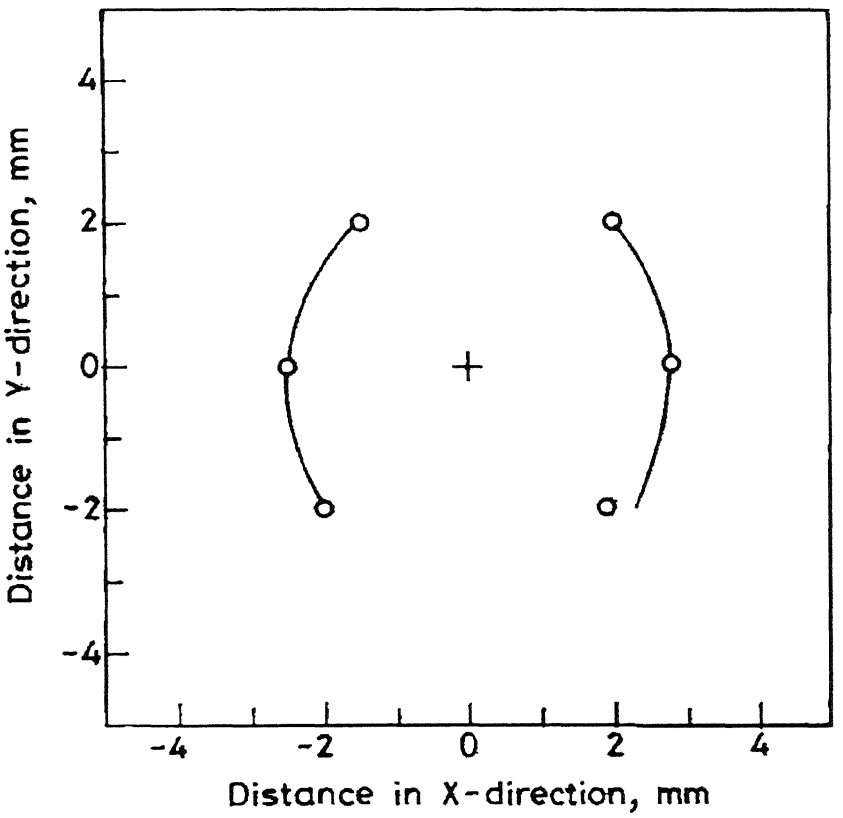

Figure 4.1.20 Iso-velocity line for the velocity of 160 m/s on the XY plane situated at Z=15 mm.

3. For any given value of Y and Z, increase in X either in positive or negative direction for all values of Z decreases the velocity of gas in the gas field (Figure 4.2.1a and 4.2.1b to 4.2.7a and 4.2.7b).
4. Increase in the value of Y both in positive or negative directions, decreases the velocities both in X and Z directions. The extent of decrease depends on the value of Y.

For example at Y=0 the velocity of gas at X=0 and Z=0 is 236 m/s, which is almost same at Y=2 mm but decreases to 140 m/s at Y= + 6 mm and to 184 m/s at Y= - 6 mm. Similar information can be obtained at other values of Y and different combinations of X and Z (Figure 4.3.1a, 4.3.2a, 4.3.3a, 4.3.4a, 4.3.5a, 4.3.6a, 4.3.7a and 4.3.8a).

Figures 4.2.8 to 4.2.15 show the variation of velocity on XY planes of gas field situated at Z= 0, ± 10 mm, 20 cm, 30 mm, 40 mm, 50 mm, 60 mm. In this representation velocity is plotted as a function of X at different values of Y varying in between – 6 mm and + 6 mm.

From Figures 4.2.8 to 4.2.15 the following observations have been made:

1. The velocity of gas on the XY plane, situated at any value of Z, decreases with either increase in X while keeping Y constant, or increase in Y while keeping X constant both in positive and negative directions (Figure 4.2.8 to 4.2.15).
2. For any given value of either Y or Z, the rate of decrease in velocity with increase in X is similar in both the positive and negative directions. It is further observed that the curve on either side is almost symmetrical to each other (Figure 4.2.8 –4.2.15).
3. For any given value of Z and X, an increase in Y, either in positive or negative direction, decreases the velocity of gas in the gas field. For example at Z=0 the velocity of gas at X=2 mm and Y=0 is 226 m/s, but decreases to 160 m/s at Y= + 6 mm and to 140 m/s at Y= - 6 mm (Figure 4.2.8a and 4.2.8b). Similar observation can be obtained at other combinations of X and Y.
4. The increase in value of Z both in positive or negative directions decreases the velocity the velocities both in Y and X directions.

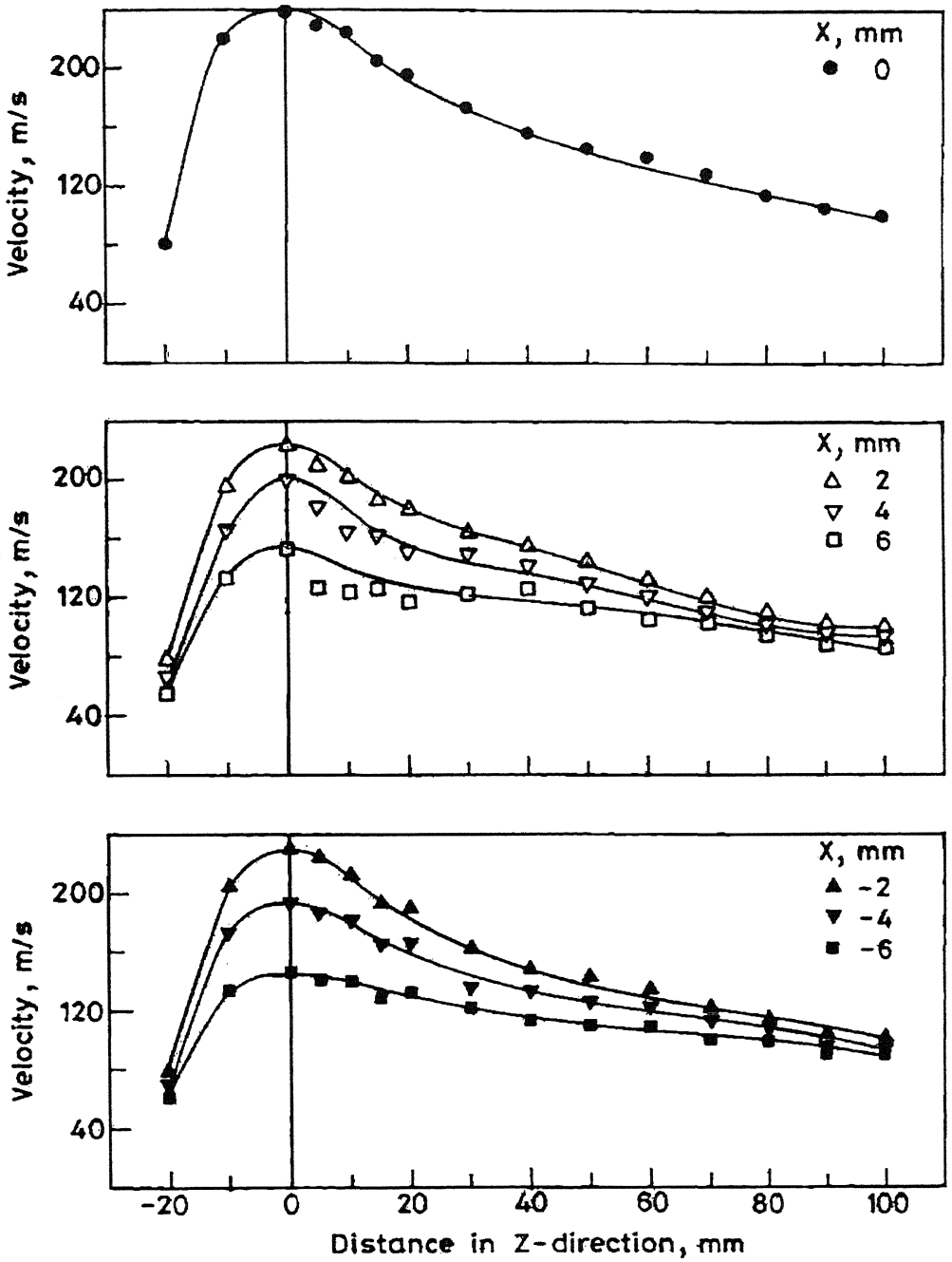

Figure 4.2.1 Variation of gas velocity on the XZ plane of gas field situated at Y =0.

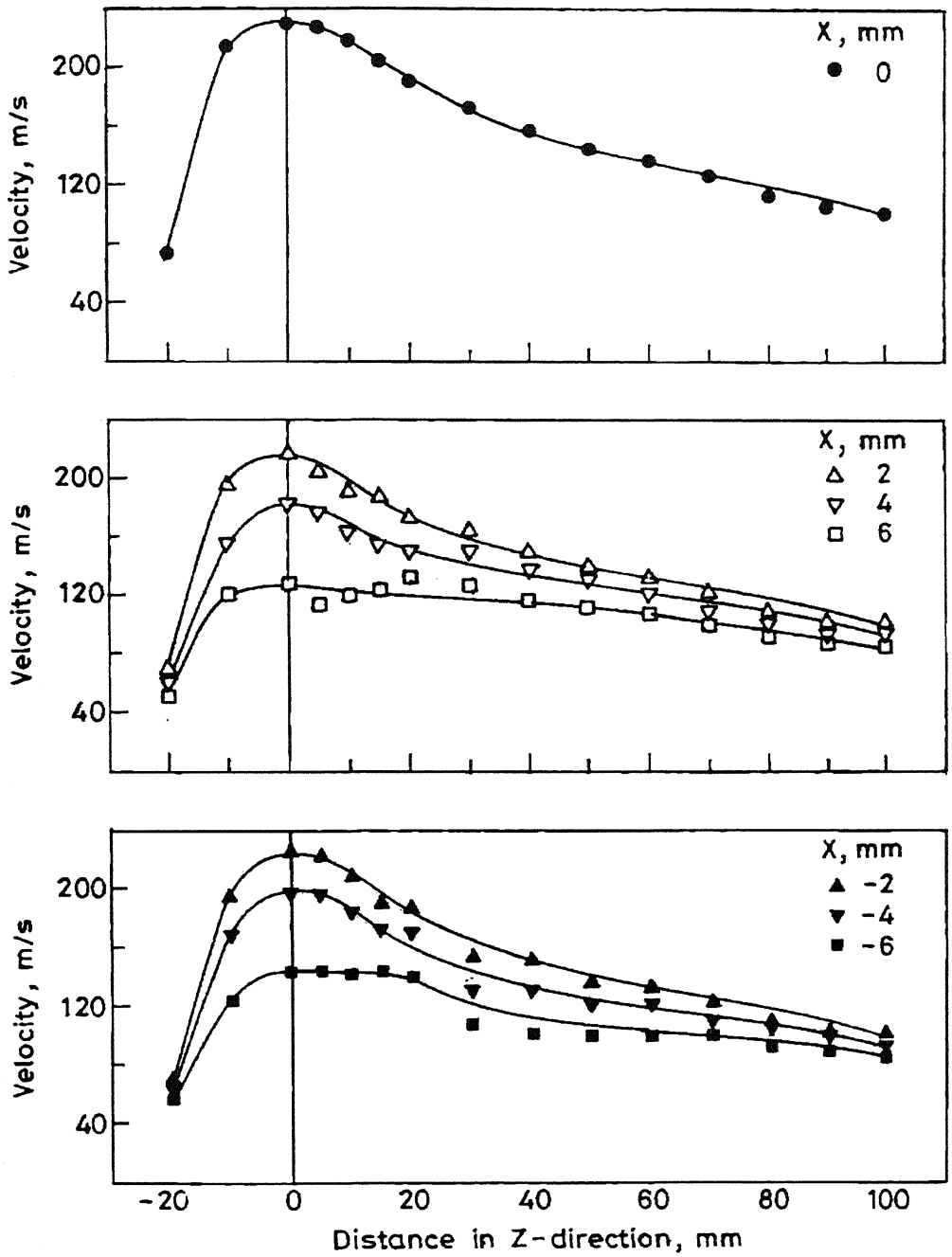

Figure 4.2.2 Variation of gas velocity on the XZ plane of gas field situated at Y = 2 mm.

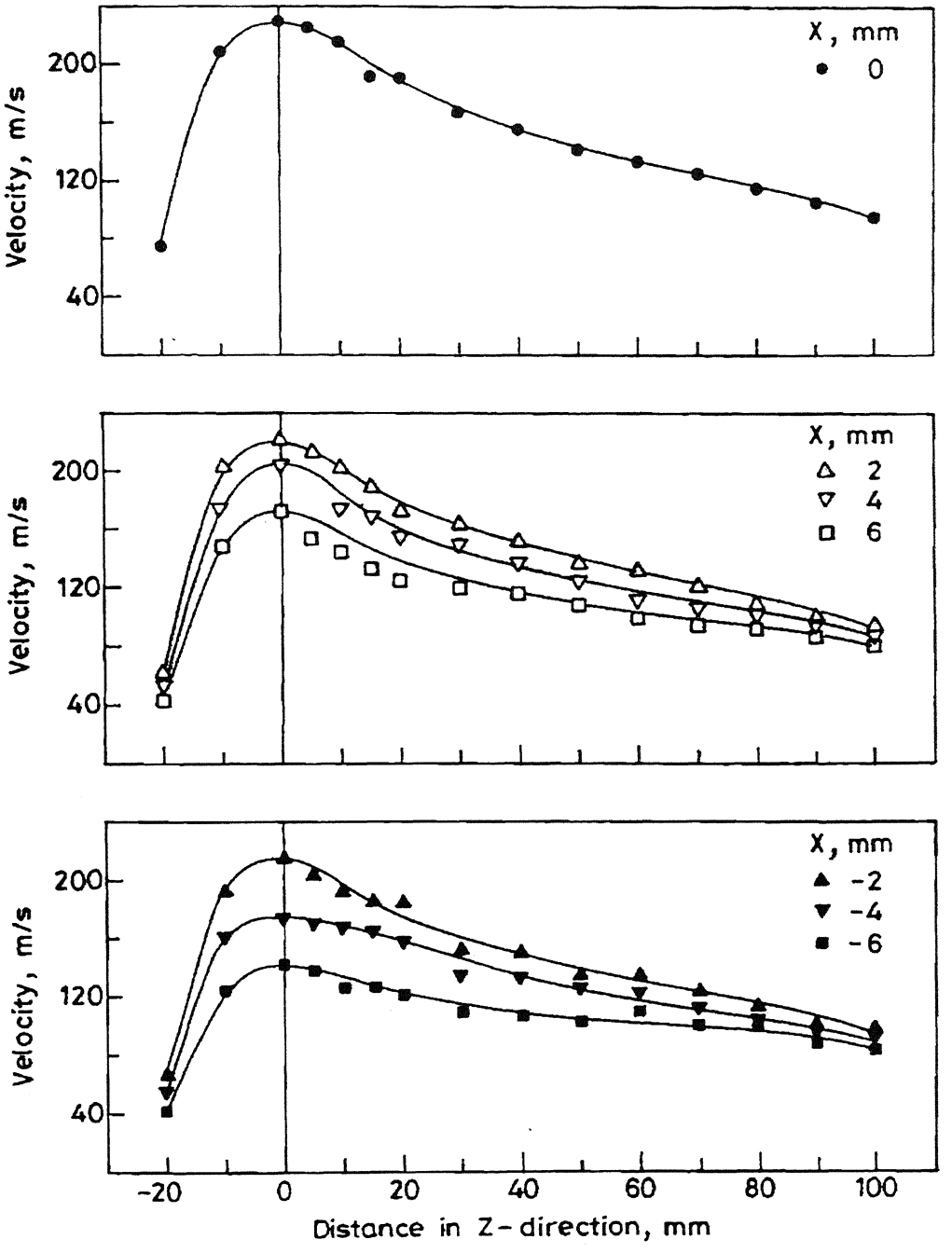

Figure 4.2.3 Variation of gas velocity on the XZ plane of gas field situated at Y = -2 mm.

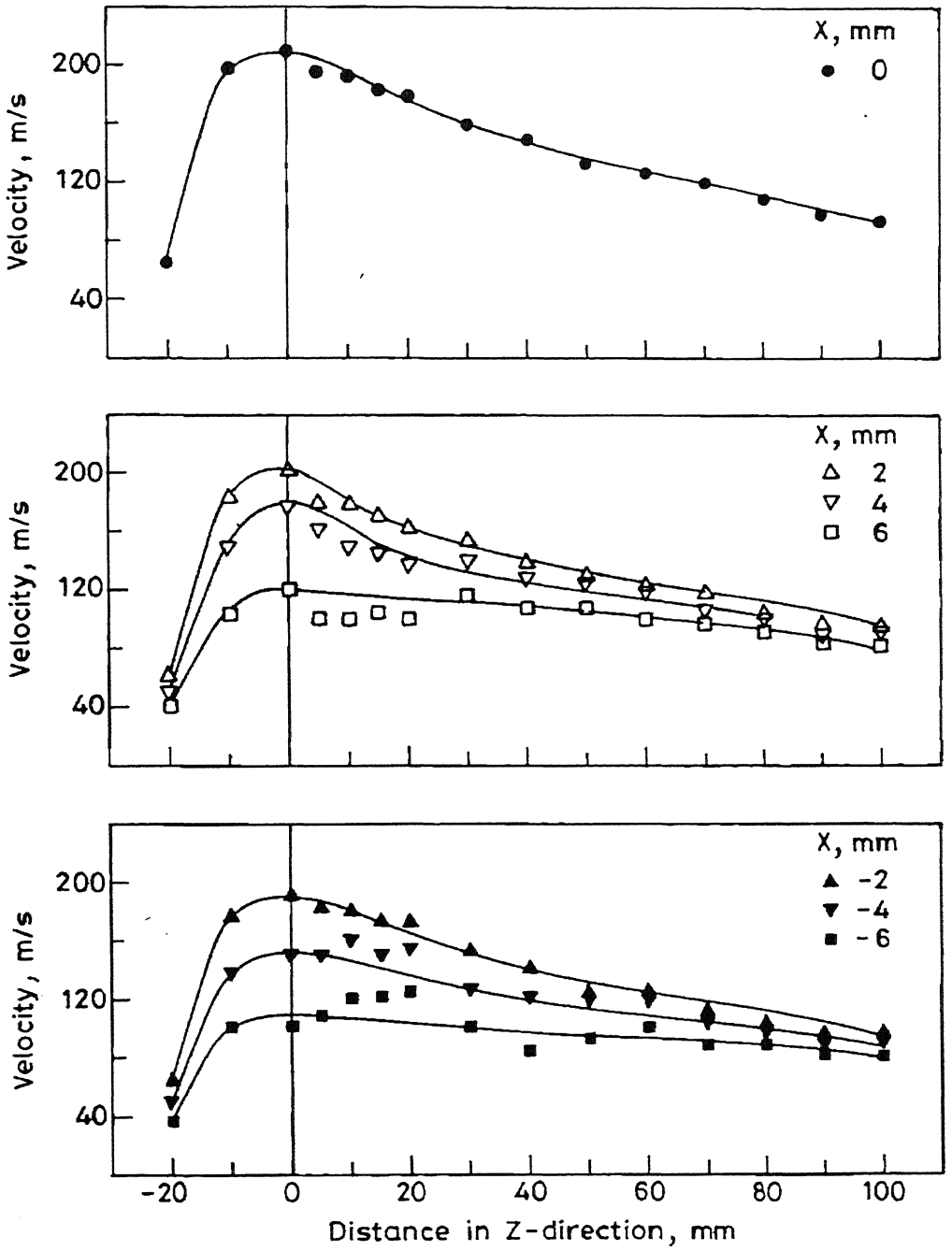

Figure 4.2.4 Variation of gas velocity on the XZ plane of gas field situated at Y = 4 mm.

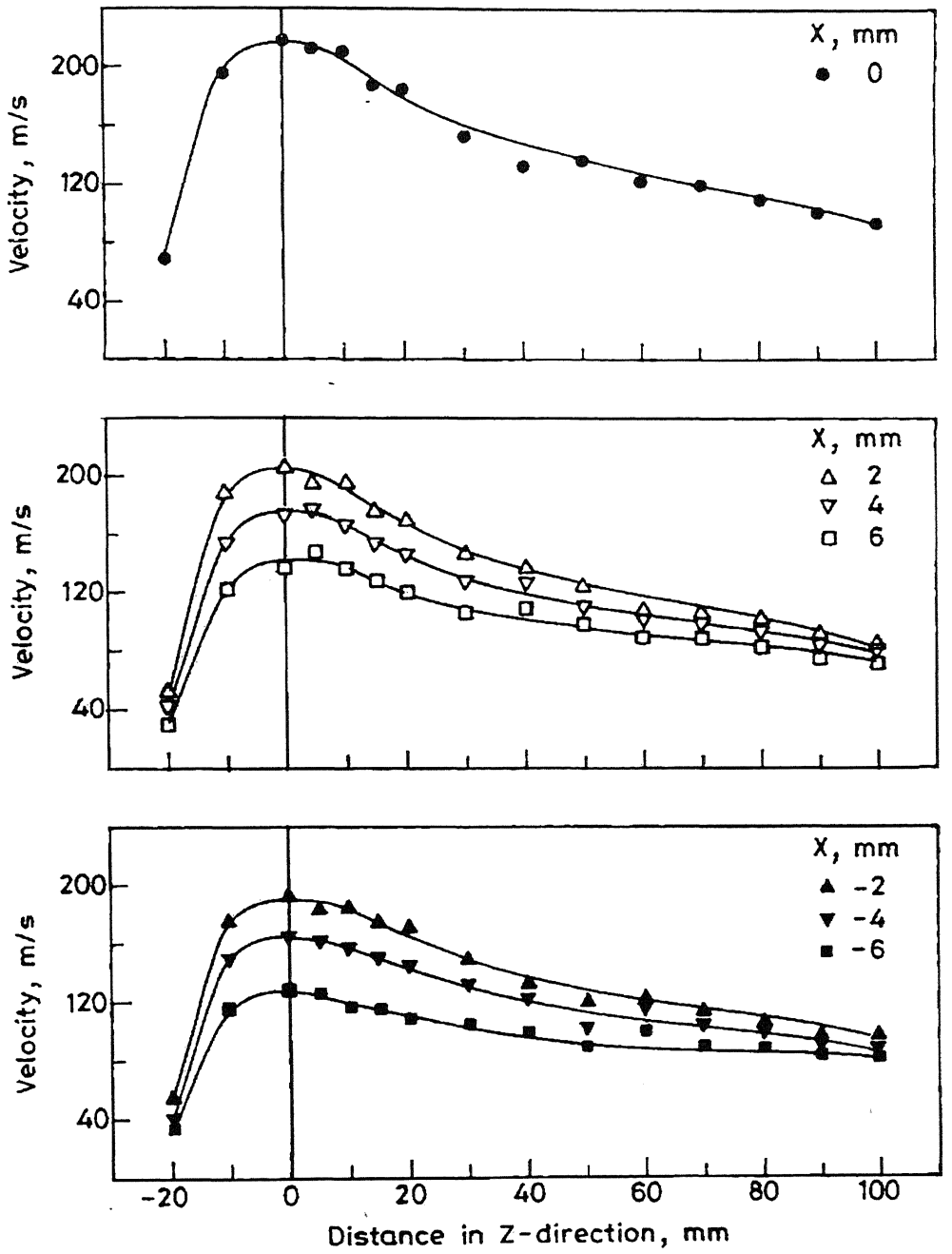

Figure 4.2.5 Variation of gas velocity on the XZ plane of gas field situated at Y = - 4 mm.

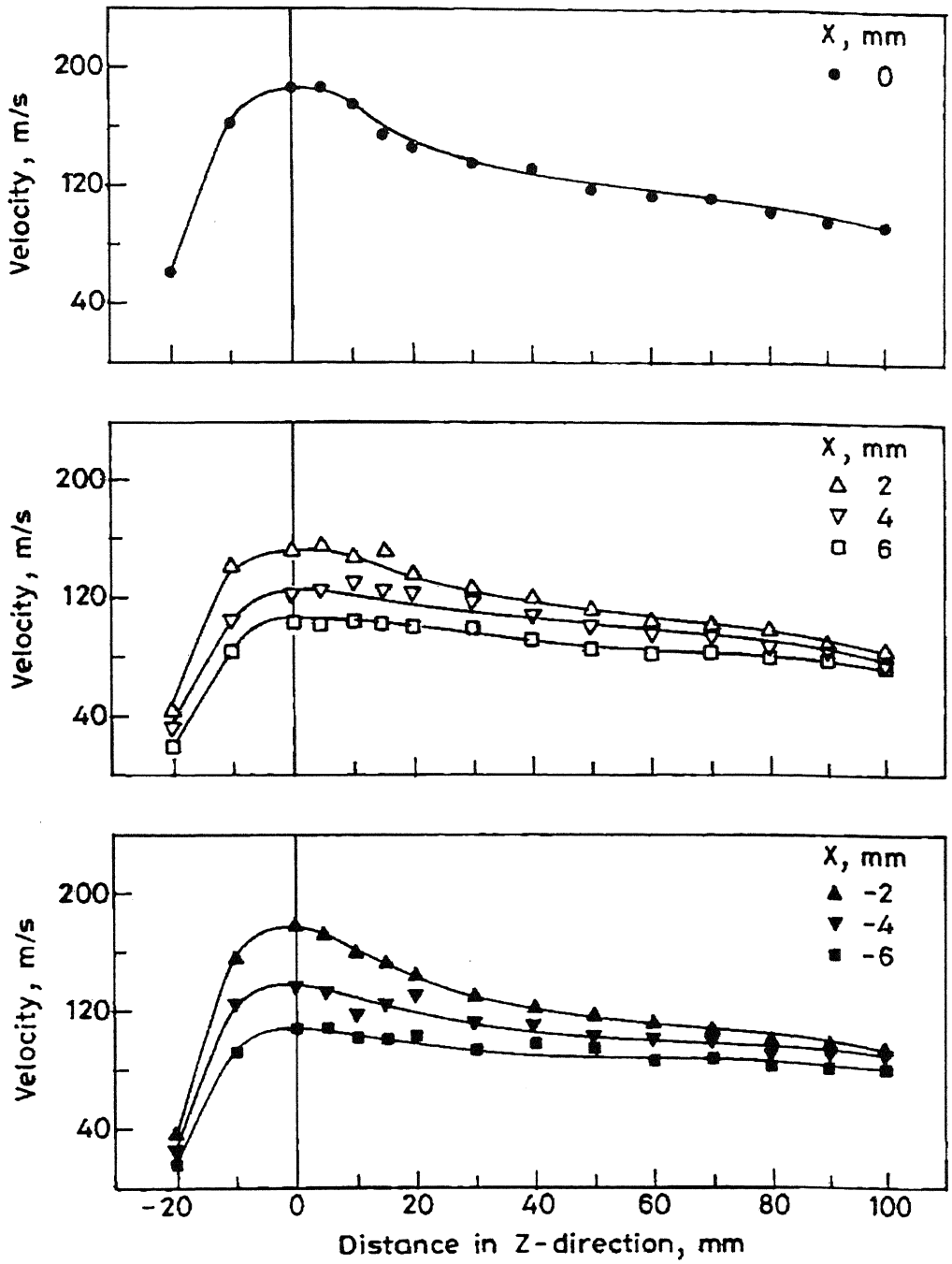

Figure 4.2.7 Variation of gas velocity on the XZ plane of gas field situated at Y= -6 mm.

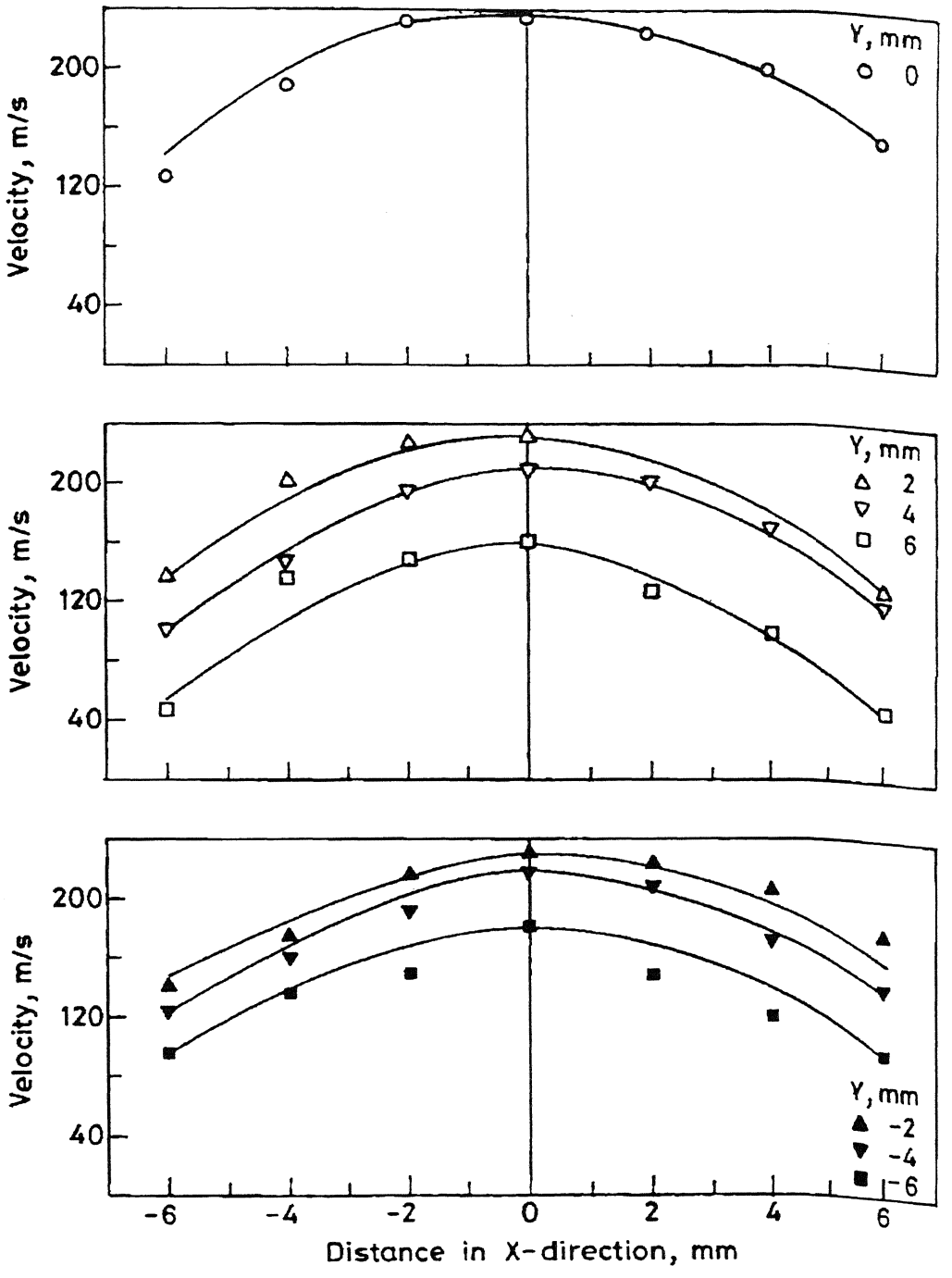

Figure 4.2.8 Variation of gas velocity on XY plane of gas field situated at Z = 0.

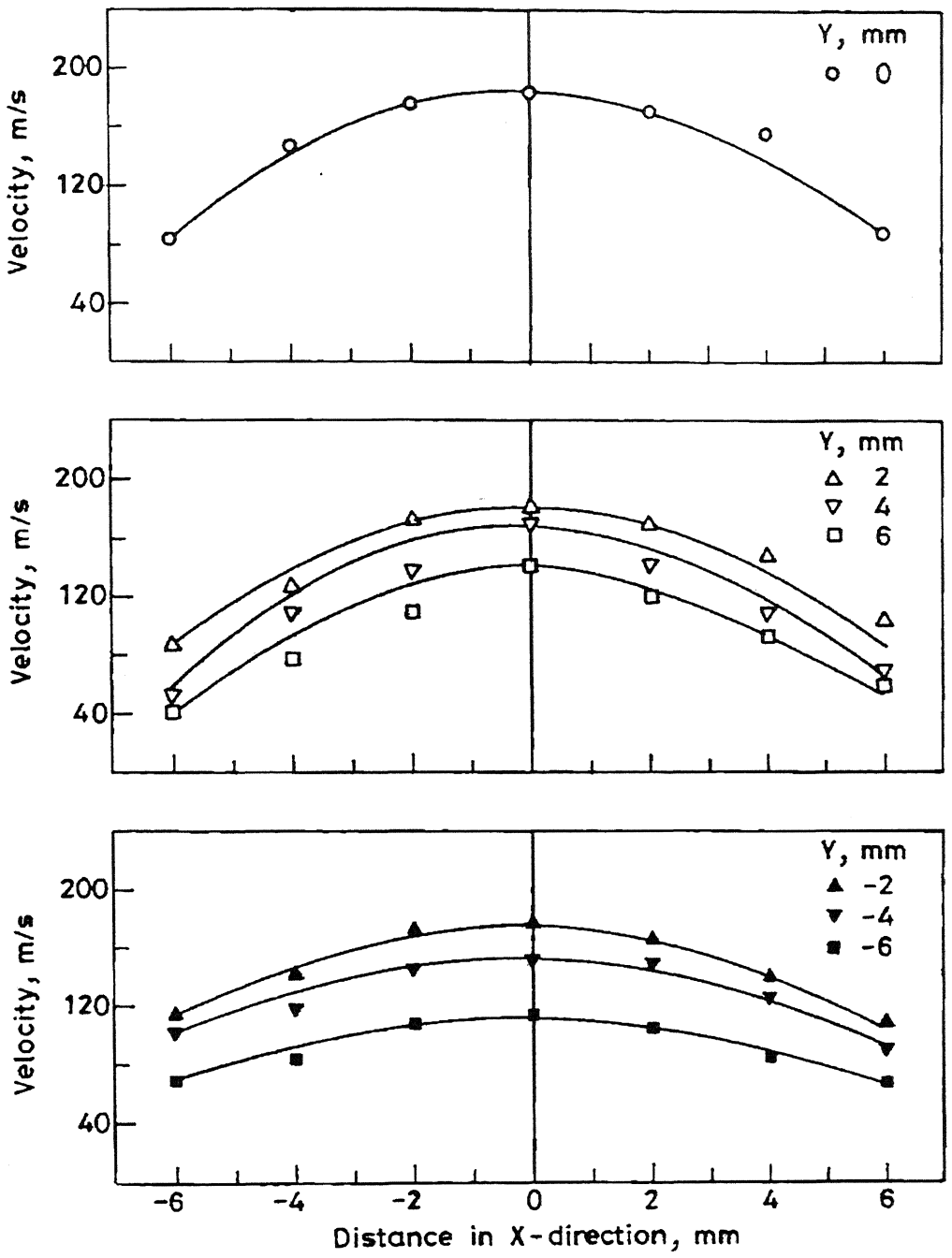

Figure 4.2.10 Variation of gas velocity on XY plane of gas field situated at Z = -10 mm.

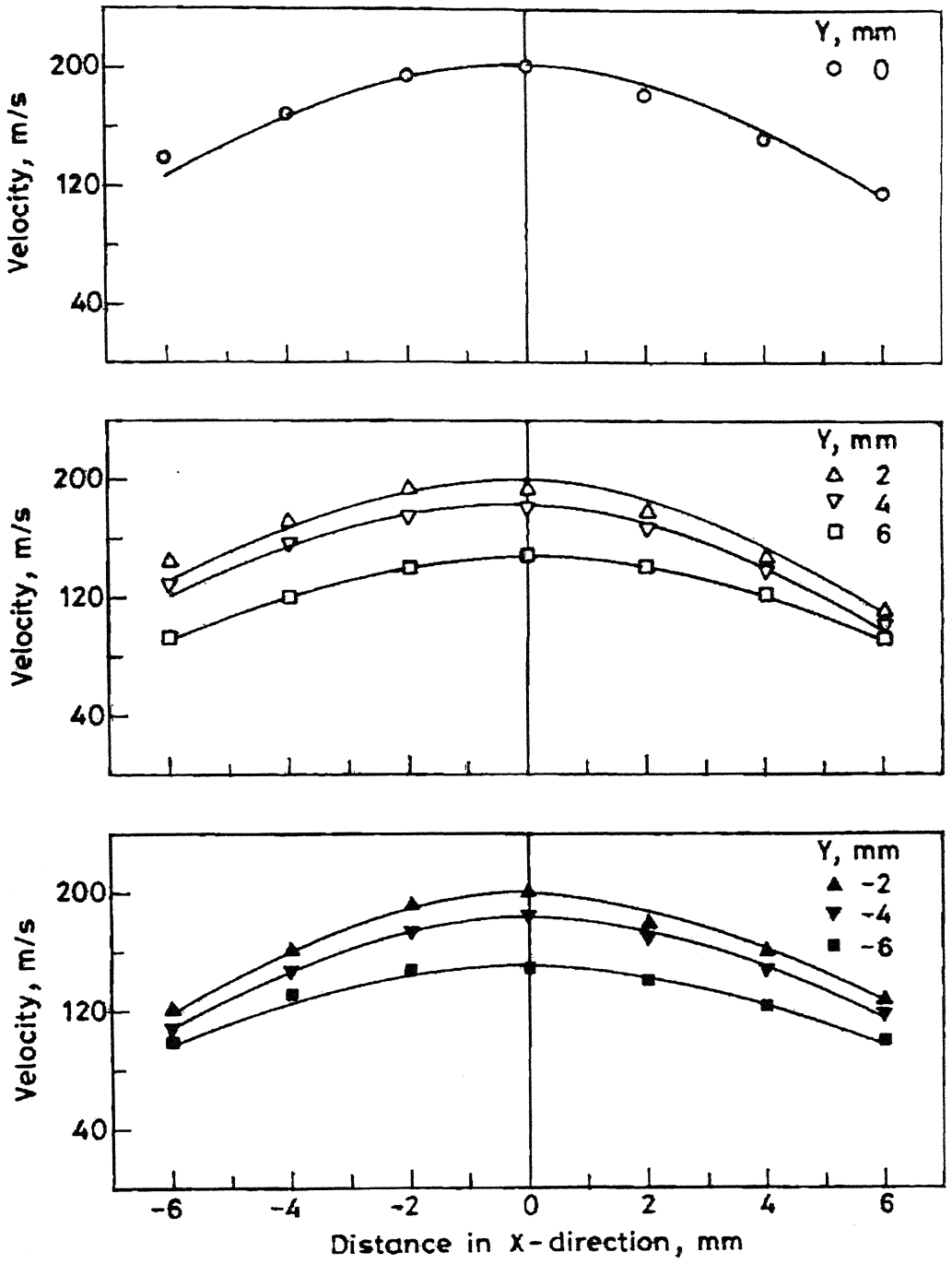

Figure 4.2.11 Variation of gas velocity on XY plane of gas field situated at Z = 20 mm.

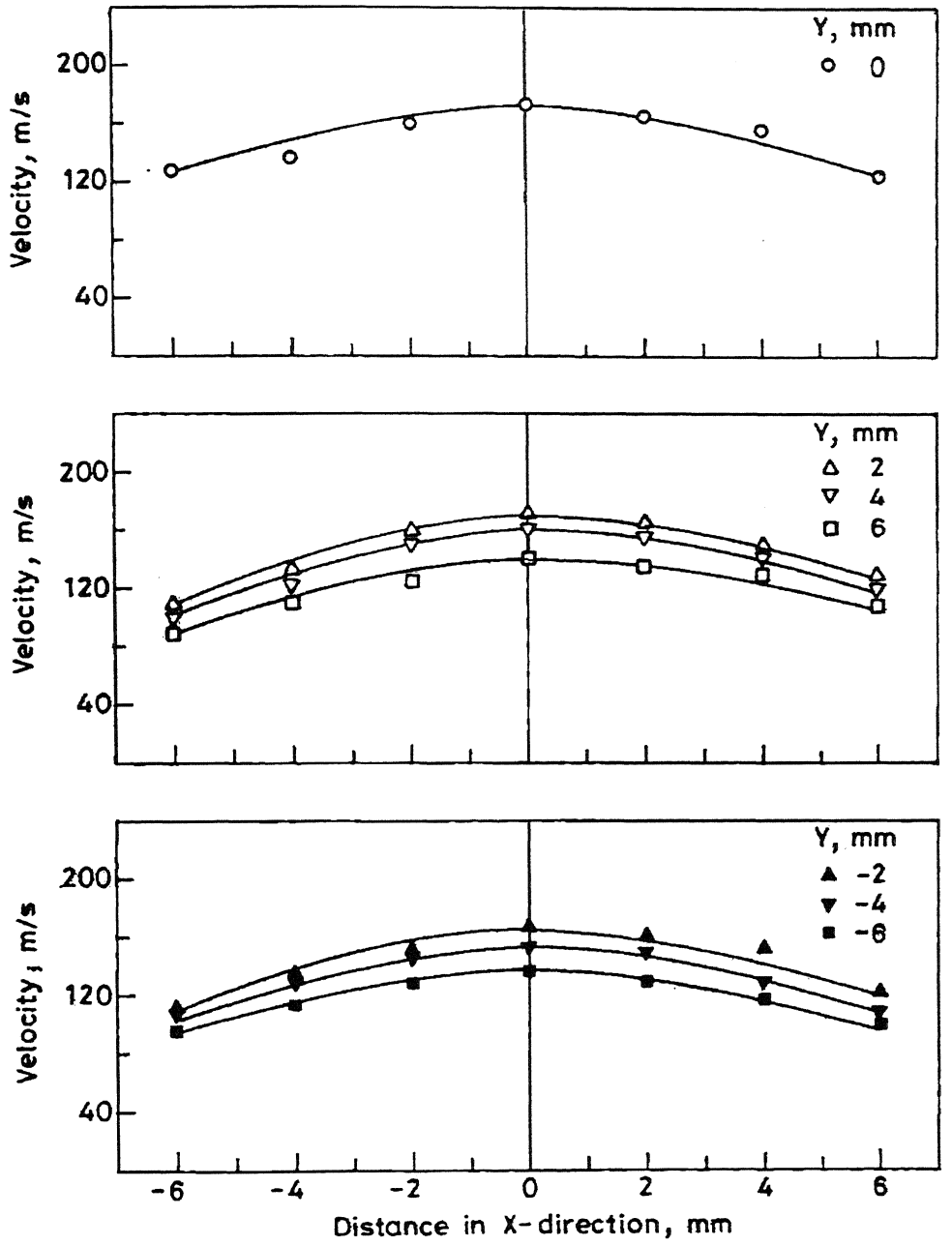

Figure 4.2.12 Variation of gas velocity on the XY plane of gas field situated at Z = 30 mm

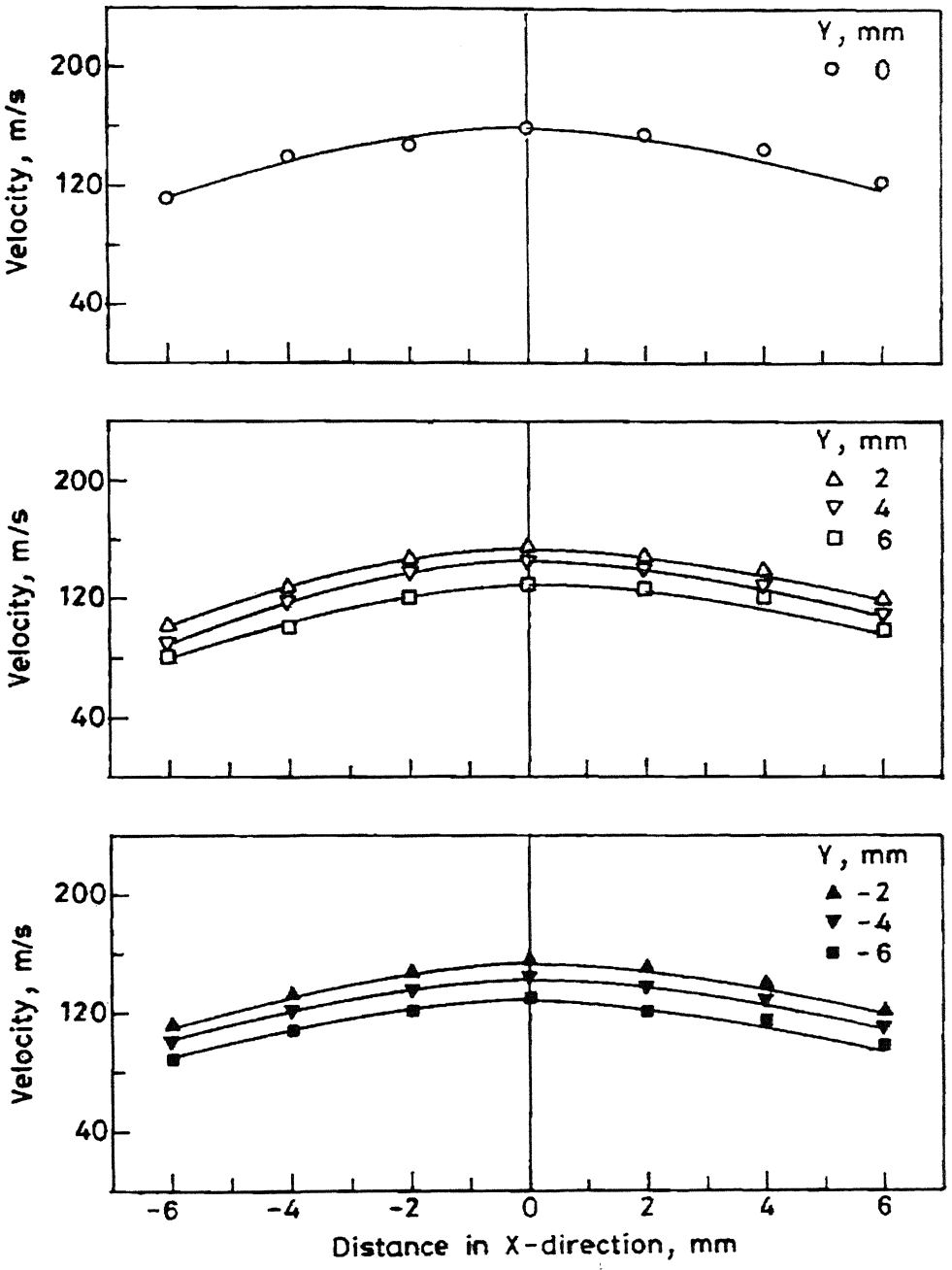

Figure 4.2.13 Variation of gas velocity on the XY plane of gas field situated at Z = 40 mm.

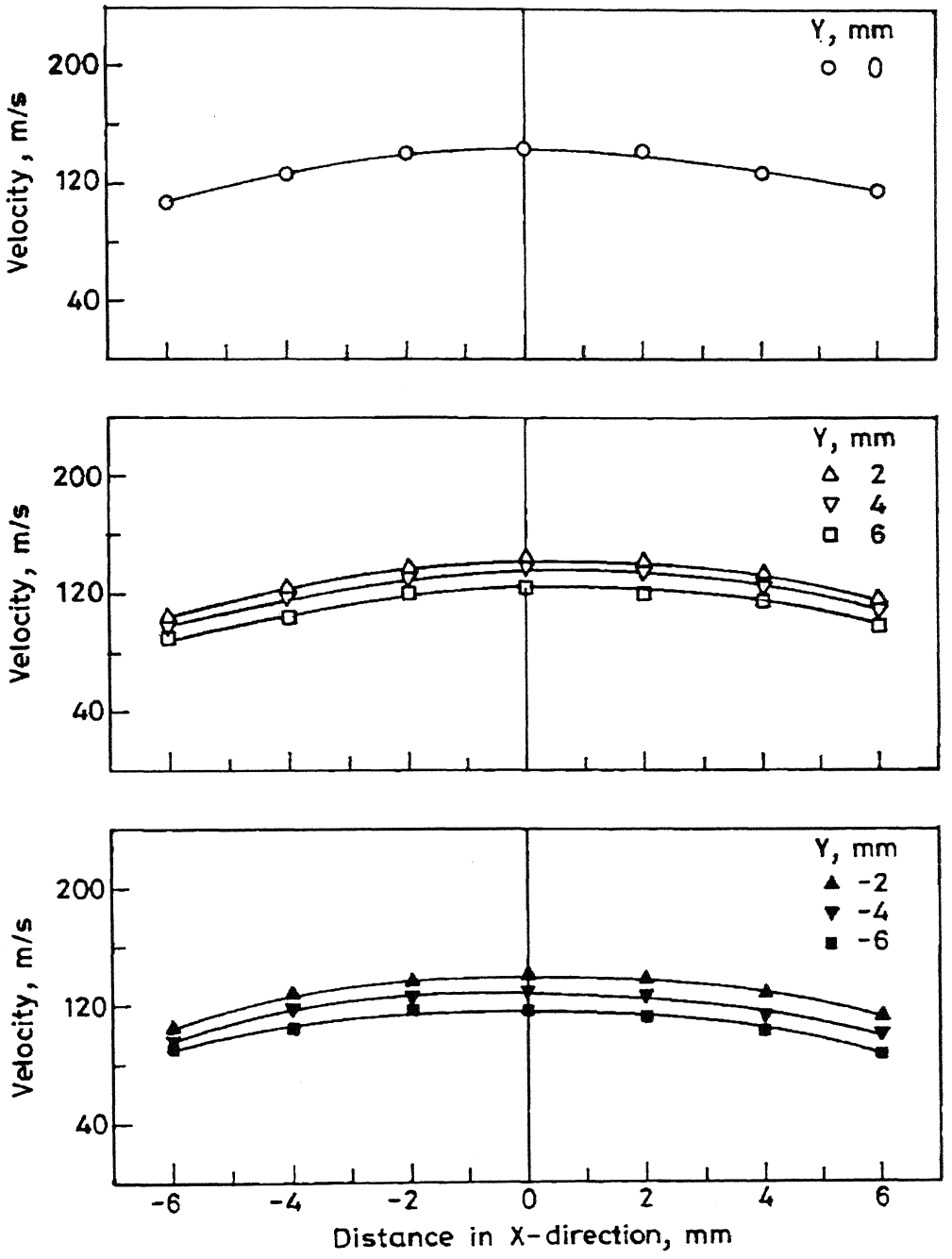

Figure 4.2.14 Variation of gas velocity on the XY plane of gas field situated at Z = 50 mm.

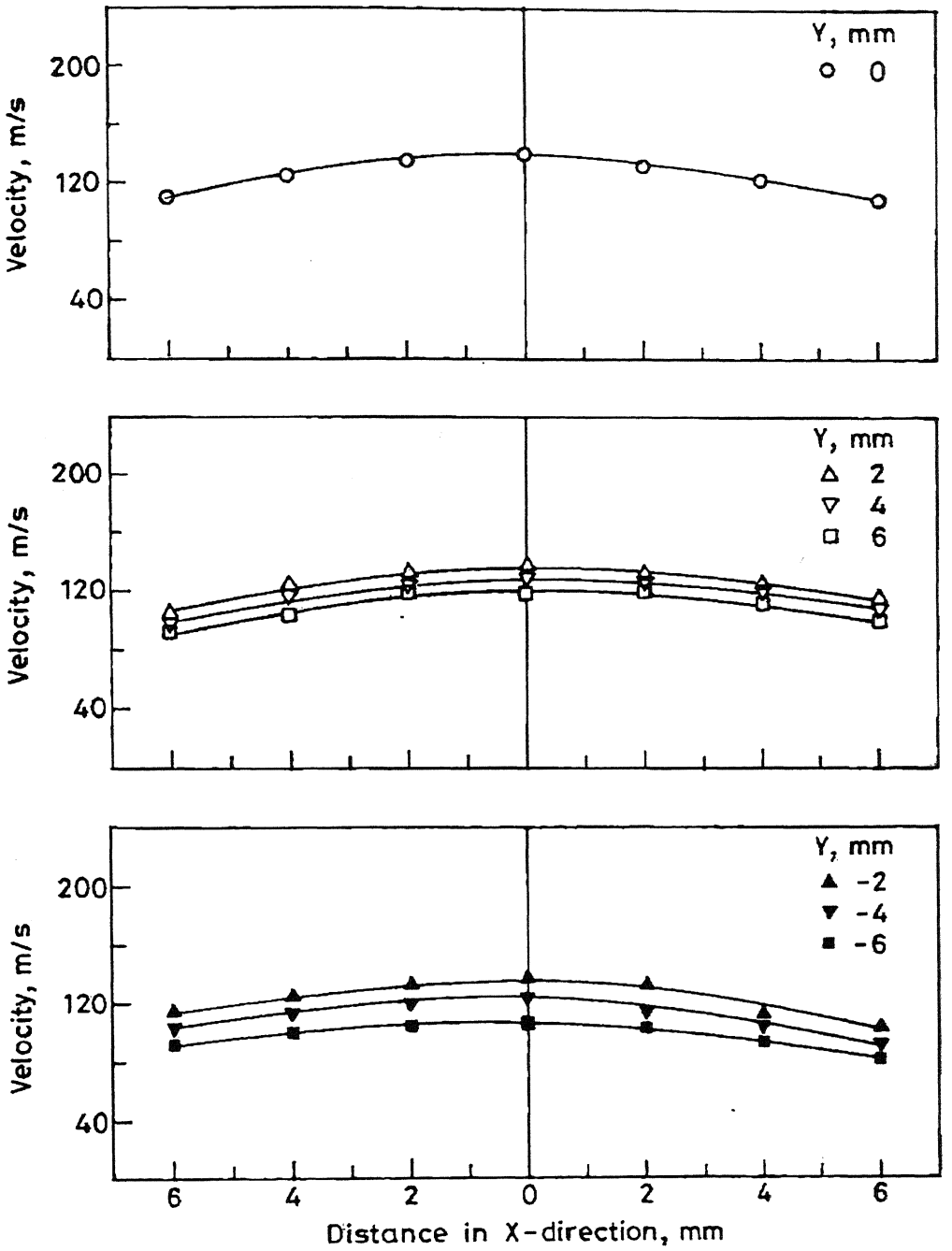

Figure 4.2.15 Variation of gas velocity on the XY plane of gas field situated at Z = 60 mm

It can be seen that the velocity is different at different points on the XY planes as seen in case of 800 kPa plenum pressure. In this representation iso-velocity lines for velocity of 160 m/s, have been shown. Figures 4.2.16 to 4.2.22 show the iso-velocity lines for velocity of 160 m/s at plenum pressure of 1000 kPa.

From above figures the following observations can be made:

1. The region up to which the gas velocity is 160 m/s is maximum for the XY plane situated at Z = 0 i.e. passing through the geometric point. The extent of this region decreases with increase in Z both in positive and negative directions.
2. The region up to which the gas velocity is 160 m/s was not found below the Z = 30 mm.
3. The iso-velocity lines are in general symmetrical to the vertical line passing through the geometric point (same as in case 800 kPa).

4.3 Variation of velocity in the Gas Field produced at 1200 kPa plenum pressure:

Figures 4.3.1 to 4.3.7 show the variation of velocity on the XZ planes of gas field situated at Y = 0, ± 2 mm, ± 4 mm, ± 6 mm. In this representation velocity is plotted as a function of Z at different values of X varying in between – 6 mm and + 6 mm.

From all the above figures the following observations can be made:

1. The geometric point of an atomizer is situated at X=0, Y=0 and Z=0, the velocity of gas on the XZ plane situated at any value of Y, decreases with either increase in Z while keeping X constant or increase in X while keeping Z constant, both in positive or negative directions (Figure 4.3.1 to 4.3.7).
2. For any given value of either X or Y, the decrease in velocity with increase in Z is faster when the value of Z is negative as compared when Z is positive (Figure 4.3.1b). The impingement of jets at the geometric point causes the downward flow of the gas at a rate faster than the upward flow. Thus the entrainment of the surrounding air into the downward flow of the gas occurs slowly as compared with into the upward flow of gas.

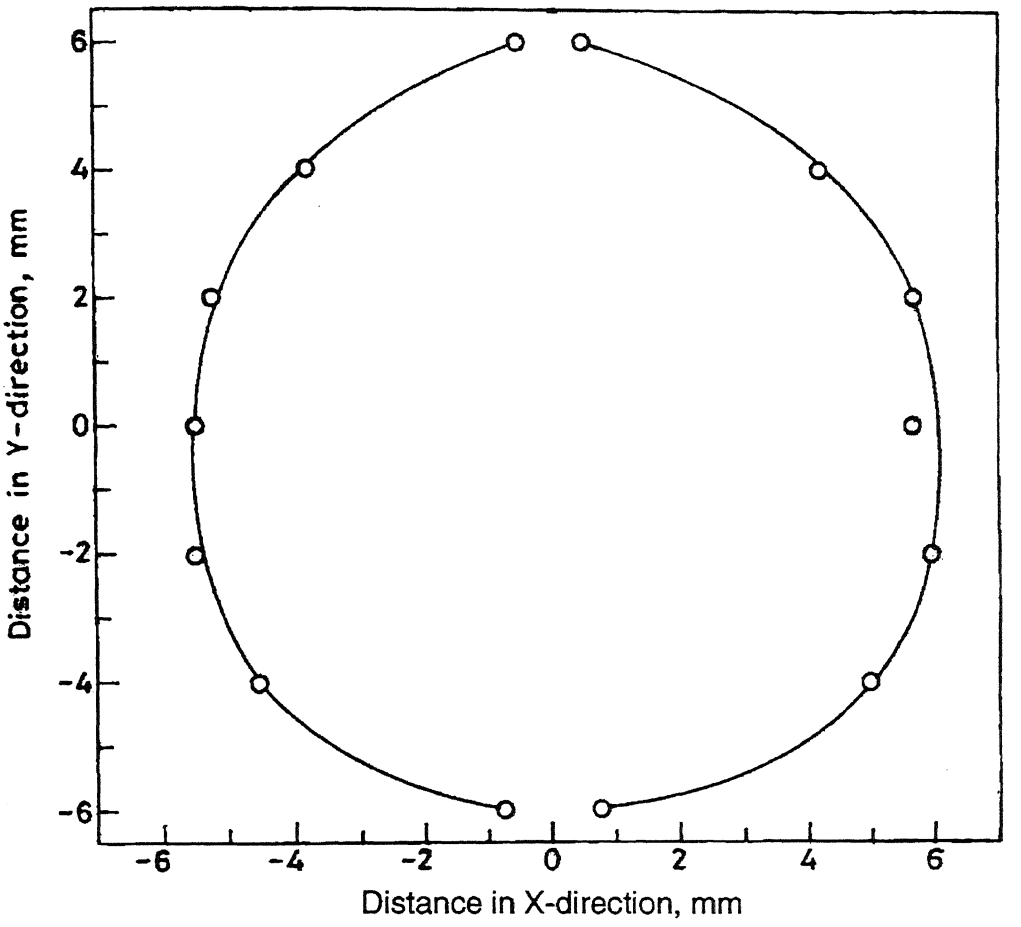

Figure 4.2.16 Iso-velocity line for the velocity of 160 m/s on the XY plane situated at Z=0.

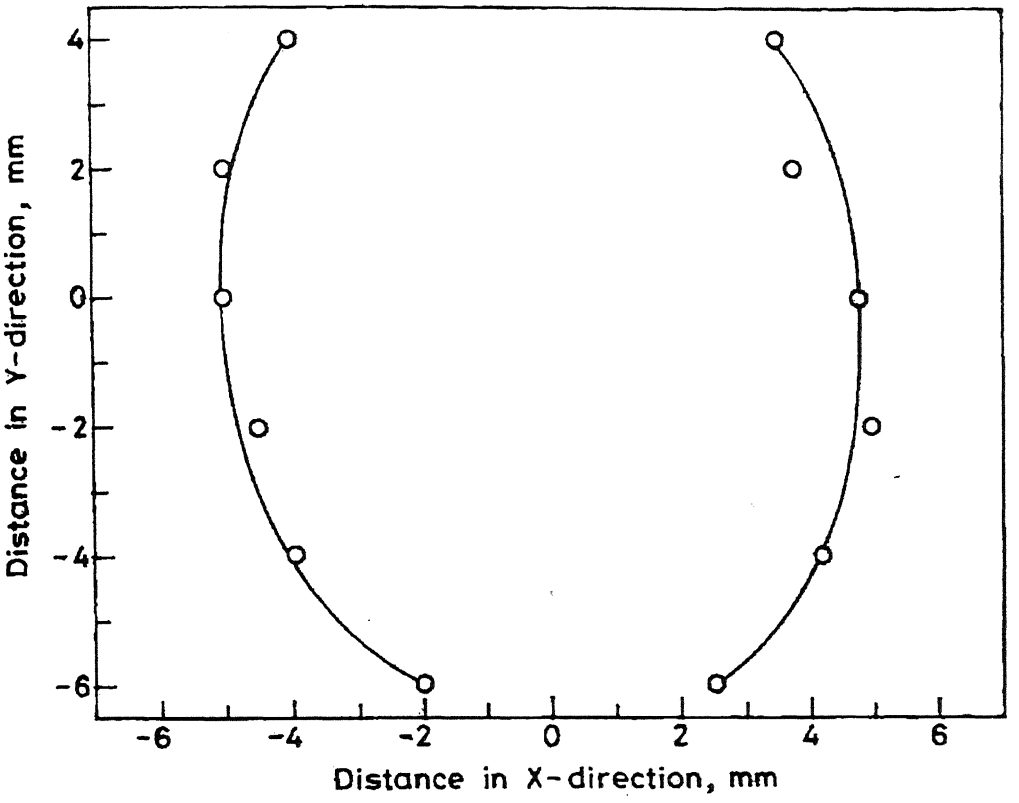

Figure 4.2.17 Iso- velocity line for the velocity of 160 m/s on the XY plane situated at Z=10 mm.

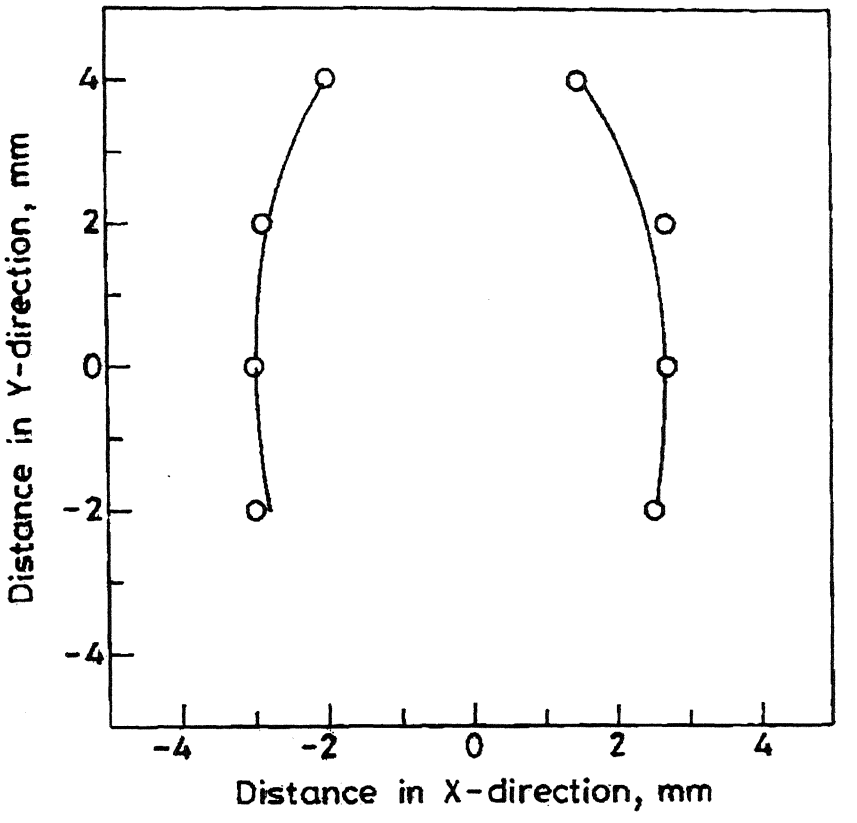

Figure 4.2.18 Iso-velocity line for the velocity of 160 m/s on the XY plane situated at Z= - 10 mm.

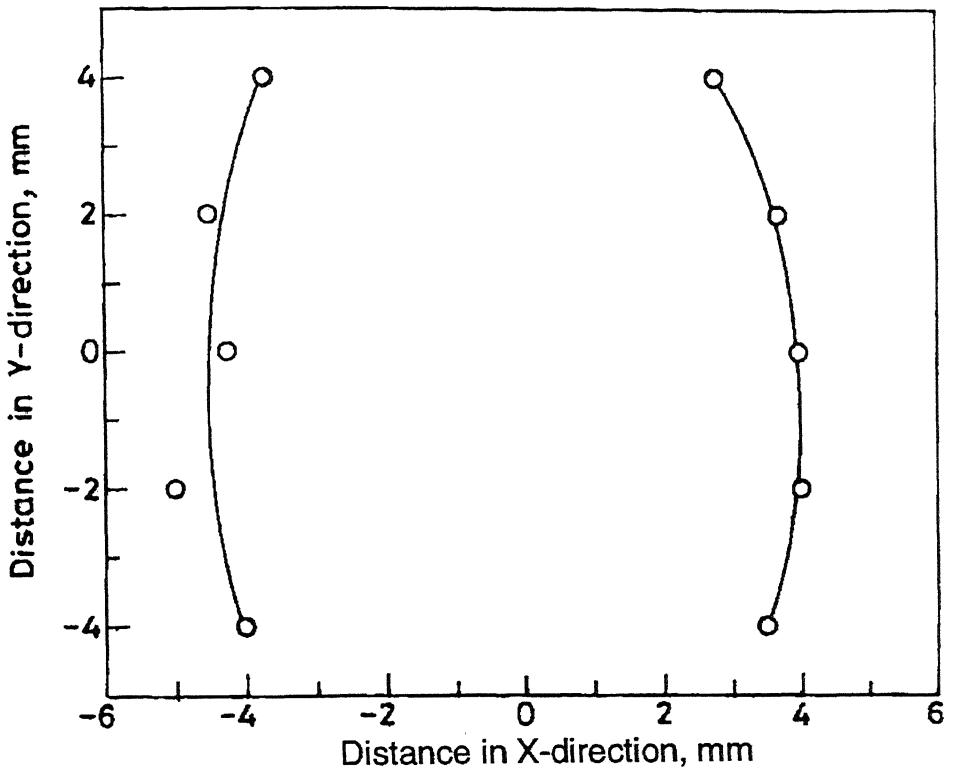

Figure 4.2.19 Iso-velocity line for the velocity of 160 m/s on the XY plane situated at Z= 20 mm.

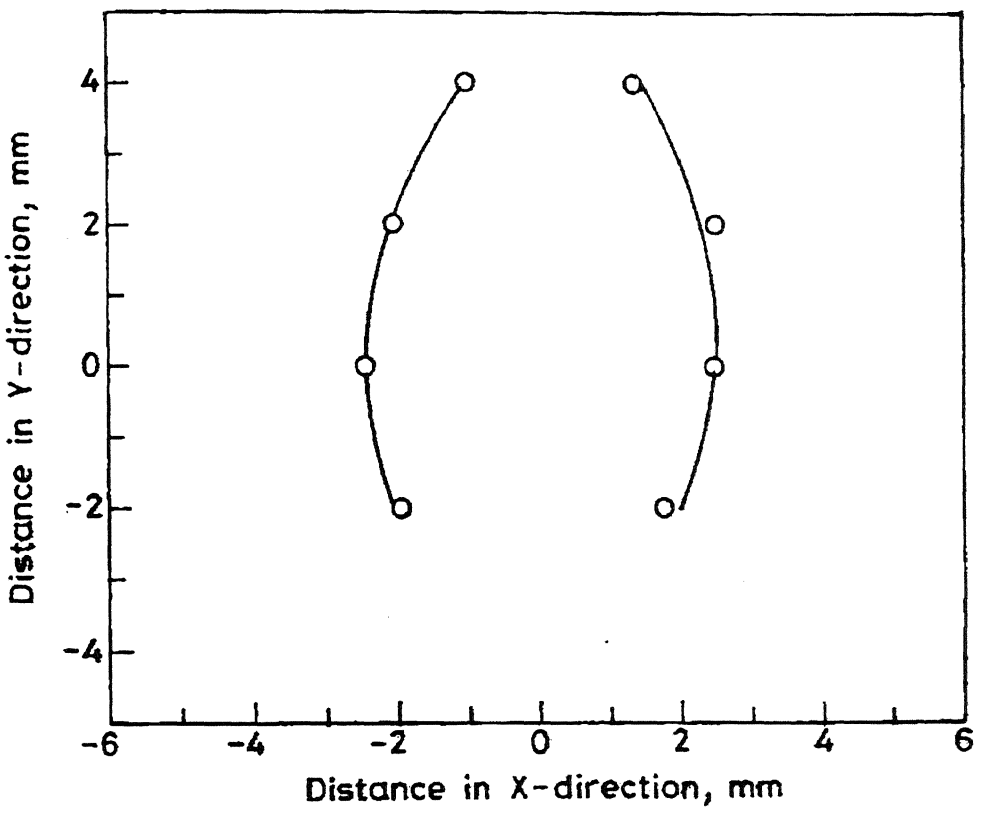

Figure 4.2.20 Iso-velocity line for the velocity of 160 m/s on the XY plane situated at Z=30 mm.

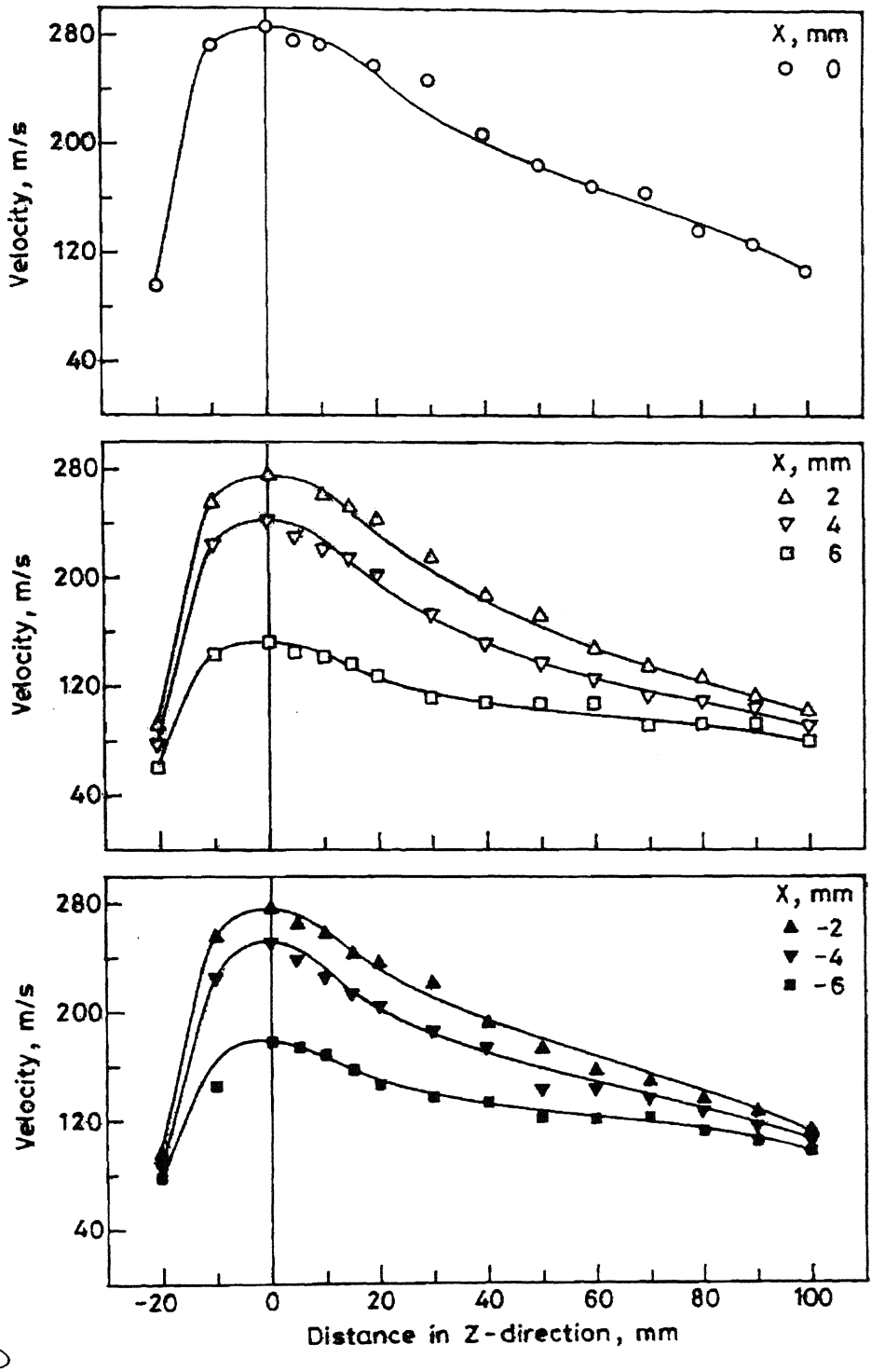

Figure 4.3.1 Variation of gas velocity on the XZ plane of gas field situated at Y =0.

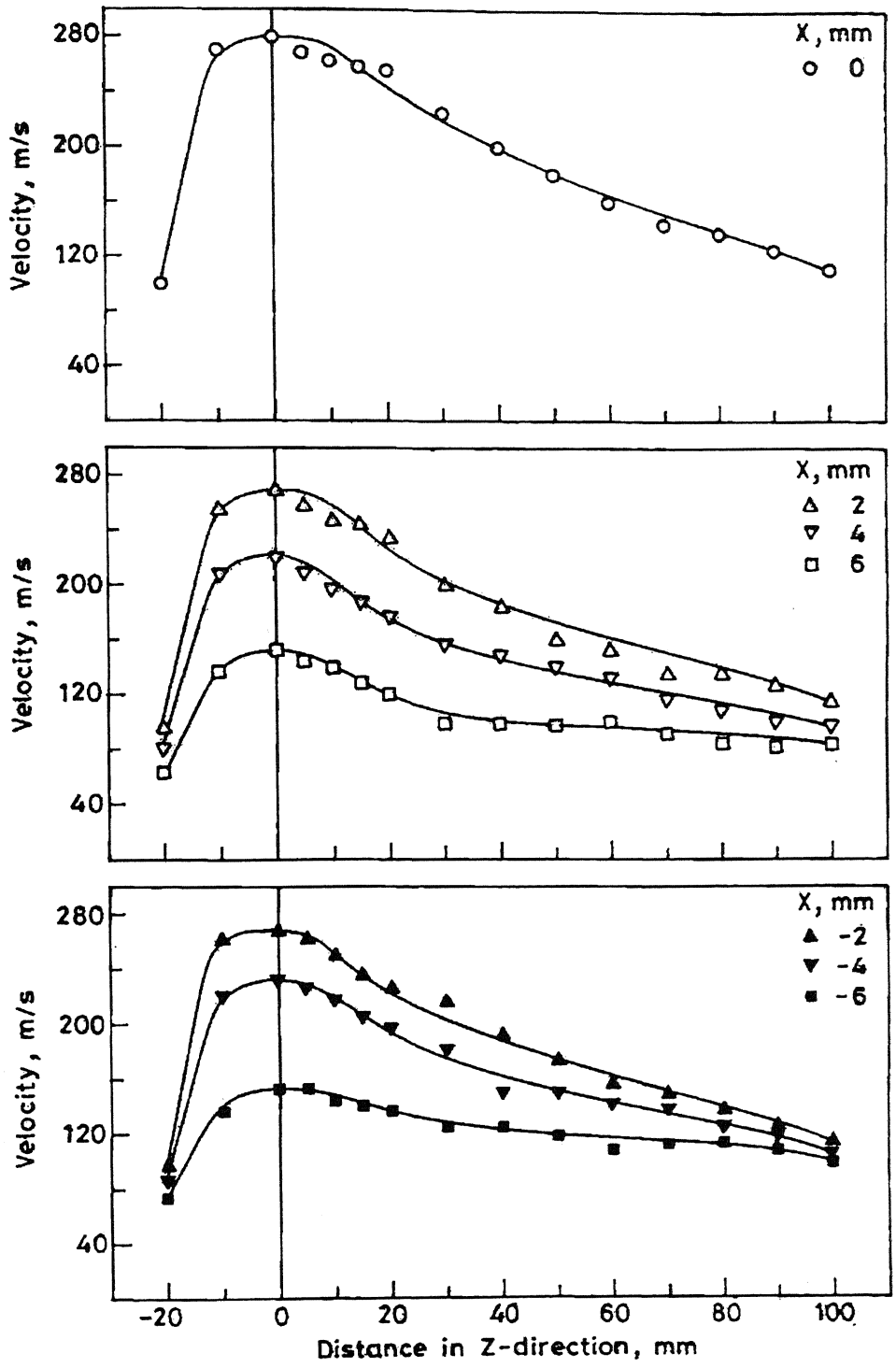

Figure 4.3.2 Variation of gas velocity on the XZ plane of gas field situated at Y = 2 mm.

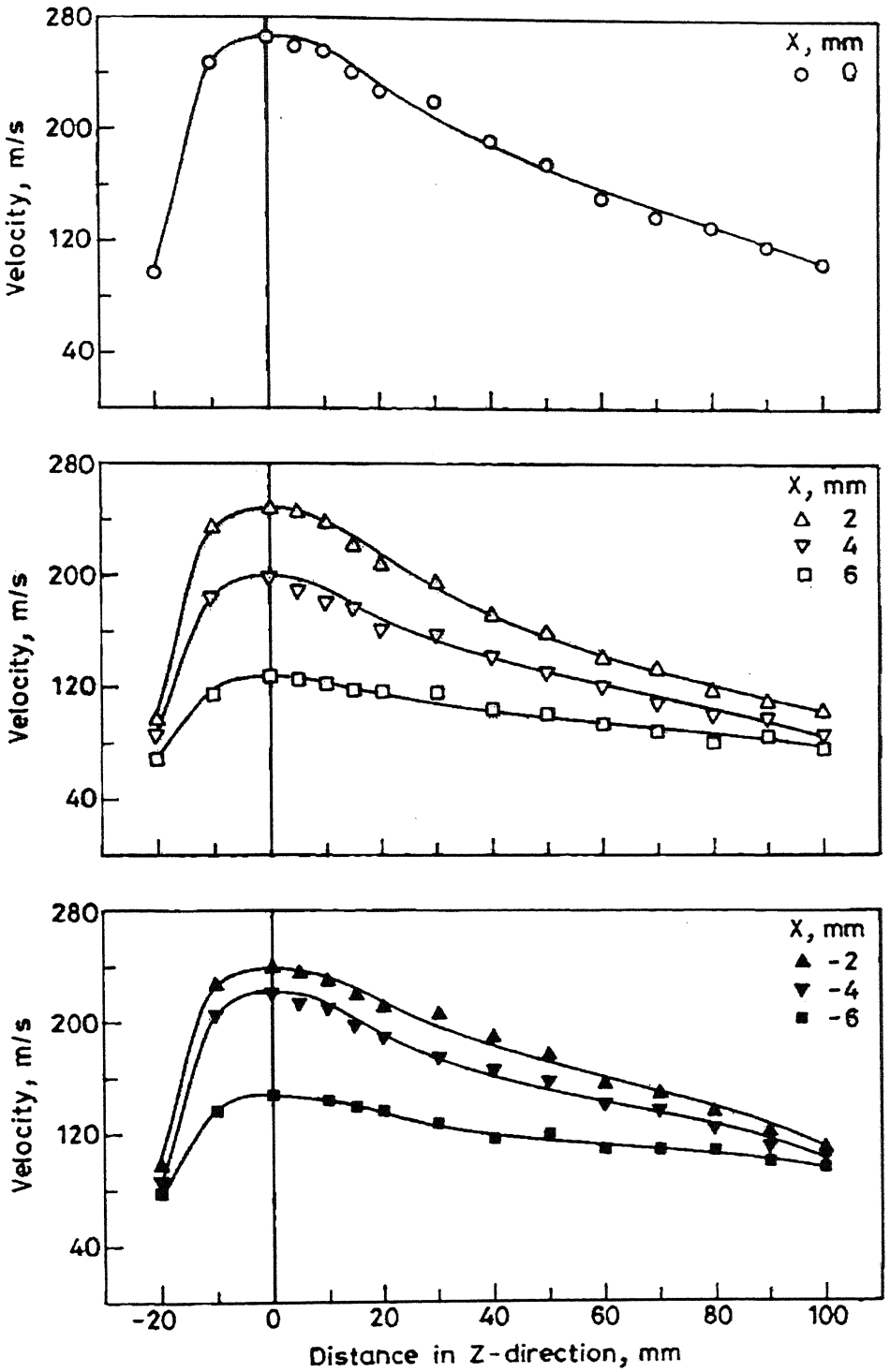

Figure 4.3.3 Variation of gas velocity on the XZ plane of gas field situated at Y = - 2 mm

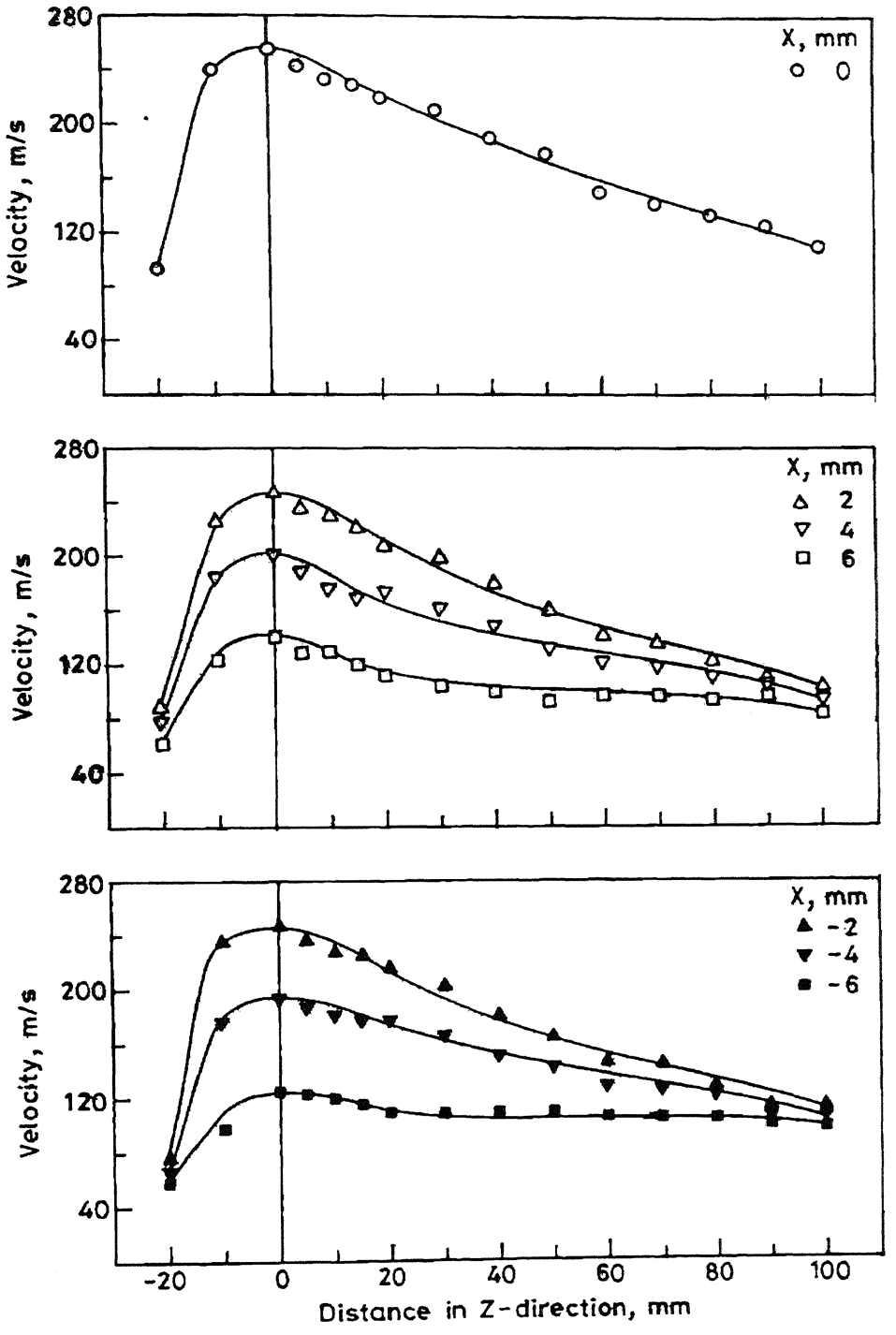

Figure 4.3.4 Variation of gas velocity on XZ plane of gas field situated at Y = 4 mm.

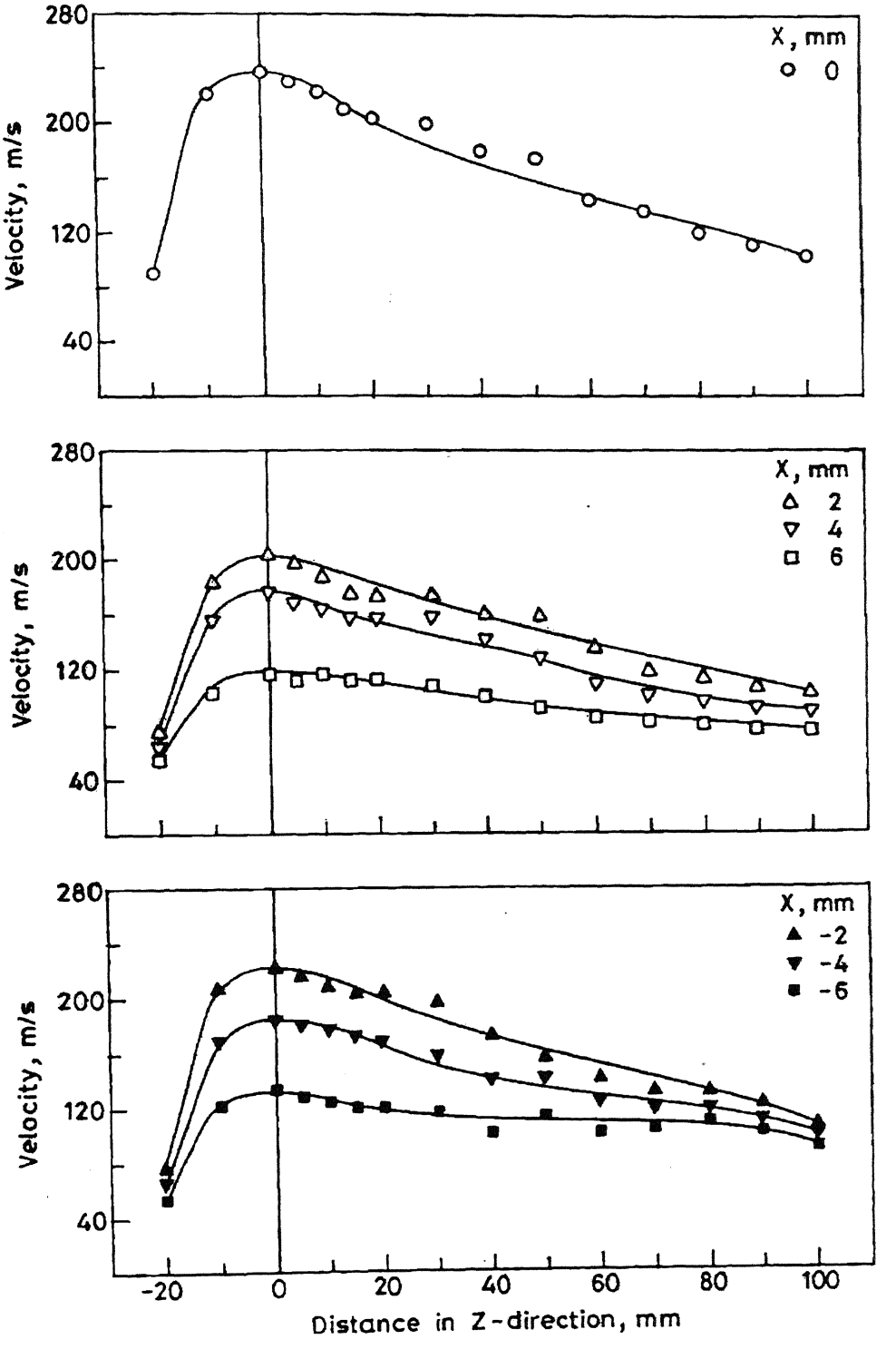

Figure 4.3.5 Variation of gas velocity on the XZ plane of gas field situated at Y= - 4 mm.

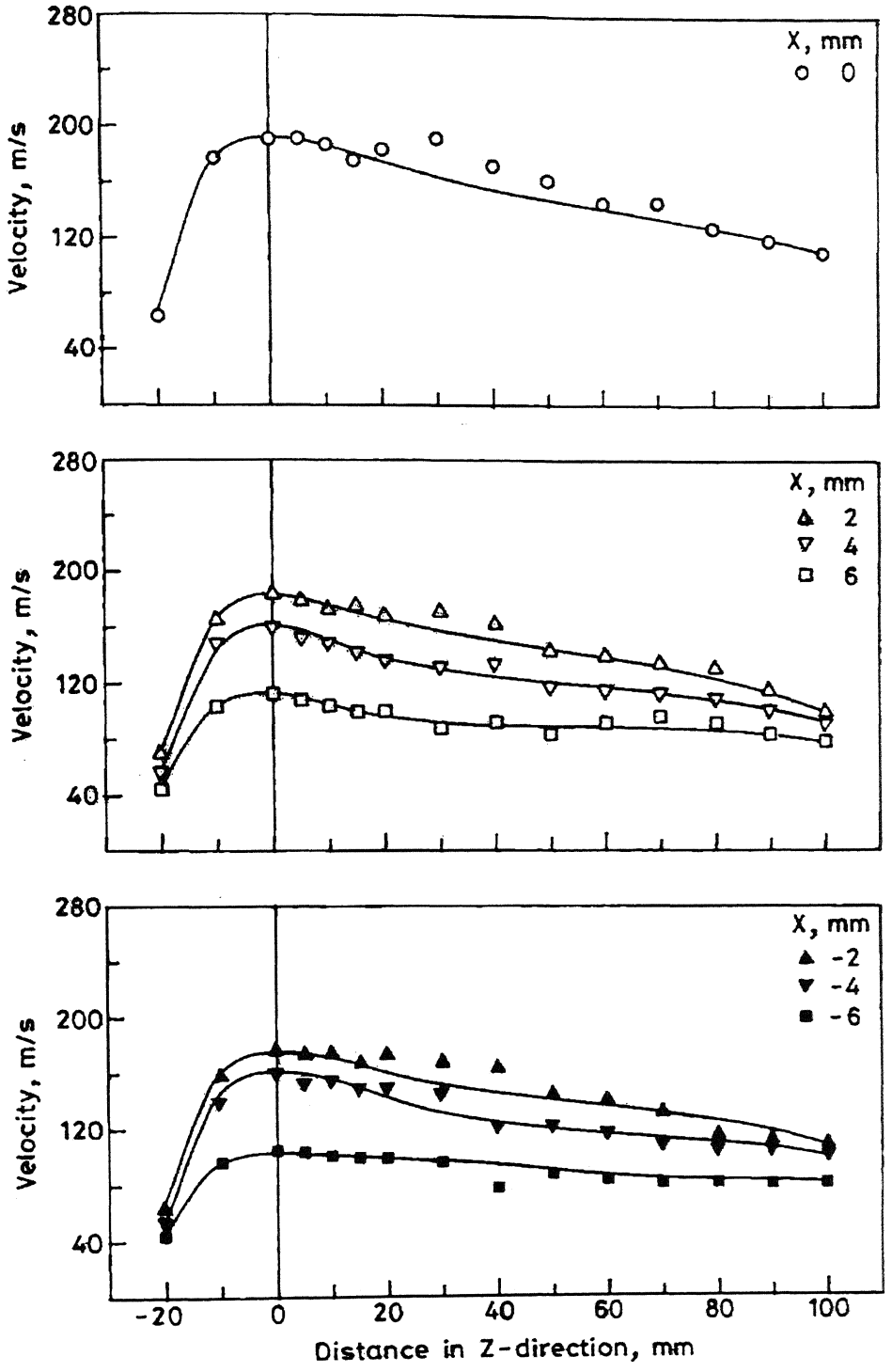

Figure 4.3.6 Variation of gas velocity on the XZ plane of gas field situated at Y = 6 mm

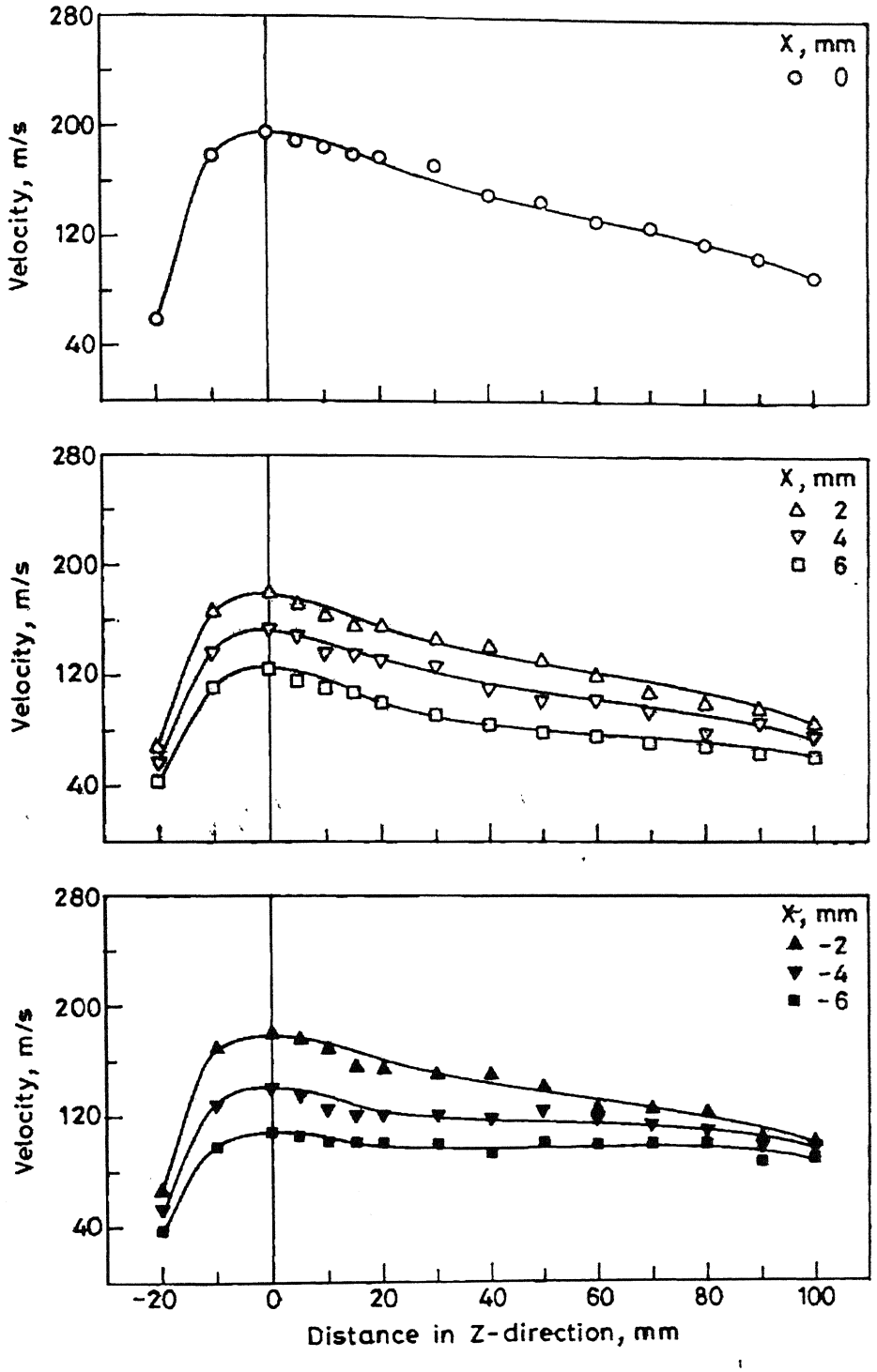

Figure 4.3.7 Variation of gas velocity on the XZ plane of gas field situated at Y = -6 mm

3. For any given value of Y and Z, increase in X either in positive or negative direction for all values of Z decreases the velocity of gas in the gas field (Figure 4.3.1a and 4.3.1b to 4.3.7a and 4.3.7b).
4. Increase in the value of Y both in positive or negative directions, decreases the velocities both in X and Z directions. The extent of decrease depends on the value of Y.

For example at Y=0 the velocity of gas at X=0 and Z=0 is 284 m/s, which is almost same at Y=2 mm but decreases to 188 m/s at Y= + 6 mm and to 195 m/s at Y= - 6 mm. Similar information can be obtained at other values of Y and different combinations of X and Z (Figure 4.3.1a, 4.3.2a, 4.3.3a, 4.3.4a, 4.3.5a, 4.3.6a and 4.3.7a).

Figures 4.3.8 to 4.3.15 show the variation of velocity on XY planes of gas field situated at Z= 0, ± 10 mm, 20 cm, 30 mm, 40 mm, 50 mm, 60 mm. In this representation velocity is plotted as a function of X at different values of Y varying in between – 6 mm and + 6 mm.

From Figures 4.3.8 to 4.3.15 the following observations have been made:

1. The velocity of gas on the XY plane, situated at any value of Z, decreases with either increase in X while keeping Y constant, or increase in Y while keeping X constant both in positive and negative directions (Figure 4.3.8 to 4.3.15).
2. For any given value of either Y or Z, the rate of decrease in velocity with increase in X is similar in both the positive and negative directions. It is further observed that the curve on either side is almost symmetrical to each other (Figure 4.3.8 –4.3.15).
3. For any given value of Z and X, an increase in Y, either in positive or negative direction, decreases the velocity of gas in the gas field. For example at Z=0 the velocity of gas at X=2 mm and Y=0 is 276 m/s, but decreases to 180 m/s at Y= + 6 mm and to 176 m/s at Y= - 6 mm (Figure 4.3.8a and 4.3.8b). Similar observation can be obtained at other combinations of X and Y.
4. The increase in value of Z both in positive or negative directions decreases the velocity the velocities both in Y and X directions.

It can be seen that the velocity is different at different points on the XY planes as seen in case of 800 kPa plenum pressure.

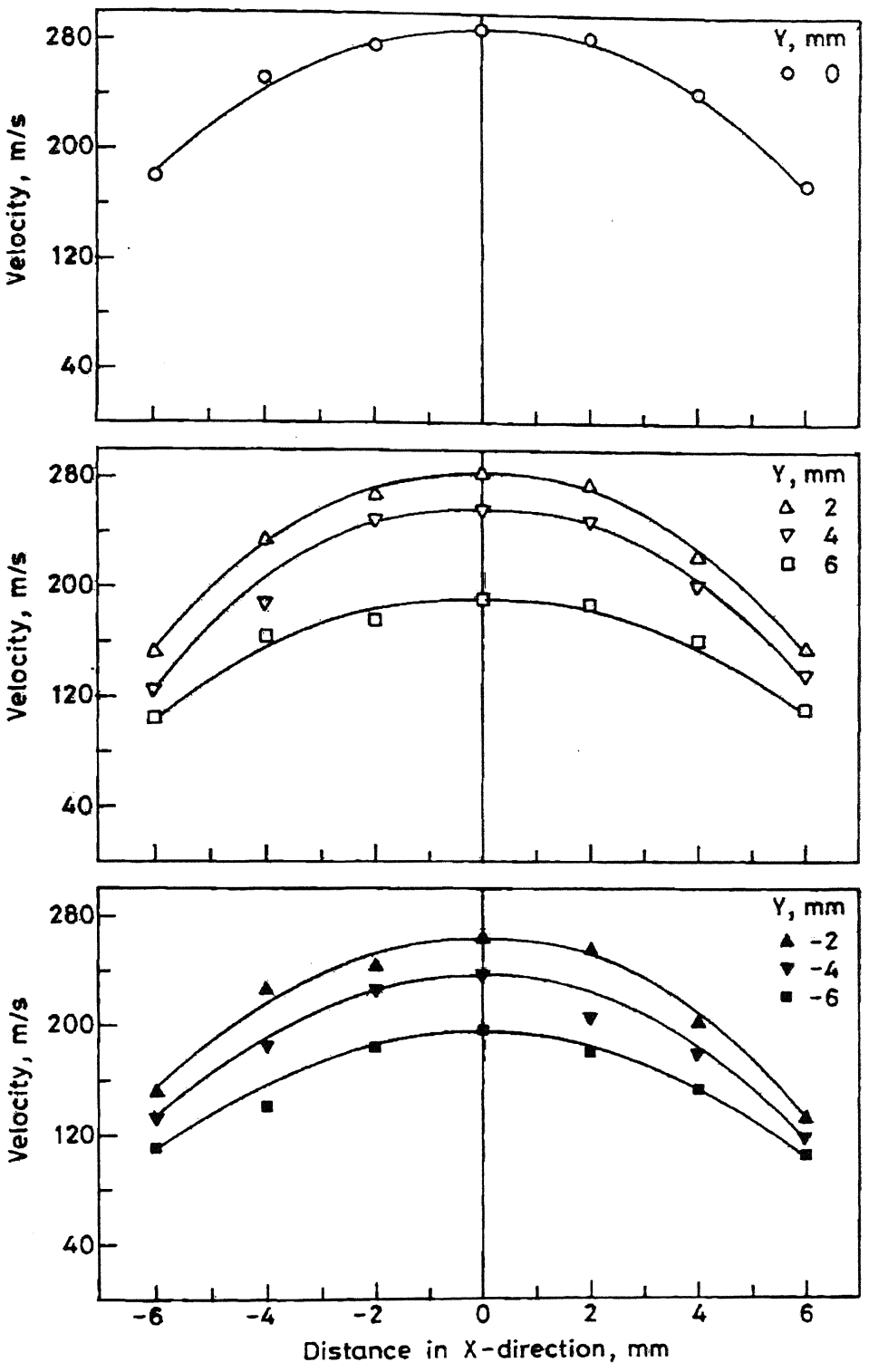

Figure 4.3.8 Variation of gas velocity on the XY plane of gas field situated at Z = 0.

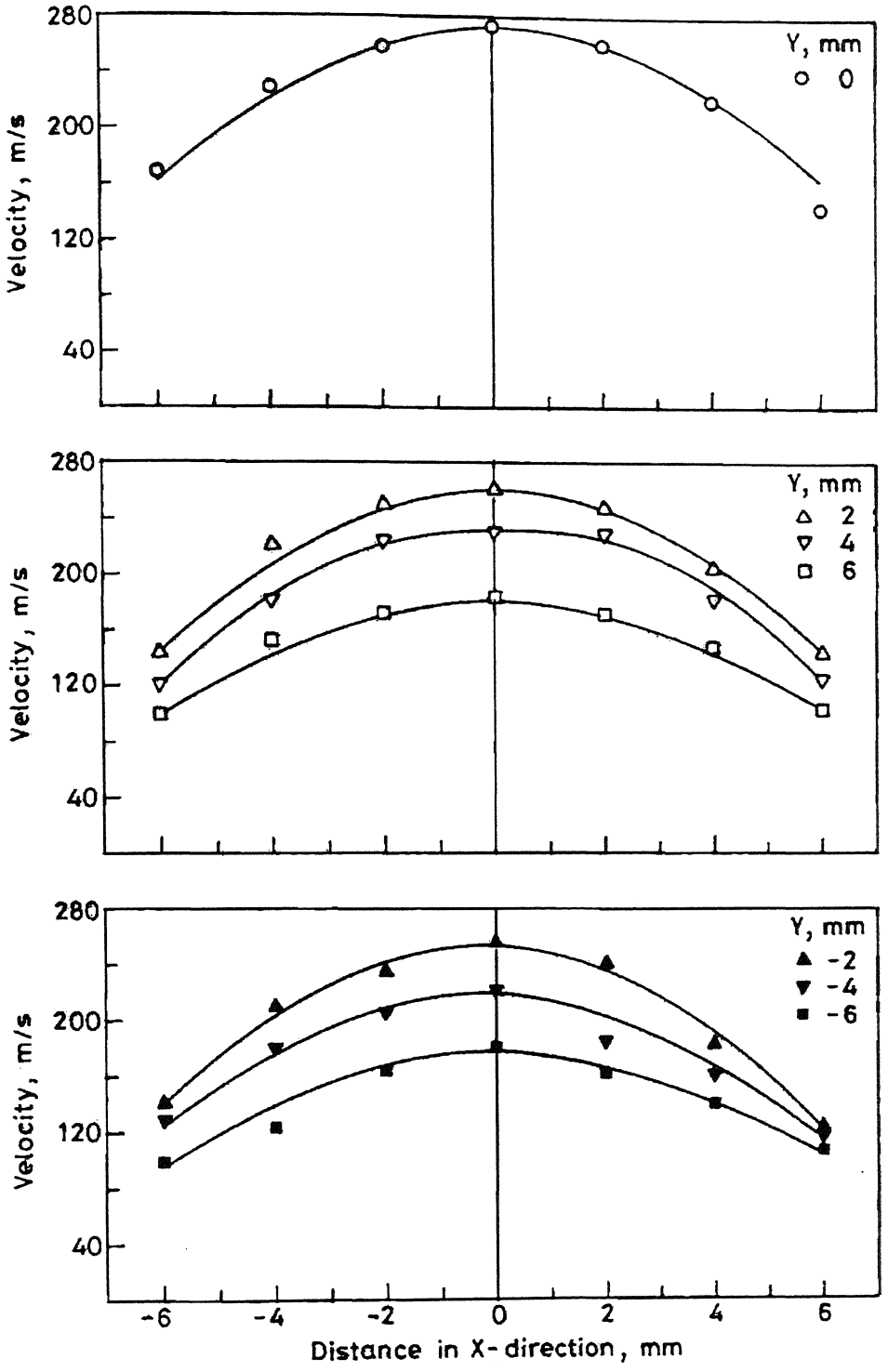

Figure 4.3.9 Variation of gas velocity on the XY plane of gas field situated at Z =10 mm.

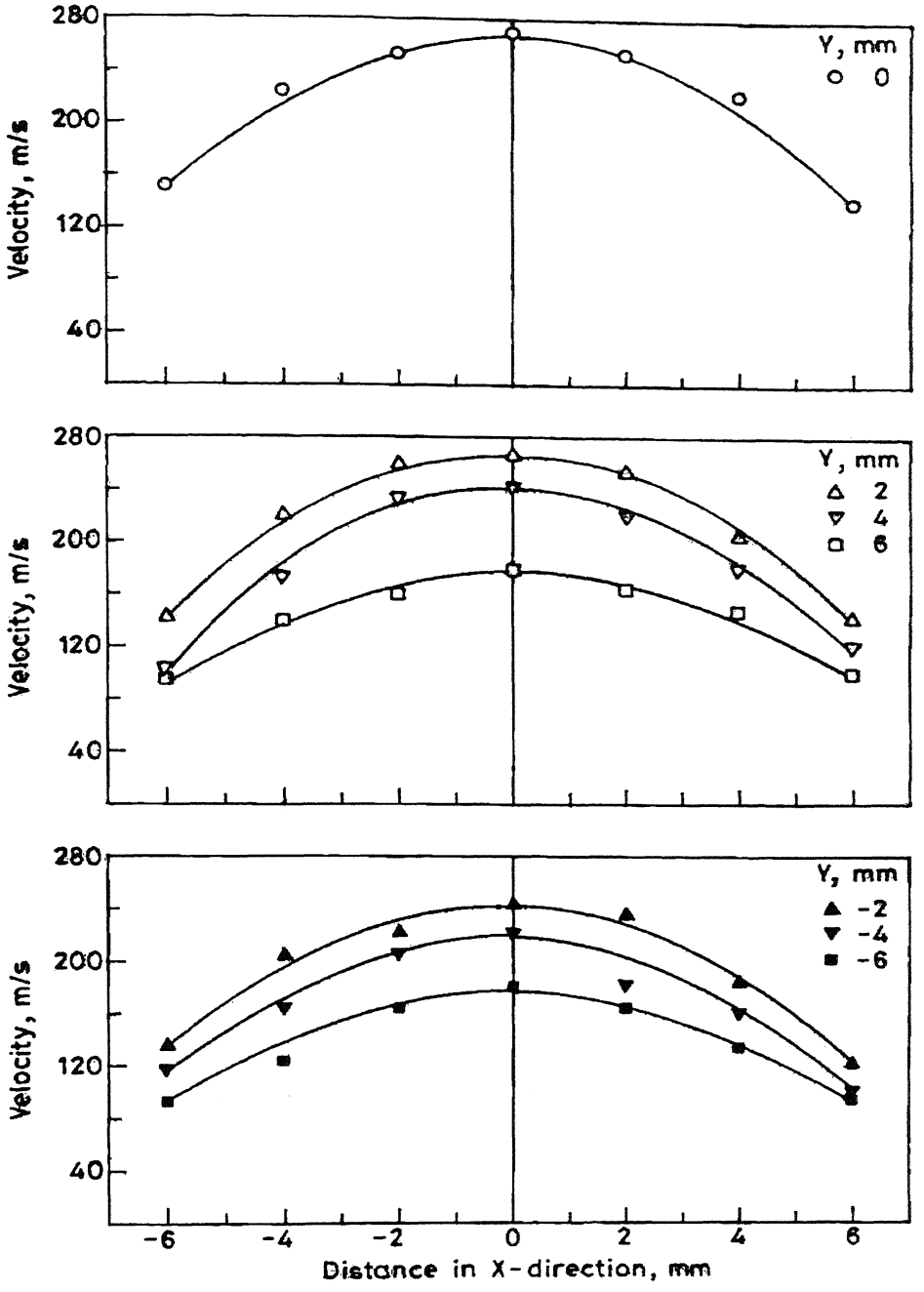

Figure 4.3.10 Variation of gas velocity on the XY plane of gas field situated at Z= -10 mm.

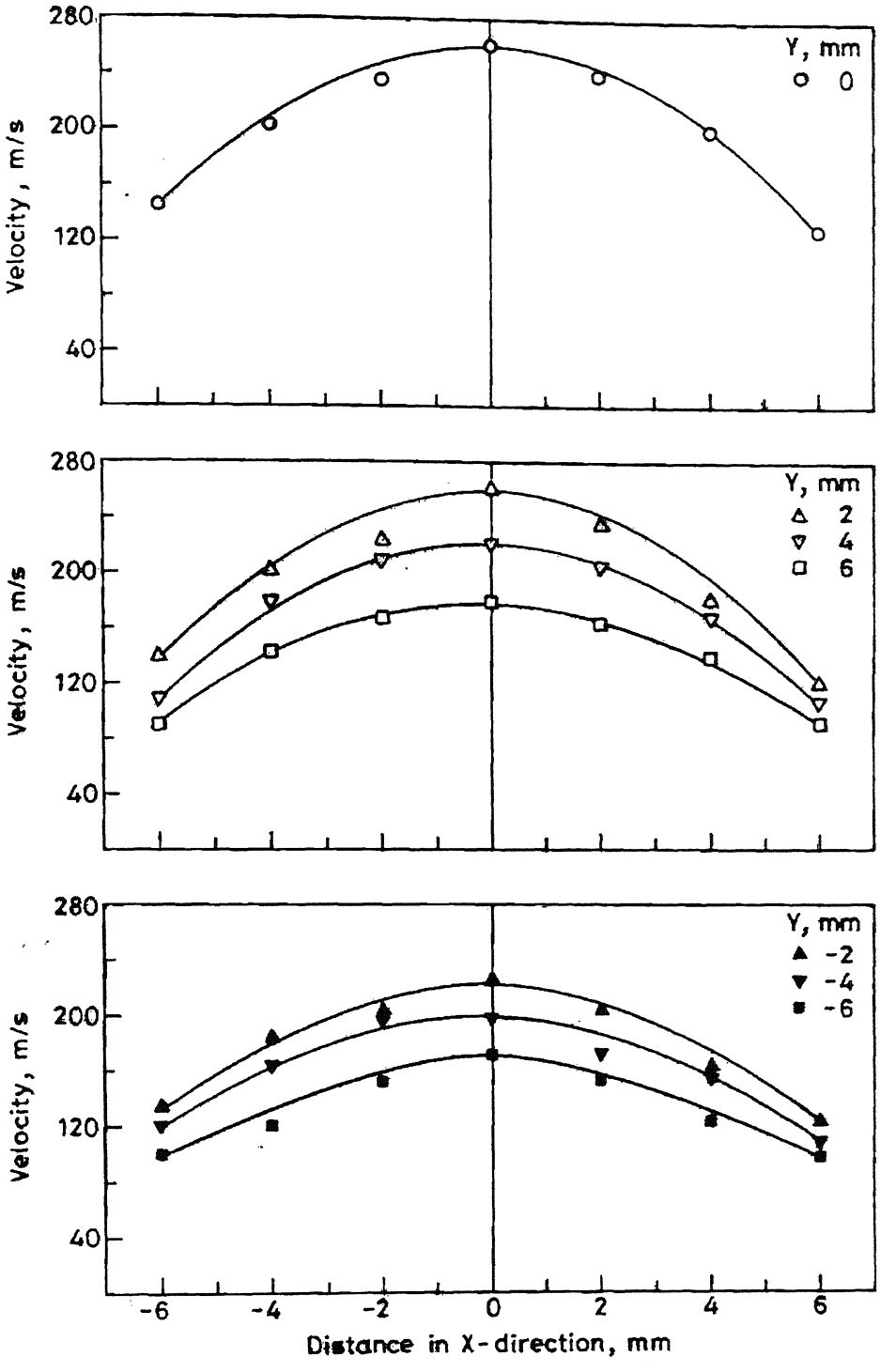

Figure 4.3.11 Variation of gas velocity on the XY plane of gas field situated at Z = 20 mm

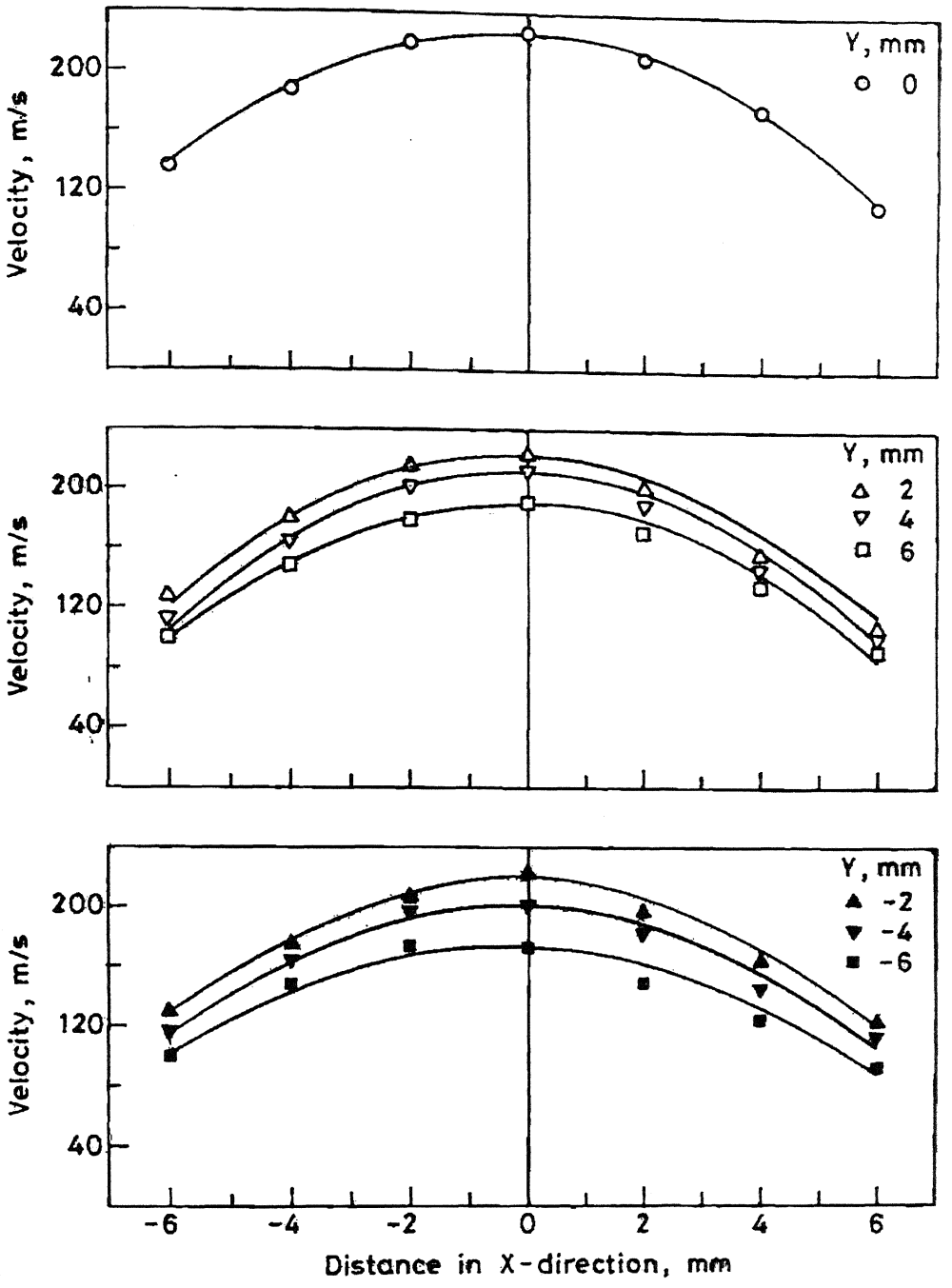

Figure 4.3.12 Variation of gas velocity on XY plane of gas field situated at Z= 30

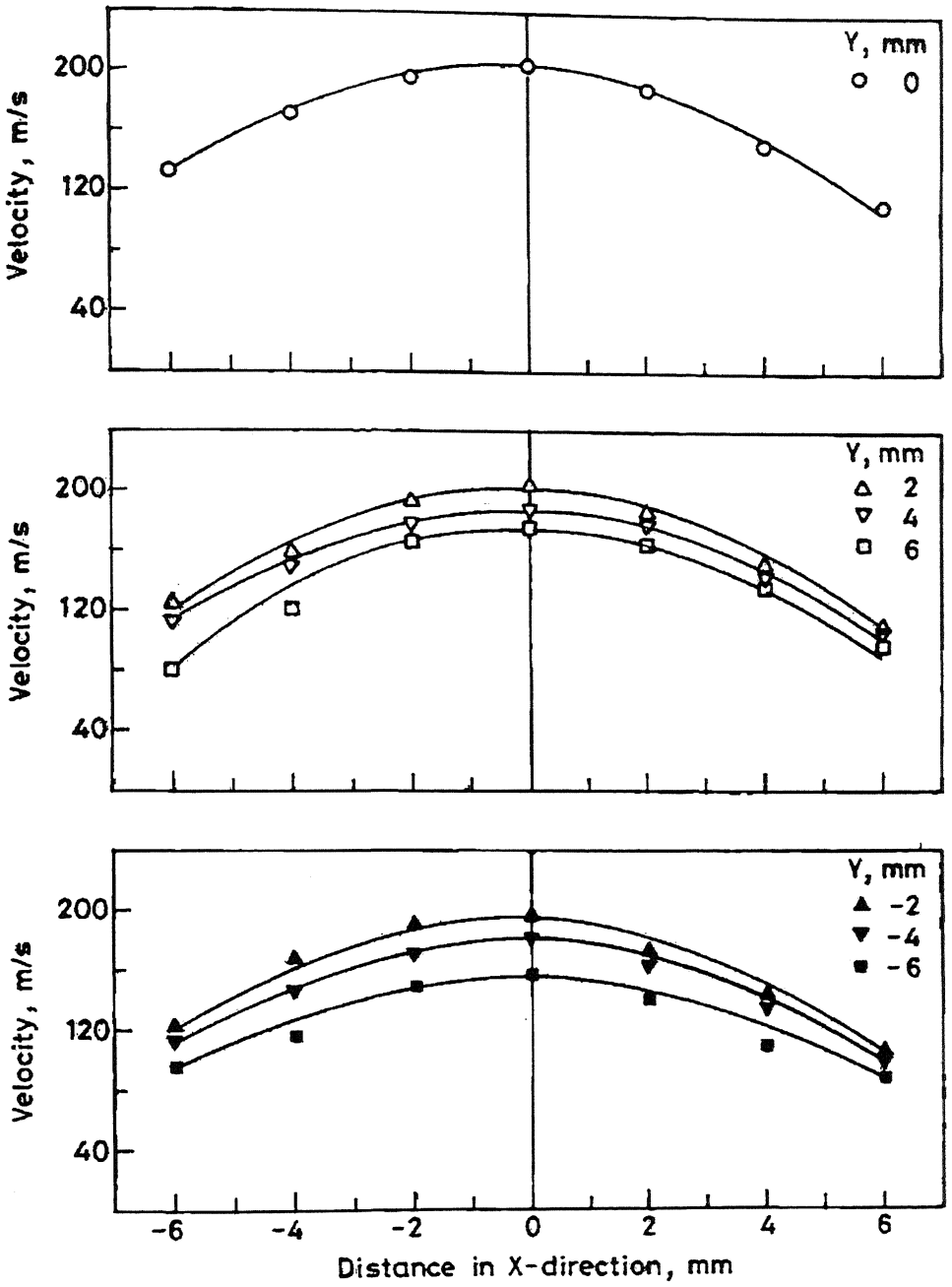

Figure 4.3.13 Variation of gas velocity on the XZ plane of gas field situated at Z = 40 mm

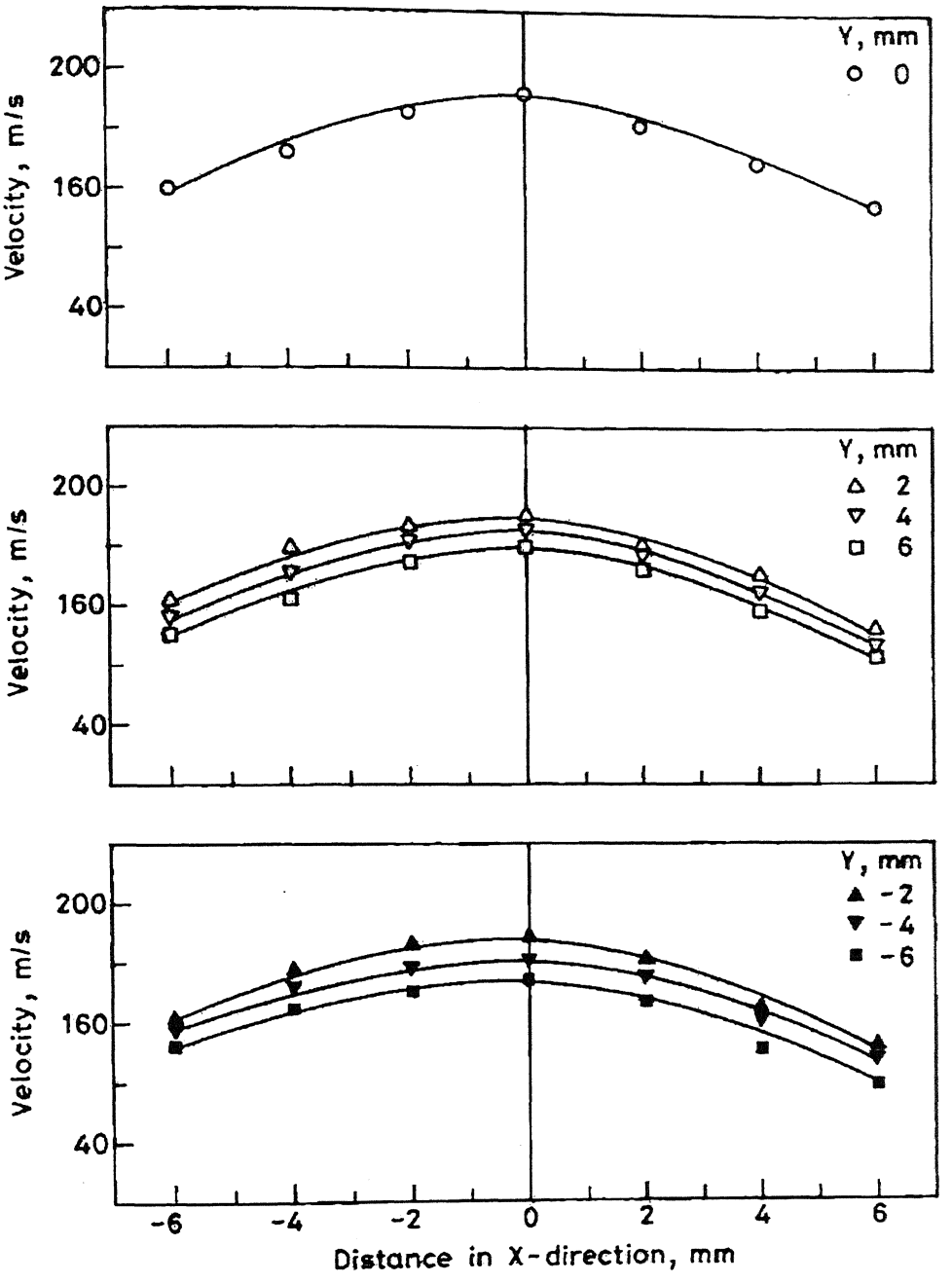

Figure 4.3.14 Variation of gas velocity on the XY plane of gas field situated at Z = 50 mm

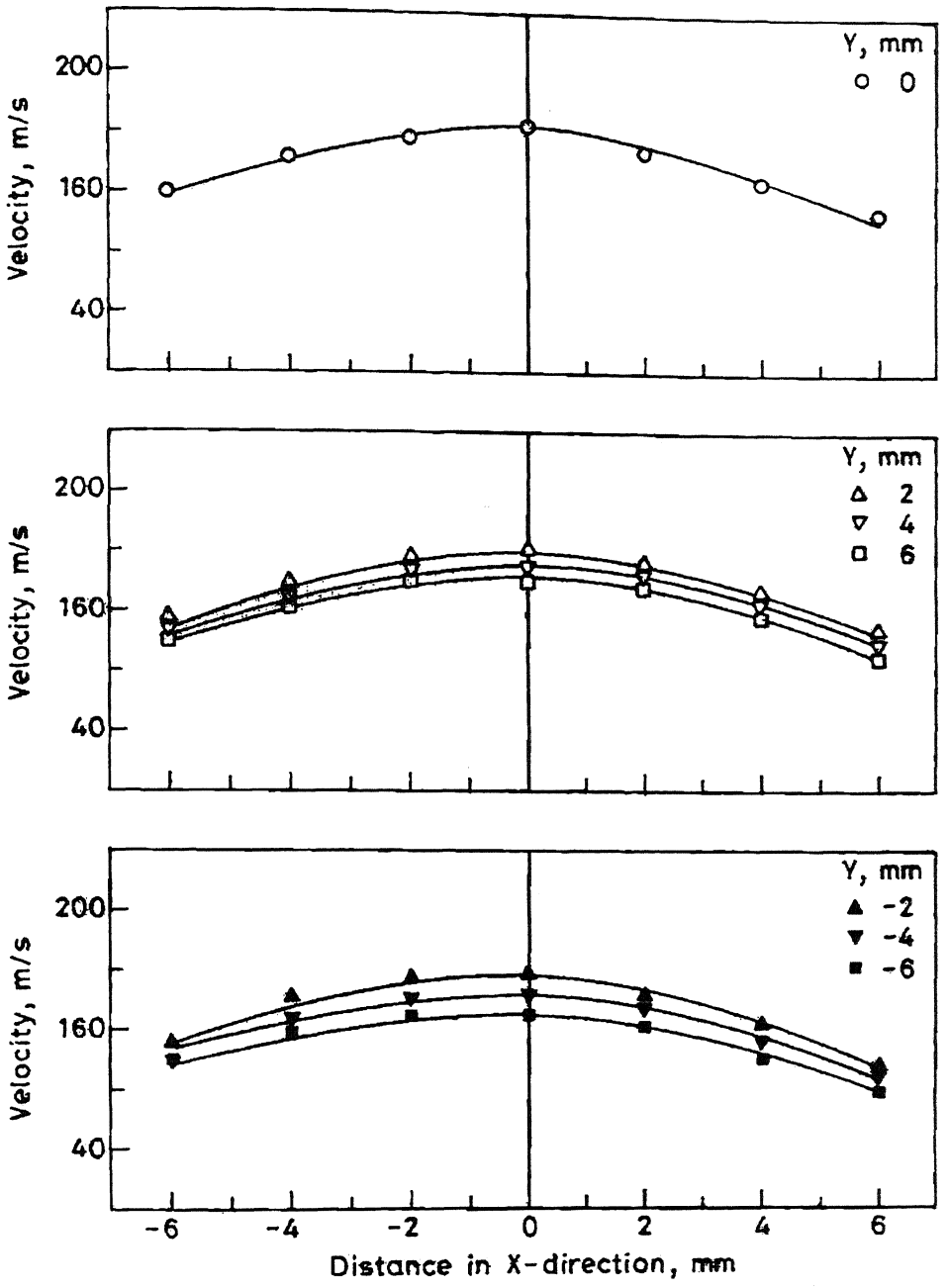

Figure 4.3.15 Variation of gas velocity on the XY plane of gas field situated at Z = 60 mm

In this representation iso-velocity lines for velocity of 160 m/s, have been shown. Figures 4.3.16 to 4.3.22 show the iso-velocity lines for velocity of 160 m/s at plenum pressure of 1200 kPa.

From above figures the following observations can be made:

1. The region up to which the gas velocity is 160 m/s is maximum for the XY plane situated at Z = 0 i.e. passing through the geometric point. The extent of this region decreases with increase in Z both in positive and negative directions.
2. The region up to which the gas velocity is 160 m/s was not found below the Z = 60 mm.
3. The isolines are in general symmetrical to the vertical line passing through the geometric point (same as in case 800 kPa and 1000 kPa).

4.4 Comparison of results obtained at various plenum pressures:

It can be seen from the above results that geometric point has different velocity at different pressures. Table 4.1 shows the gas velocities at different points on XY plane situated at Z = 0 as a functions of plenum pressure. From the table it is clear that with increase in plenum pressure, the gas velocity at geometric point increases. Further it can be seen that the velocity of gas decreases with either increase in X or Y in both directions. It is also clear from the iso-velocity lines plots that the region, up to which gas velocity is 160 m/s, increases with increase in plenum pressure at any given XY plane.

4.4 Importance of the present study for free fall gas atomization:

In the free fall atomization, the liquid metal stream falls freely up to a certain distance vertically downward before it is disintegrated in the gas field around the geometric point of an atomizer. The present study shows that the gas field around the geometric point at any given plenum pressure has a typical shape. Figure shows schematically a typical shape of iso-velocity lines for velocity 120 m/s, 140 m/s, and 160 m/s at plenum pressure of 1000 kPa on XZ plane situated at Y = 0. The same shape will be obtained on XY plane at X = 0.

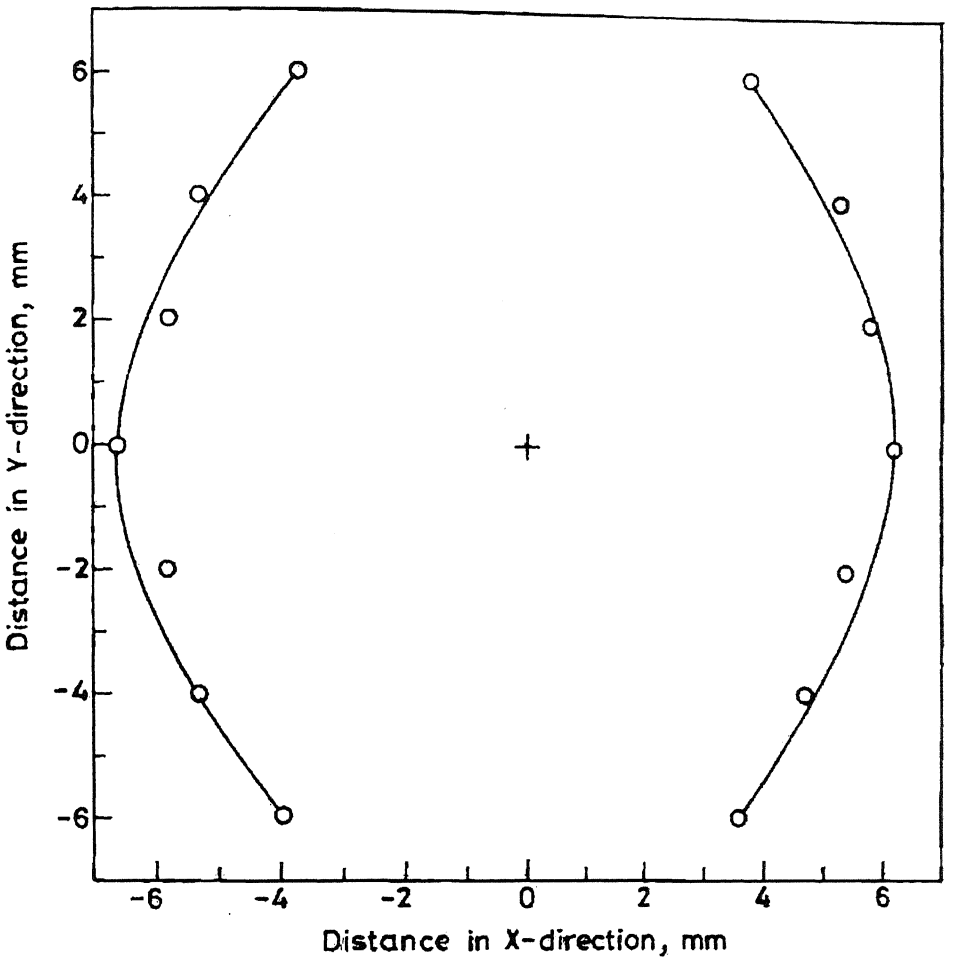

Figure 4.3.16 Iso-velocity line for the velocity of 160 m/s on the XY plane situated at Z=0.

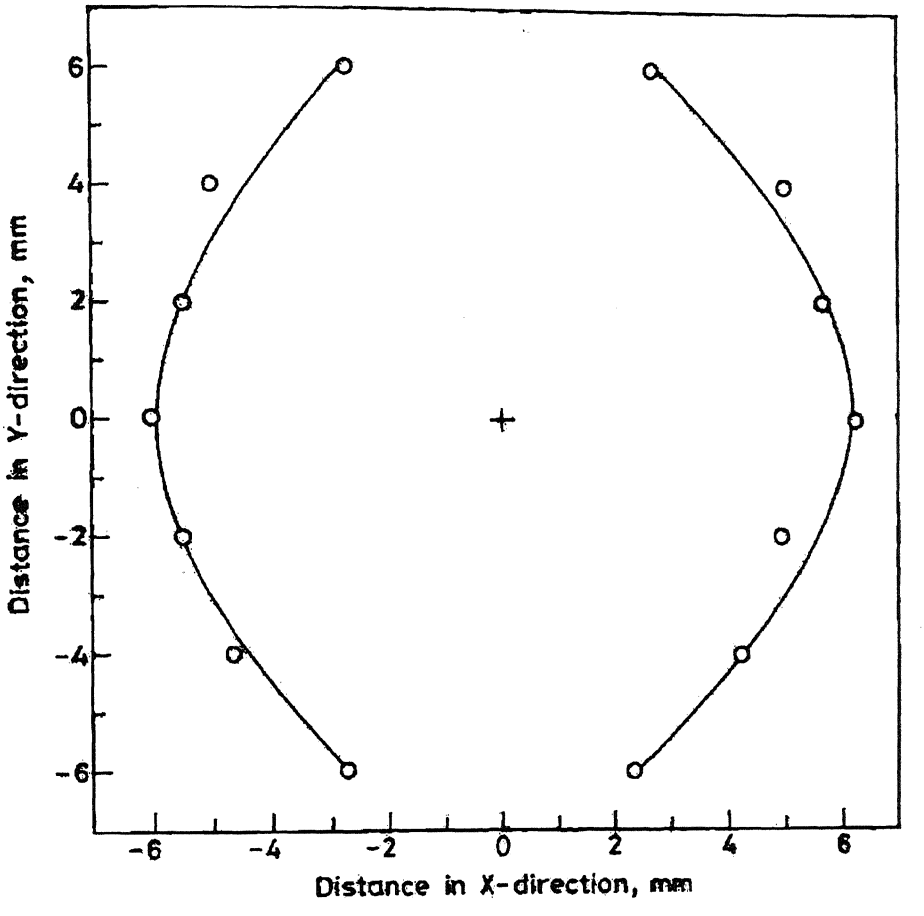

Figure 4.3.17 Iso-velocity line for the velocity of 160 m/s on the XY plane situated at Z=10 mm

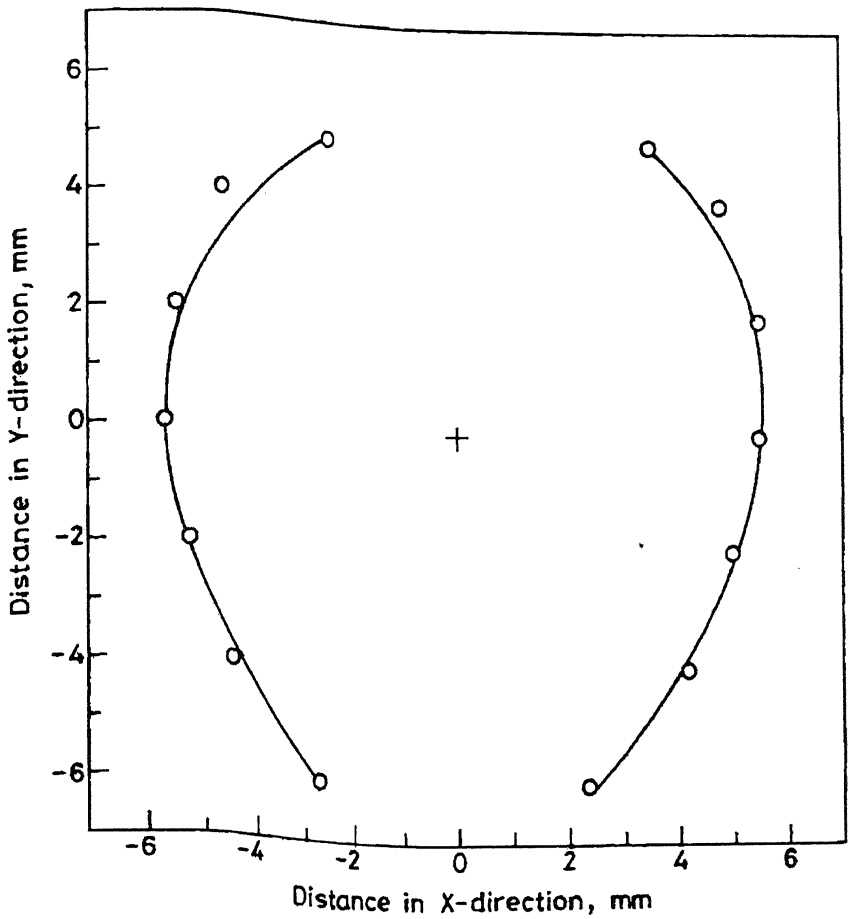

Figure 4.3.18 Iso-velocity line for the velocity of 160 m/s on the XY plane situated at Z= -10 mm.

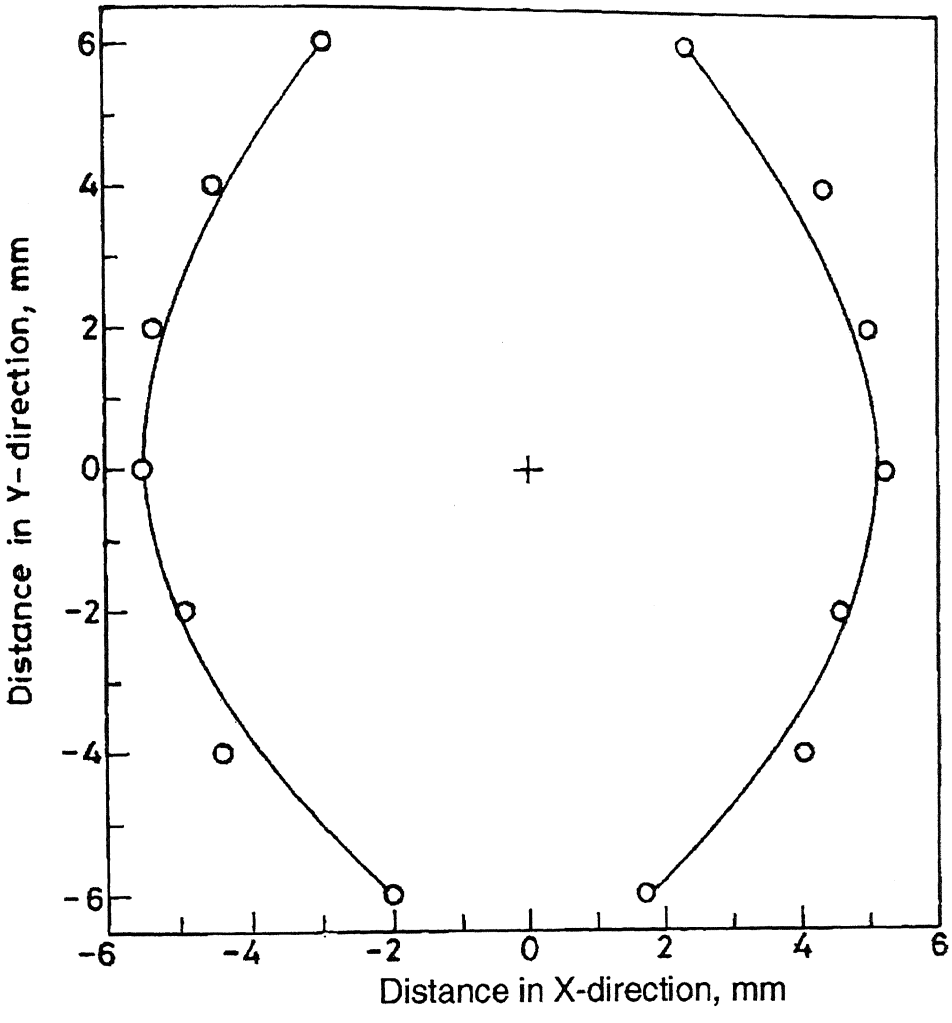

Figure 4.3.19 Iso-velocity line for the velocity of 160 m/s on the XY plane situated at Z=20 mm

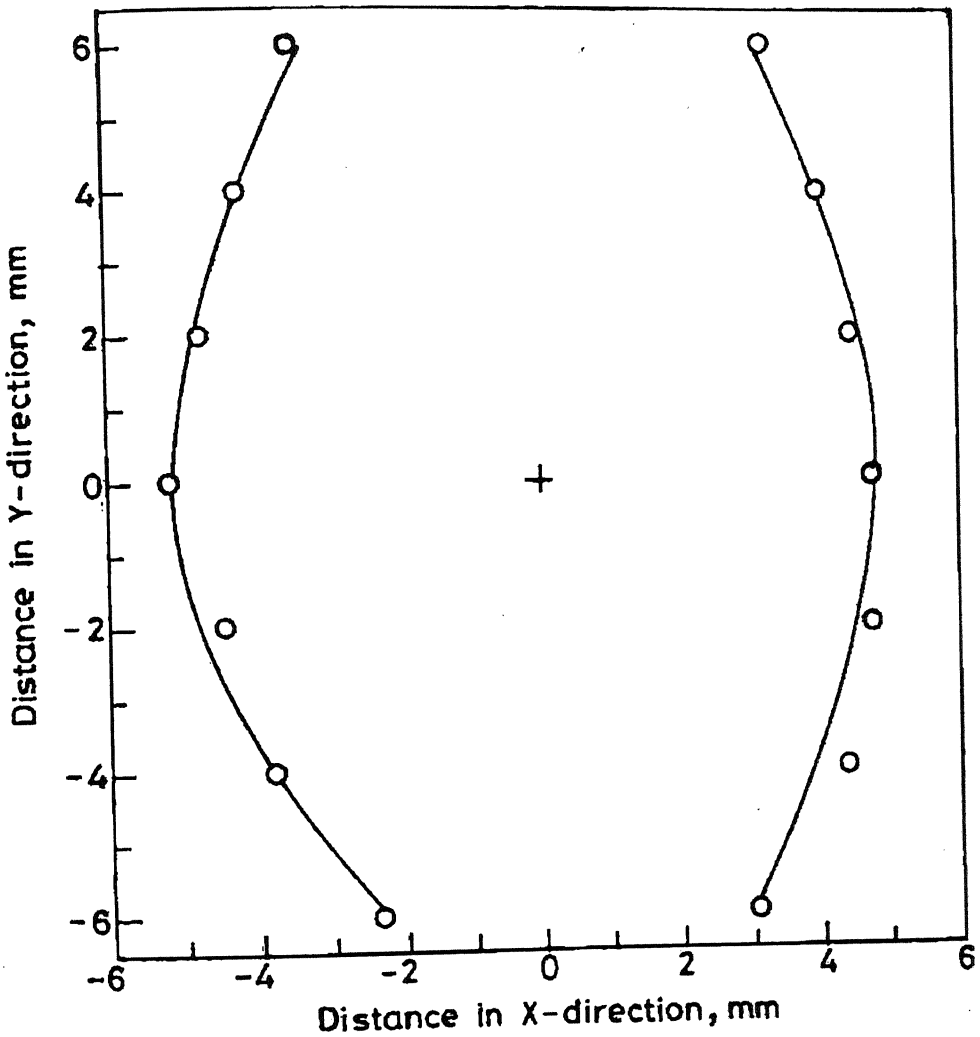

Figure 4.3.20 Iso-velocity line for the velocity of 160 m/s on the XY plane situated at Z=30 mm

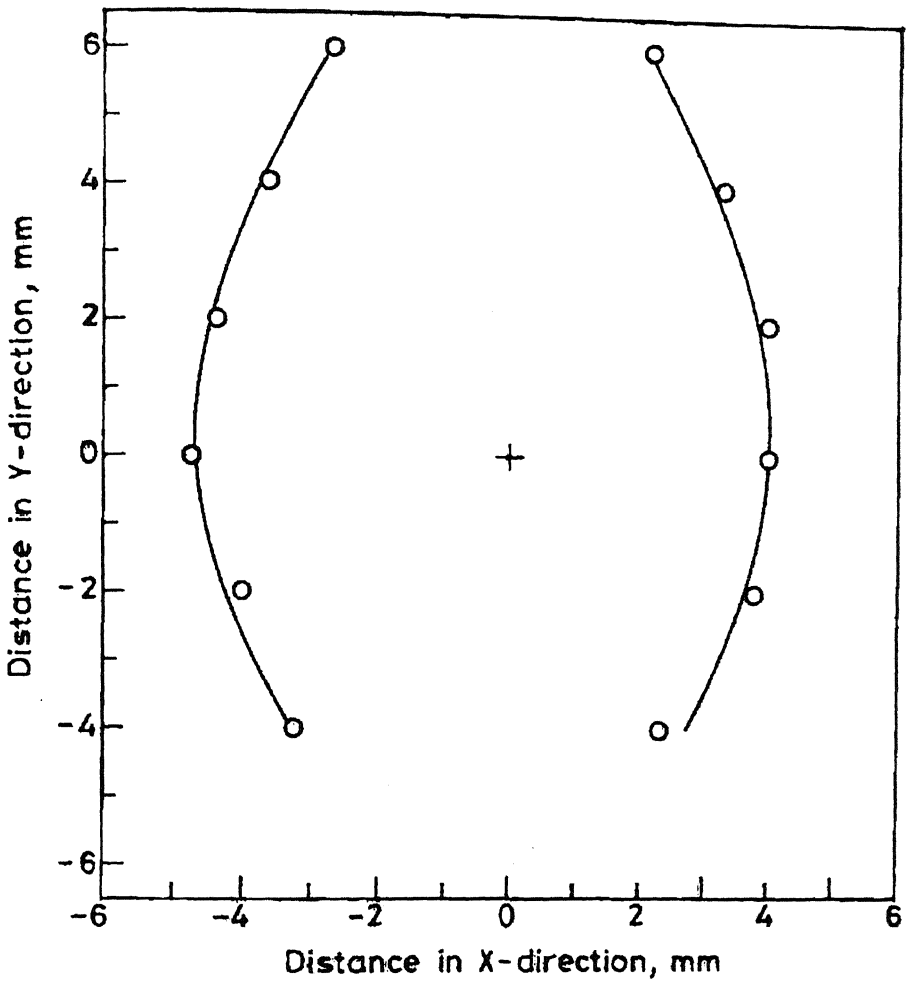

Figure 4.3.21 Iso-velocity line for the velocity of 160 m/s on the XY plane situated at Z=40 mm.

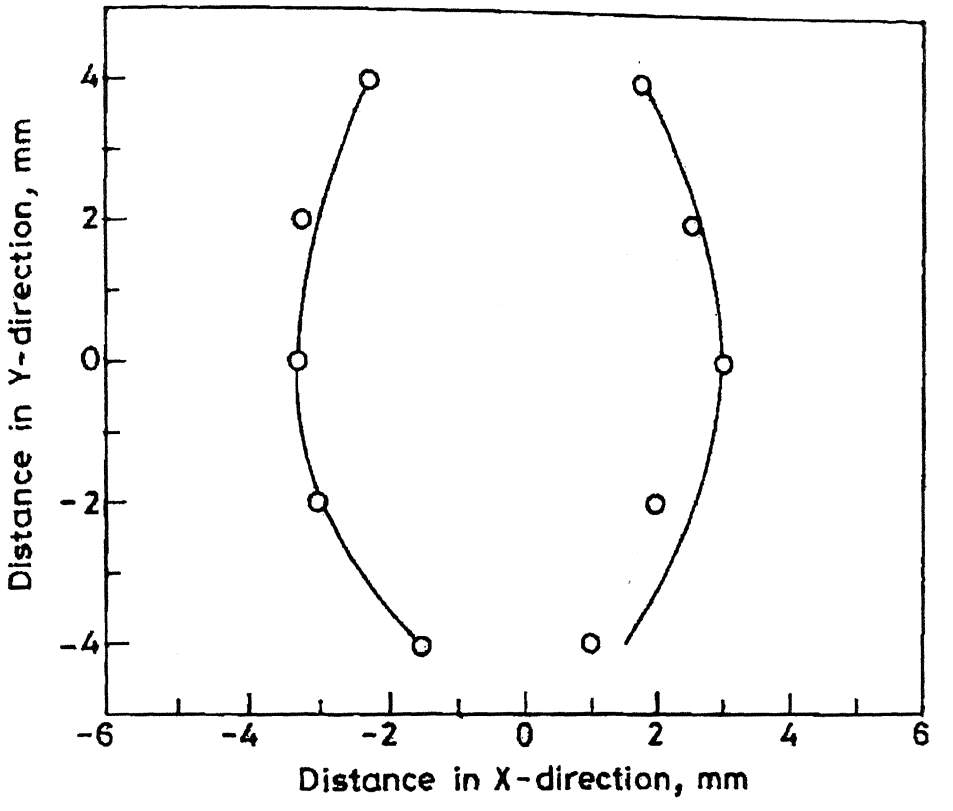

Figure 4.3.22 Iso-velocity line for the velocity of 160 m/s on the XY plane situated at Z=50 mm.

Table: 4.1 Gas velocity at different points on XY plane situated at Z = 0 as a function of plenum pressure.

(X, Y) coordinates of the points, mm	Velocity at plenum pressure of 800 kPa	Velocity at plenum pressure of 1000 kPa	Velocity at plenum pressure of 1200 kPa
(0,0)	205	235	282
(0,2)	202	229	280
(0, -2)	192	232	264
(0,4)	187	207	253
(0, -4)	177	218	238
(0,6)	157	140	193
(0, -6)	156	184	196
(2,0)	195	225	276
(-2,0)	192	233	27 8
(4,0)	178	199	242
(-4,0)	167	192	248
(6,0)	144	153	158
(-6,0)	137	165	175

Following observations can be made from the above figure:

1.As the metal stream of given diameter meets the gas field for the first time it interacts with gas field having different velocities at different points on the horizontal cross-section of the gas field.

2. As a result of first interaction of the molten stream with gas field, it disintegrates to droplets, which move downwards in the gas field. It is apparent that liquid droplets further interact with gas field having different velocities in X, Y, and Z directions.

3.For any given gas velocity the droplets moving along the vertical line passing through the geometric point will remains relatively for a long time as compared with the droplets moving in all other directions.

4.As a result of different velocities of gas within the gas field, it is plausible to expect the different size of droplets formed due to disintegration of liquid metal stream; leading to size distribution in the powder collectives.

Chapter-5
CONCLUSIONS

Numerous experiments were carried out to measure pitot pressure within the gas field formed by impingement of gas jets in free fall gas atomization. Then pressure readings were converted to velocity.

The following conclusions are made:

1. It has been found that the gas field created by an atomizer shows large variation in velocities around the geometric point.
2. The atomizing gas is found to possess maximum velocity at the geometric point and the velocity at the geometric point increases with increase in plenum pressure.
3. The gas velocity on XZ plane situated at any value of Y, decreases with either increase in ± Z or ± X at any plenum pressure.
4. The velocity of gas on the XY plane, situated at any value of Z, decreases with either increase in ± X or ± Y at any plenum pressure.
5. The region included by iso-velocity line of any given value at a given pressure is maximum on the horizontal XY plane passing through the geometric point. The extent of this region decreases more rapidly on the horizontal XY plane, situated towards the negative directions of Z than those situated towards positive directions of Z. This is valid for all plenum pressure.
6. Due to different velocities of gas within the gas field, disintegration of the molten metal stream results in different size of droplets and this leads to size distribution in a powder collective.

Chapter-6

SCOPE FOR FUTURE WORK

Further work is proposed:

1. To measure pitot pressure in gas field, produced by atomizer of different apex angle and focal length.
2. To perform atomization of liquid metal stream of different diameter and to correlate to size distribution of resultant powder collective with gas field.

REFERENCES

1. A.Lawley, 'Atomization, the production of metal powders, Monographs in P/M series', MPIF, Princeton, New jersey, 1992.
2. E.J Lavernia and Y .Wu,' Spray Atomization and Deposition', John Wiley and sons, Chichester, 1996.
3. J. Bruce See, C. Runkle and T. B. King, 'The Disintegration of Liquid Lead Streams by Nitrogen Jets', Met. Trans., Vol. 4(11), 1973, p.2669.
4. J. B. See and G. H Johnston, 'Interaction between Nitrogen Jets and Liquid Lead and Tin Streams', Powder Technology, Vol.21, 1978, p.119.
5. G. Helmerssion, A. Hede, T. Johannesson, B. Bergman and H. Hallen, 'On the control of Powder-size Distribution in Full – Scale Gas Atomization of Nickel – based Alloys', Scandianavian Journal Met., 26, 1997, p. 93.
6. John J. Dunkley, Powder Metallurgy, Metals Handbook, Vol.7, 9th edition, 1984, American society for Materials, Materials park, Ohio, p. 35.
7. B.P Bewlay and B. Cantor, 'Gas velocity Measurements from a close-coupled Spray Deposition Atomizer', Materials Science and Engineering, A118 (1989), pp. 207-222.
8. S.A Moir and H. Jones, 'The Gas Velocity Profile of a Free Fall Atomizer and its Relation to Solidification Microstructure of Collected Spray Droplets of 2014 aluminum alloy' Materials Science and Engineering, A173 (1993), pp. 161-164.
9. S.A Moir, H. Jones and S.B.M Beek, 'Gas Velocities from Free Fall Gas Atomizer' Powder Metallurgy, 1996, Vol. 39, n.4, p. 271.
10. G.Helmersson and K.Burgdorf, 'Effect of process parameters on microstructure of gas atomized powder', International Journal of Powder Metallurgy, 1996,n.25, pp. 51-58.
11. I Uslan, S.Saritas and T.J Davies, Powder Metallurgy, 1999, Vol.42, n.2, p.157.
12. D.Singh, S.C Koria and R.K Dube, 'Velocity of gas from free fall type atomizers', Powder Metallurgy, 1999, Vol.42, n.2, p. 79.
13. D.Singh, S.C Koria and R.K Dube, 'Study of free fall gas atomization of liquid metals to produce powder', Powder Metallurgy, 2001, Vol.44, n.2, pp. 177.

14. R.K Dube, S.C Koria and R.Subramanian, 'Atomization of Aluminum by Multiple Discrete Nitrogen Jets', Powder Metallurgy International, Vol.20 (6), 1988, pp. 14-18.

15. S.L Shinde and G.S Tendulkar, ' Analysis of Atomization – A review', Powder Met. Int., Vol.9 (4), 1977, p. 180.

16. M.H. Aksel and O.C. Enralp, 'Gas Dynamics', Prentice Hall, London, 1994, pp.79-124, pp. 197-198.

APPENDIX – A

Method for calculation of gas velocity from pressure readings:

The Mach number was calculated by using equation 3.1 and the velocity of gas was obtained by substitute this value of Mach number in equation 3.4.

An example of calculation of gas velocity is given as follows:

Step 1:

Calculation of pressure in kPa from manometer reading:

If the difference between two ends of mercury level is h, then Pitot pressure is = ρgh in kPa, where, ρ is density of mercury and g is acceleration due to gravity = 9.8 m/s^2. If h = 9.4 cm. Then Pitot pressure will be 12.5 kPa.

Step 2:

Stagnation pressure = Pitot pressure, kPa + atmospheric pressure, in kPa.

= 12.5 + 101.3

= 113.8 kPa.

Step 3:

The value of Mach number was obtained as 0.41 by substituting the appropriate values, in equation 3.1. Tthe gas velocity was obtained as144.2 m/s by substituting the value of Mach number in equation 3.4.

APPENDIX – B

Table: B. 1 Gas velocity at different points on XY plane situated at Z = 0 at plenum pressure of 800 kPa.

(X, Y) coordinates of the points, mm	Gas Velocity, m/s
(0,0)	205
(2,0)	195
(-2,0)	192
(4,0)	178
(-4,0)	167
(6,0)	137
(-6,0)	144
(0,2	202
(2,2)	194
(-2, 2)	177
(4,2)	162
(-4,2)	130
(6,2)	116
(-6,2)	110
(0,4)	187
(2,4)	162
(-2,4)	155
(4,4)	111
(-4,4)	84
(6,4)	62
(-6,4)	67
(0,6)	156
(2,6)	113
(-2,6)	135
(4,6)	87
(-4,6)	74
(6,6)	40
(-6,6)	43
(0, -2)	192
(2, -2)	183
(-2, -2)	186

(4, -2)	161
(-4, -2)	170
(6, -2)	120
(-6, -2)	132
(0, -4)	177
(2, -4)	170
(-2, -4)	173
(4, -4)	136
(-4, -4)	153
(6, -4)	93
(-6, -4)	93
(0, -6)	157
(2, -6)	137
(-2, -6)	144
(4, -6)	96
(-4, -6)	93
(6, -6)	43
(-6, -6)	42

Table: B. 2 Gas velocity at different points on XY plane situated at Z = 10 mm at plenum pressure of 800 kPa.

(X, Y) coordinates of the points, mm	**Gas Velocity, m/s**
(0,0)	192
(2,0)	180
(-2,0)	180
(4,0)	161
(-4,0)	161
(6,0)	128
(-6,0)	133
(0,2	178
(2,2)	165
(-2, 2)	172
(4,2)	137
(-4,2)	150
(6,2)	103
(-6,2)	103
(0,4)	156
(2,4)	138
(-2,4)	153

(4,4)	103
(-4,4)	126
(6,4)	63
(-6,4)	103
(0,6)	133
(2,6)	105
(-2,6)	128
(4,6)	73
(-4,6)	93
(6, 6)	46
(-6,6)	47
(0, -2)	189
(2, -2)	178
(-2, -2)	179
(4, -2)	151
(-4, -2)	156
(6, -2)	121
(-6, -2)	129
(0, -4)	170
(2, -4)	147
(-2, -4)	158
(4, -4)	113
(-4, -4)	129
(6, -4)	93
(-6, -4)	109
(0, -6)	122
(2, -6)	106
(-2, -6)	113
(4, -6)	86
(-4, -6)	102
(6, -6)	47
(-6, -6)	87

Table: B. 3 Gas velocity at different points on XY plane situated at Z = 20 mm at plenum pressure of 800 kPa.

(X, Y) coordinates of the points, mm	Gas Velocity, m/s
(0,0)	156.6
(2,0)	156.6
(-2,0)	148
(4,0)	144
(-4,0)	123
(6,0)	128
(-6,0)	93
(0,2	154
(2,2)	150
(-2, 2)	140
(4,2)	143
(-4,2)	117
(6,2)	128
(-6,2)	92
(0,4)	143
(2,4)	138
(-2,4)	131
(4,4)	127
(-4,4)	111.3
(6,4)	103
(-6,4)	84
(0,6)	126
(2,6)	113.35
(-2,6)	115.6
(4,6)	103.38
(-4,6)	101.87
(6, 6)	81
(-6,6)	72.3
(0, -2)	142.9
(2, -2)	139.8
(-2, -2)	138.8
(4, -2)	131
(-4, -2)	122
(6, -2)	116.6
(-6, -2)	97.95
(0, -4)	128.33
(2, -4)	120.5
(-2, -4)	125.39
(4, -4)	111.3
(-4, -4)	110
(6, -4)	98
(-6, -4)	98

(0, -6)	105.6
(2, -6)	101.87
(-2, -6)	101.87
(4, -6)	92
(-4, -6)	97
(6, -6)	73
(-6, -6)	86

Table: B. 4 Gas velocity at different points on XY plane situated at Z = 30 mm at plenum pressure of 800 kPa.

(X, Y) coordinates of the points, mm	**Gas Velocity, m/s**
(0,0)	137
(2,0)	137
(-2,0)	130
(4,0)	132
(-4,0)	114
(6,0)	115.3
(-6,0)	93
(0,2	135.6
(2,2)	134.5
(-2, 2)	129.4
(4,2)	120.5
(-4,2)	113.35
(6,2)	107.79
(-6,2)	87
(0,4)	121.7
(2,4)	113.35
(-2,4)	113.35
(4,4)	105.6
(-4,4)	103.38
(6,4)	91
(-6,4)	86
(0,6)	101.87
(2,6)	97.95
(-2,6)	101.87
(4,6)	84
(-4,6)	91.3
(6, 6)	78
(-6,6)	78
(0, -2)	138.79
(2, -2)	132.86

(-2, -2)	132.86
(4, -2)	129.5
(-4, -2)	120.5
(6, -2)	111.3
(-6, -2)	103.38
(0, -4)	123.58
(2, -4)	121.74
(-2, -4)	120.5
(4, -4)	116.6
(-4, -4)	107.79
(6, -4)	108.8
(-6, -4)	101.87
(0, -6)	105.6
(2, -6)	105.6
(-2, -6)	103.38
(4, -6)	103.38
(-4, -6)	101.87
(6, -6)	95.5
(-6, -6)	93

Table: B 5 Gas velocity at different points on XY plane situated at Z = 40 mm at plenum pressure of 800 kPa.

(X, Y) coordinates of the points, mm	**Gas Velocity, m/s**
(0,0)	125.39
(2,0)	120.5
(-2,0)	123.5
(4,0)	113.35
(-4,0)	107.8
(6,0)	101.8
(-6,0)	96
(0,2	117.9
(2,2)	117.9
(-2, 2)	115.3
(4,2)	113.35
(-4,2)	105.6
(6,2)	101.87
(-6,2)	93
(0,4)	109.9
(2,4)	107.7
(-2,4)	107.9
(4,4)	101.87

(-4,4)	98
(6,4)	95
(-6,4)	86
(0,6)	97.9
(2,6)	95.5
(-2,6)	97.9
(4,6)	87.7
(-4,6)	91.3
(6, 6)	84
(-6,6)	81
(0, -2)	113.35
(2, -2)	111.3
(-2, -2)	107.79
(4, -2)	109.9
(-4, -2)	97.95
(6, -2)	103.38
(-6, -2)	95.5
(0, -4)	111.3
(2, -4)	107.79
(-2, -4)	105.6
(4, -4)	101.87
(-4, -4)	105.6
(6, -4)	93
(-6, -4)	93
(0, -6)	98
(2, -6)	08
(-2, -6)	98
(4, -6)	91.3
(-4, -6)	91.3
(6, -6)	81
(-6, -6)	86

Table: B. 6 Gas velocity at different points on XY plane situated at Z =50 mm at plenum pressure of 800 kPa

(X, Y) coordinates of the points, mm	**Gas Velocity, m/s**
(0,0)	113.35
(2,0)	113.35
(-2,0)	111.3
(4,0)	107.78
(-4,0)	103.38
(6,0)	101.87
(-6,0)	93
(0,2	109.9

(2,2)	109.9
(-2, 2)	107.7
(4,2)	103.38
(-4,2)	101.87
(6,2)	98
(-6,2)	91.3
(0,4)	105.6
(2,4)	105.6
(-2,4)	105.6
(4,4)	101.87
(-4,4)	97.9
(6,4)	91.3
(-6,4)	86
(0,6)	95.5
(2,6)	93
(-2,6)	93
(4,6)	88
(-4,6)	86
(6, 6)	81
(-6,6)	84
(0, -2)	109.9
(2, -2)	109.9
(-2, -2)	107
(4, -2)	105.6
(-4, -2)	101.87
(6, -2)	101.87
(-6, -2)	93
(0, -4)	105.6
(2, -4)	105.6
(-2, -4)	103.38
(4, -4)	101.87
(-4, -4)	101.87
(6, -4)	91.3
(-6, -4)	91.3
(0, -6)	95.5
(2, -6)	98
(-2, -6)	93
(4, -6)	91.3
(-4, -6)	93
(6, -6)	78
(-6, -6)	84

Table: B. 7 Gas velocity at different points on XY plane situated at Z = 60 mm at plenum pressure of 800 kPa.

(X, Y) coordinates of the points, mm	Gas Velocity, m/s
(0,0)	105.6
(2,0)	101.87
(-2,0)	101.87
(4,0)	101.87
(-4,0)	93
(6,0)	93
(-6,0)	88
(0,2	101.38
(2,2)	101.38
(-2, 2)	93
(4,2)	98
(-4,2)	91.3
(6,2)	91.3
(-6,2)	86
(0,4)	97.8
(2,4)	95.5
(-2,4)	91.3
(4,4)	93
(-4,4)	86
(6,4)	91.3
(-6,4)	78
(0,6)	87.7
(2,6)	86
(-2,6)	84.3
(4,6)	81
(-4,6)	81
(6, 6)	78
(-6,6)	78
(0, -2)	105.6
(2, -2)	101.87
(-2, -2)	101.87
(4, -2)	99.5
(-4, -2)	93
(6, -2)	93
(-6, -2)	86
(0, -4)	97.9
(2, -4)	93
(-2, -4)	93
(4, -4)	91.3
(-4, -4)	91.3
(6, -4)	87.7
(-6, -4)	85.6

(0, -6)	91.3
(2, -6)	87.7
(-2, -6)	87.7
(4, -6)	85.6
(-4, -6)	84.3
(6, -6)	78
(-6, -6)	78

Table: B. 8 Gas velocity at different points on XY plane situated at Z = 70 mm at plenum pressure of 800 kPa

(X, Y) coordinates of the points, mm	**Gas Velocity, m/s**
(0,0)	97.9
(2,0)	95.5
(-2,0)	93
(4,0)	93
(-4,0)	91.3
(6,0)	87.7
(-6,0)	84.3
(0,2	95.5
(2,2)	95.5
(-2, 2)	95.5
(4,2)	93
(-4,2)	91.3
(6,2)	85.6
(-6,2)	84.3
(0,4)	91.3
(2,4)	91.3
(-2,4)	93
(4,4)	87.7
(-4,4)	84.3
(6,4)	81
(-6,4)	78
(0,6)	85.6
(2,6)	81
(-2,6)	84.3
(4,6)	78
(-4,6)	81
(6, 6)	78
(-6,6)	72.7
(0, -2)	97.9

(2, -2)	91.3
(-2, -2)	93
(4, -2)	87.7
(-4, -2)	91.3
(6, -2)	85.6
(-6, -2)	84.3
(0, -4)	91.3
(2, -4)	87.7
(-2, -4)	85.7
(4, -4)	85.9
(-4, -4)	85.9
(6, -4)	81
(-6, -4)	81.2
(0, -6)	85.9
(2, -6)	84.3
(-2, -6)	85.9
(4, -6)	81.12
(-4, -6)	84.3
(6, -6)	72.7
(-6, -6)	78

Table: B. 9 Gas velocity at different points on XY plane situated at Z = 80 mm at plenum pressure of 800 kPa.

(X, Y) coordinates of the points, mm	**Gas Velocity, m/s**
(0,0)	93
(2,0)	93
(-2,0)	91.3
(4,0)	87.7
(-4,0)	87.7
(6,0)	84.3
(-6,0)	84.3
(0,2	91.3
(2,2)	91.3
(-2, 2)	87.7
(4,2)	85.9
(-4,2)	85.9
(6,2)	84.3
(-6,2)	84.3
(0,4)	85.9
(2,4)	84.3
(-2,4)	84.3
(4,4)	84.3

(-4,4)	84.3
(6,4)	78
(-6,4)	78
(0,6)	81
(2,6)	81
(-2,6)	84.3
(4,6)	78
(-4,6)	78
(6, 6)	76
(-6,6)	78
(0, -2)	93
(2, -2)	85.9
(-2, -2)	87.7
(4, -2)	85.9
(-4, -2)	84.3
(6, -2)	84.3
(-6, -2)	84.3
(0, -4)	87.7
(2, -4)	84.3
(-2, -4)	85.9
(4, -4)	84.3
(-4, -4)	84.3
(6, -4)	78
(-6, -4)	78
(0, -6)	81
(2, -6)	81
(-2, -6)	78
(4, -6)	78
(-4, -6)	72.7
(6, -6)	65.7
(-6, -6)	72.7

Table: B 10 Gas velocity at different points on XY plane situated at Z = 90 mm at plenum pressure of 800 kPa.

(X, Y) coordinates of the points, mm	**Gas Velocity, m/s**
(0,0)	85.9
(2,0)	87.7
(-2,0)	84.3
(4,0)	84.3
(-4,0)	84.3
(6,0)	81
(-6,0)	78
(0,2	84.3

(2,2)	85.9
(-2, 2)	84.3
(4,2)	84.3
(-4,2)	81
(6,2)	78
(-6,2)	78
(0,4)	84.3
(2,4)	81
(-2,4)	84.3
(4,4)	78
(-4,4)	78
(6,4)	76
(-6,4)	78
(0,6)	78
(2,6)	78
(-2,6)	76
(4,6)	72.7
(-4,6)	72.7
(6, 6)	72.7
(-6,6)	63
(0, -2)	84.3
(2, -2)	81
(-2, -2)	84.3
(4, -2)	81
(-4, -2)	78
(6, -2)	78
(-6, -2)	72.7
(0, -4)	81
(2, -4)	78
(-2, -4)	78
(4, -4)	78
(-4, -4)	78
(6, -4)	69
(-6, -4)	69
(0, -6)	78
(2, -6)	78
(-2, -6)	78
(4, -6)	69
(-4, -6)	72.7
(6, -6)	63
(-6, -6)	65.7

Table: B. 11 Gas velocity at different points on XY plane situated at Z = 100 mm at plenum pressure of 800 kPa.

(X, Y) coordinates of the points, mm	Gas Velocity, m/s
(0,0)	78
(2,0)	78
(-2,0)	78
(4,0)	78
(-4,0)	75.6
(6,0)	75.6
(-6,0)	72.6
(0,2	78
(2,2)	78
(-2, 2)	78
(4,2)	75.7
(-4,2)	75.9
(6,2)	72.7
(-6,2)	72.7
(0,4)	78
(2,4)	75.9
(-2,4)	78
(4,4)	72.7
(-4,4)	72.7
(6,4)	72.7
(-6,4)	69.3
(0,6)	72.7
(2,6)	72.7
(-2,6)	72.7
(4,6)	65.6
(-4,6)	65.6
(6, 6)	63
(-6,6)	63
(0, -2)	78
(2, -2)	78
(-2, -2)	80.12
(4, -2)	75.9
(-4, -2)	78
(6, -2)	72.7
(-6, -2)	75.9
(0, -4)	78
(2, -4)	75.9
(-2, -4)	78
(4, -4)	75.9
(-4, -4)	78
(6, -4)	72.7
(-6, -4)	75.9

(0, -6)	78
(2, -6)	75.9
(-2, -6)	78
(4, -6)	72.7
(-4, -6)	72.7
(6, -6)	65
(-6, -6)	69.3

Table: B. 12 Gas velocity at different points on XY plane situated at Z = - 10 mm at plenum pressure of 800 kPa.

(X, Y) coordinates of the points, mm	**Gas Velocity, m/s**
(0,0)	184.5
(2,0)	172.7
(-2,0)	176.5
(4,0)	156.6
(-4,0)	148.5
(6,0)	88
(-6,0)	84
(0,2	180
(2,2)	172.3
(-2, 2)	168
(4,2)	148
(-4,2)	128
(6,2)	104
(-6,2)	84
(0,4)	172
(2,4)	140.5
(-2,4)	128
(4,4)	112
(-4,4)	112
(6,4)	68
(-6,4)	56
(0,6)	140
(2,6)	124
(-2,6)	112
(4,6)	96
(-4,6)	80
(6, 6)	84
(-6,6)	44

(0, -2)	176
(2, -2)	168.3
(-2, -2)	172
(4, -2)	140.5
(-4, -2)	144.5
(6, -2)	108
(-6, -2)	116
(0, -4)	152.5
(2, -4)	152.5
(-2, -4)	146
(4, -4)	128
(-4, -4)	120
(6, -4)	92
(-6, -4)	104
(0, -6)	112.5
(2, -6)	104
(-2, -6)	116
(4, -6)	88
(-4, -6)	88
(6, -6)	72
(-6, -6)	72

Table: B. 13 Gas velocity at different points on XY plane situated at Z = - 10 mm at plenum pressure of 1000 kPa.

(X, Y) coordinates of the points, mm	**Gas Velocity, m/s**
(0,0)	220.5
(2,0)	200.5
(-2,0)	208.5
(4,0)	168.8
(-4,0)	172
(6,0)	132.5
(-6,0)	136
(0,2	216
(2,2)	192
(-2, 2)	196
(4,2)	152.5
(-4,2)	168.5
(6,2)	124
(-6,2)	128
(0,4)	192.5
(2,4)	184.8
(-2,4)	176
(4,4)	148

(-4,4)	136
(6,4)	108
(-6,4)	101.87
(0,6)	144
(2,6)	133
(-2,6)	136
(4,6)	116.6
(-4,6)	108.5
(6, 6)	88
(-6,6)	88
(0, -2)	208
(2, -2)	204
(-2, -2)	192
(4, -2)	172
(-4, -2)	164
(6, -2)	148
(-6, -2)	128
(0, -4)	192
(2, -4)	186
(-2, -4)	176
(4, -4)	154
(-4, -4)	148
(6, -4)	126
(-6, -4)	118.5
(0, -6)	160
(2, -6)	140
(-2, -6)	156
(4, -6)	106
(-4, -6)	128
(6, -6)	88
(-6, -6)	92

Table: B. 14 Gas velocity at different points on XY plane situated at Z = 0 mm at plenum pressure of 1000 kPa.

(X, Y) coordinates of the points, mm	**Gas Velocity, m/s**
(0,0)	235.47
(2,0)	225.7
(-2,0)	232.9
(4,0)	199.77
(-4,0)	191.45
(6,0)	153

(-6,0)	129.8
(0,2	229.6
(2,2)	217.5
(-2, 2)	224
(4,2)	183
(-4,2)	199
(6,2)	126.5
(-6,2)	137.2
(0,4)	207.79
(2,4)	204.6
(-2,4)	195.6
(4,4)	177.4
(-4,4)	150
(6,4)	121.7
(-6,4)	101.8
(0,6)	161.3
(2,6)	144
(-2,6)	124
(4,6)	129
(-4,6)	100
(6, 6)	48
(-6,6)	48
(0, -2)	232
(2, -2)	223
(-2, -2)	217.6
(4, -2)	206.3
(-4, -2)	176
(6, -2)	172
(-6, -2)	78
(0, -4)	218
(2, -4)	210
(-2, -4)	194
(4, -4)	176
(-4, -4)	98
(6, -4)	139
(-6, -4)	56
(0, -6)	184
(2, -6)	140
(-2, -6)	149
(4, -6)	91.3
(-4, -6)	91.3
(6, -6)	59
(-6, -6)	46.6

Table: B. 15 Gas velocity at different points on XY plane situated at Z =10 mm at plenum pressure of 1000 kPa

(X, Y) coordinates of the points, mm	Gas Velocity, m/s
(0,0)	222
(2,0)	205.5
(-2,0)	215.4
(4,0)	166.9
(-4,0)	186
(6,0)	121.74
(-6,0)	139.84
(0,2	217.6
(2,2)	199.77
(-2, 2)	210.9
(4,2)	163.6
(-4,2)	186
(6,2)	107.79
(-6,2)	142.9
(0,4)	194
(2,4)	182
(-2,4)	186.7
(4,4)	151.6
(-4,4)	163.57
(6,4)	103.38
(-6,4)	126.57
(0,6)	137.2
(2,6)	143.9
(-2,6)	113
(4,6)	129
(-4,6)	81
(6, 6)	91
(-6,6)	57
(0, -2)	213
(2, -2)	201
(-2, -2)	194
(4, -2)	177.4
(-4, -2)	140
(6, -2)	146
(-6, -2)	98

(0, -4)	212
(2, -4)	196
(-2, -4)	199
(4, -4)	167.7
(-4, -4)	138
(6, -4)	138
(-6, -4)	78
(0, -6)	172
(2, -6)	156
(-2, -6)	161
(4, -6)	132
(-4, -6)	116.6
(6, -6)	105.6
(-6, -6)	72

Table: B. 16 Gas velocity at different points on XY plane situated at Z = 20 mm at plenum pressure of 1000 kPa.

(X, Y) coordinates of the points, mm	**Gas Velocity, m/s**
(0,0)	200
(2,0)	180
(-2,0)	196
(4,0)	152
(-4,0)	168.5
(6,0)	116.4
(-6,0)	123.5
(0,2	200
(2,2)	180
(-2, 2)	188
(4,2)	144
(-4,2)	168
(6,2)	106
(-6,2)	140
(0,4)	180
(2,4)	167
(-2,4)	176
(4,4)	139
(-4,4)	158
(6,4)	105.6
(-6,4)	128.3
(0,6)	147.8
(2,6)	142.9
(-2,6)	138.8

(4,6)	123.6
(-4,6)	121.7
(6, 6)	91.3
(-6,6)	93
(0, -2)	199.7
(2, -2)	182.1
(-2, -2)	194
(4, -2)	151
(-4, -2)	170
(6, -2)	116.6
(-6, -2)	138.7
(0, -4)	183.7
(2, -4)	171
(-2, -4)	175
(4, -4)	149
(-4, -4)	146.8
(6, -4)	123.6
(-6, -4)	109.9
(0, -6)	146.8
(2, -6)	139.8
(-2, -6)	146.8
(4, -6)	125.4
(-4, -6)	132.8
(6, -6)	101.87
(-6, -6)	101.87

Table: B. 17 Gas velocity at different points on XY plane situated at Z = 30 mm at plenum pressure of 1000 kPa.

(X, Y) coordinates of the points, mm	**Gas Velocity, m/s**
(0,0)	172
(2,0)	168
(-2,0)	161
(4,0)	156.6
(-4,0)	135.6
(6,0)	125.6
(-6,0)	129.5
(0,2	170
(2,2)	167
(-2, 2)	158

(4,2)	155.4
(-4,2)	131
(6,2)	129
(-6,2)	107.79
(0,4)	161.5
(2,4)	156.6
(-2,4)	149.3
(4,4)	143.9
(-4,4)	125.4
(6,4)	121.7
(-6,4)	101.87
(0,6)	140.8
(2,6)	138.79
(-2,6)	123.58
(4,6)	131.18
(-4,6)	109.9
(6, 6)	107.79
(-6,6)	87.7
(0, -2)	164.8
(2, -2)	163.2
(-2, -2)	155.3
(4, -2)	151.6
(-4, -2)	135.6
(6, -2)	120.5
(-6, -2)	111.3
(0, -4)	153
(2, -4)	149
(-2, -4)	150
(4, -4)	129.5
(-4, -4)	132.86
(6, -4)	107.79
(-6, -4)	107.79
(0, -6)	137.2
(2, -6)	129.5
(-2, -6)	129.8
(4, -6)	123.6
(-4, -6)	113.35
(6, -6)	103.38
(-6, -6)	93

Table: B. 18 Gas velocity at different points on XY plane situated at Z = 40 mm at plenum pressure of 1000 kPa.

(X, Y) coordinates	**Gas**

of the points, mm	Velocity, m/s
(0,0)	158.8
(2,0)	156.65
(-2,0)	150.23
(4,0)	143.9
(-4,0)	135.6
(6,0)	126.57
(-6,0)	111.3
(0,2	156.65
(2,2)	151.64
(-2, 2)	149.28
(4,2)	139.84
(-4,2)	129.48
(6,2)	121.74
(-6,2)	103.38
(0,4)	149.8
(2,4)	143.9
(-2,4)	139.8
(4,4)	132.86
(-4,4)	121.74
(6,4)	115.34
(-6,4)	91.29
(0,6)	134.5
(2,6)	131.8
(-2,6)	126.57
(4,6)	121.74
(-4,6)	105.6
(6, 6)	103.38
(-6,6)	84
(0, -2)	157.98
(2, -2)	155.3
(-2, -2)	149.28
(4, -2)	139.8
(-4, -2)	132.86
(6, -2)	119.8
(-6, -2)	107.79
(0, -4)	146.87
(2, -4)	139.84
(-2, -4)	137.2
(4, -4)	132.86
(-4, -4)	125.4
(6, -4)	109.9
(-6, -4)	101.87
(0, -6)	132.86
(2, -6)	122.8

(-2, -6)	126.57
(4, -6)	115.35
(-4, -6)	113.35
(6, -6)	97.95
(-6, -6)	99.5

Table: B. 19 Gas velocity at different points on XY plane situated at Z = 50 mm at plenum pressure of 1000 kPa.

(X, Y) coordinates of the points, mm	**Gas Velocity, m/s**
(0,0)	143.9
(2,0)	142.9
(-2,0)	142.9
(4,0)	128.28
(-4,0)	128.48
(6,0)	116.6
(-6,0)	109.9
(0,2	143.9
(2,2)	140.9
(-2, 2)	138.8
(4,2)	132.8
(-4,2)	123.58
(6,2)	116.6
(-6,2)	103.38
(0,4)	135.6
(2,4)	135.6
(-2,4)	131.2
(4,4)	128.33
(-4,4)	120.5
(6,4)	113.35
(-6,4)	98
(0,6)	128.33
(2,6)	122.9
(-2,6)	121.7
(4,6)	116.6
(-4,6)	105.6
(6, 6)	101.8
(-6,6)	93
(0, -2)	138.7
(2, -2)	137
(-2, -2)	137

(4, -2)	128.3
(-4, -2)	128.3
(6, -2)	113.35
(-6, -2)	105.6
(0, -4)	131.2
(2, -4)	128.3
(-2, -4)	128.3
(4, -4)	113.35
(-4, -4)	120.5
(6, -4)	103.4
(-6, -4)	105.6
(0, -6)	117.96
(2, -6)	113.4
(-2, -6)	116.6
(4, -6)	103.4
(-4, -6)	103.3
(6, -6)	86
(-6, -6)	97

Table: B.20 Gas velocity at different points on XY plane situated at Z = 60 mm at plenum pressure of 1000 kPa.

(X, Y) coordinates of the points, mm	**Gas Velocity, m/s**
(0,0)	138.8
(2,0)	132.86
(-2,0)	135.6
(4,0)	123.58
(-4,0)	126.57
(6,0)	107.8
(-6,0)	111.3
(0,2	137.2
(2,2)	134.5
(-2, 2)	132.86
(4,2)	123.6
(-4,2)	123.58
(6,2)	111.3
(-6,2)	105.6
(0,4)	129.5

(2,4)	126.6
(-2,4)	128.3
(4,4)	120.5
(-4,4)	120.5
(6,4)	107.79
(-6,4)	101.87
(0,6)	120.5
(2,6)	120.5
(-2,6)	120.5
(4,6)	111.3
(-4,6)	105.6
(6, 6)	101.87
(-6,6)	95.5
(0, -2)	137
(2, -2)	132
(-2, -2)	132
(4, -2)	113.35
(-4, -2)	125.4
(6, -2)	103.38
(-6, -2)	113
(0, -4)	123.59
(2, -4)	111.3
(-2, -4)	120.5
(4, -4)	105.6
(-4, -4)	114.7
(6, -4)	92
(-6, -4)	105.6
(0, -6)	107.79
(2, -6)	103.38
(-2, -6)	109.9
(4, -6)	95.5
(-4, -6)	101.87
(6, -6)	84
(-6, -6)	91.2

Table: B 21 Gas velocity at different points on XY plane situated at Z = 70 mm at plenum pressure of 1000 kPa.

(X, Y) coordinates of the points, mm	**Gas Velocity, m/s**
(0,0)	128.33
(2,0)	120.5
(-2,0)	121.74
(4,0)	109.9

(-4,0)	109
(6,0)	105.6
(-6,0)	103.38
(0,2	128.33
(2,2)	125.4
(-2, 2)	121.7
(4,2)	109.9
(-4,2)	109.9
(6,2)	105.6
(-6,2)	101.87
(0,4)	123.58
(2,4)	120.5
(-2,4)	113.35
(4,4)	109.9
(-4,4)	105.6
(6,4)	103.38
(-6,4)	95.5
(0,6)	111.3
(2,6)	113.35
(-2,6)	109.9
(4,6)	105.6
(-4,6)	101.87
(6, 6)	101.87
(-6,6)	91.2
(0, -2)	125.4
(2, -2)	120.5
(-2, -2)	121.7
(4, -2)	105.6
(-4, -2)	109.9
(6, -2)	97.8
(-6, -2)	101.8
(0, -4)	120.5
(2, -4)	113.35
(-2, -4)	115.4
(4, -4)	103.4
(-4, -4)	107.8
(6, -4)	95.5
(-6, -4)	95.5
(0, -6)	111.3
(2, -6)	103.38
(-2, -6)	107
(4, -6)	99.5
(-4, -6)	103.38
(6, -6)	87.7
(-6, -6)	93

Table: B. 22 Gas velocity at different points on XY plane situated at Z = 80 mm at plenum pressure of 1000 kPa.

(X, Y) coordinates of the points, mm	Gas Velocity, m/s
(0,0)	116.66
(2,0)	113.4
(-2,0)	115.4
(4,0)	107.7
(-4,0)	109
(6,0)	97.9
(-6,0)	103.38
(0,2	113.35
(2,2)	111.3
(-2, 2)	109
(4,2)	107.79
(-4,2)	105.6
(6,2)	97.7
(-6,2)	97.7
(0,4)	107.7
(2,4)	107.7
(-2,4)	107.9
(4,4)	105.6
(-4,4)	101.87
(6,4)	99.5
(-6,4)	93
(0,6)	101.87
(2,6)	101.87
(-2,6)	95.5
(4,6)	97
(-4,6)	91.2
(6, 6)	93
(-6,6)	85.9
(0, -2)	109.6
(2, -2)	111.3
(-2, -2)	113.35
(4, -2)	103.38
(-4, -2)	105.6
(6, -2)	93
(-6, -2)	101.87
(0, -4)	111.3
(2, -4)	105.6
(-2, -4)	107.79

(4, -4)	97.6
(-4, -4)	105.6
(6, -4)	87.7
(-6, -4)	97.5
(0, -6)	101.87
(2, -6)	101.87
(-2, -6)	97.95
(4, -6)	91.2
(-4, -6)	95.5
(6, -6)	105.6
(-6, -6)	93

Table: B. 23 Gas velocity at different points on XY plane situated at Z = 90 mm at plenum pressure of 1000 kPa.

(X, Y) coordinates of the points, mm	**Gas Velocity, m/s**
(0,0)	105.6
(2,0)	103.38
(-2,0)	103.39
(4,0)	101.87
(-4,0)	99.5
(6,0)	93
(-6,0)	93
(0,2	105.6
(2,2)	103.5
(-2, 2)	103.3
(4,2)	101.87
(-4,2)	99.5
(6,2)	95.5
(-6,2)	93
(0,4)	103.37
(2,4)	99.5
(-2,4)	97.9
(4,4)	97.9
(-4,4)	93
(6,4)	93
(-6,4)	91.2
(0,6)	97.9
(2,6)	97.9

(-2,6)	95.5
(4,6)	95.5
(-4,6)	91.2
(6, 6)	91.2
(-6,6)	85.6
(0, -2)	105.6
(2, -2)	101.87
(-2, -2)	101.87
(4, -2)	95.5
(-4, -2)	99.5
(6, -2)	91.2
(-6, -2)	91.2
(0, -4)	101.87
(2, -4)	101.87
(-2, -4)	97.9
(4, -4)	93
(-4, -4)	95.5
(6, -4)	85.7
(-6, -4)	91.2
(0, -6)	95.5
(2, -6)	93
(-2, -6)	93
(4, -6)	85.6
(-4, -6)	93
(6, -6)	81.2
(-6, -6)	84

Table: B. 24 Gas velocity at different points on XY plane situated at Z =100 mm at plenum pressure of 1000 kPa.

(X, Y) coordinates of the points, mm	**Gas Velocity, m/s**
(0,0)	101.87
(2,0)	101.87
(-2,0)	99
(4,0)	95.6
(-4,0)	97.6
(6,0)	91.2
(-6,0)	95.6
(0,2	101.87
(2,2)	101.87
(-2, 2)	99
(4,2)	95.6
(-4,2)	93

(6,2)	91
(-6,2)	87.7
(0,4)	99.5
(2,4)	97.8
(-2,4)	97.7
(4,4)	93
(-4,4)	93
(6,4)	85.6
(-6,4)	87.7
(0,6)	93
(2,6)	93
(-2,6)	91.2
(4,6)	86
(-4,6)	87.7
(6, 6)	84
(-6,6)	84
(0, -2)	97.9
(2, -2)	95.5
(-2, -2)	97.9
(4, -2)	91.2
(-4, -2)	93
(6, -2)	85.9
(-6, -2)	87.7
(0, -4)	97.9
(2, -4)	91.2
(-2, -4)	97.9
(4, -4)	87.7
(-4, -4)	87.7
(6, -4)	81.2
(-6, -4)	85.6
(0, -6)	93
(2, -6)	85.9
(-2, -6)	91.3
(4, -6)	84
(-4, -6)	85.9
(6, -6)	81.12
(-6, -6)	84

Table: B.25 Gas velocity at different points on XY plane situated at Z =0 mm at plenum pressure of 1200 kPa.

(X, Y) coordinates of the points, mm	**Gas Velocity, m/s**

(4, -6)	148
(-4, -6)	140
(6, -6)	104
(-6, -6)	108

Table: B.26 Gas velocity at different points on XY plane situated at Z =10 mm at plenum pressure of 1200 kPa.

(X, Y) coordinates of the points, mm	**Gas Velocity, m/s**
(0,0)	272
(2,0)	260
(-2,0)	263
(4,0)	222
(-4,0)	220.5
(6,0)	142
(-6,0)	164
(0,2)	260
(2,2)	244
(-2, 2)	246
(4,2)	202
(-4,2)	220.5
(6,2)	142
(-6,2)	144
(0,4)	229
(2,4)	228.6
(-2,4)	242
(4,4)	182
(-4,4)	181.5
(6,4)	124
(-6,4)	120.5
(0,6)	180
(2,6)	168
(-2,6)	164
(4,6)	144
(-4,6)	128
(6, 6)	104
(-6,6)	100.5
(0, -2)	252
(2, -2)	242
(-2, -2)	238
(4, -2)	180
(-4, -2)	208
(6, -2)	120.5

(-6, -2)	140
(0, -4)	220
(2, -4)	180
(-2, -4)	202
(4, -4)	160
(-4, -4)	180
(6, -4)	122
(-6, -4)	124
(0, -6)	178
(2, -6)	180
(-2, -6)	162
(4, -6)	140
(-4, -6)	120
(6, -6)	102
(-6, -6)	100.5

Table: B.27 Gas velocity at different points on XY plane situated at Z =20 mm at plenum pressure of 1200 kPa.

(X, Y) coordinates of the points, mm	**Gas Velocity, m/s**
(0,0)	260
(2,0)	238
(-2,0)	240
(4,0)	200
(-4,0)	200
(6,0)	124
(-6,0)	144
(0,2)	260
(2,2)	238
(-2, 2)	220
(4,2)	180
(-4,2)	200
(6,2)	120
(-6,2)	140
(0,4)	216
(2,4)	202
(-2,4)	204
(4,4)	166
(-4,4)	180
(6,4)	108
(-6,4)	108
(0,6)	158
(2,6)	162
(-2,6)	164

(4,6)	140
(-4,6)	140
(6, 6)	88
(-6,6)	92
(0, -2)	240
(2, -2)	200
(-2, -2)	200
(4, -2)	160
(-4, -2)	180
(6, -2)	122
(-6, -2)	133
(0, -4)	200
(2, -4)	168
(-2, -4)	148
(4, -4)	158
(-4, -4)	164
(6, -4)	105
(-6, -4)	120
(0, -6)	168
(2, -6)	147
(-2, -6)	156
(4, -6)	122
(-4, -6)	120
(6, -6)	100
(-6, -6)	100

Table: B.28 Gas velocity at different points on XY plane situated at Z =30 mm at plenum pressure of 1200 kPa.

(X, Y) coordinates of the points, mm	**Gas Velocity, m/s**
(0,0)	226
(2,0)	208
(-2,0)	220
(4,0)	168
(-4,0)	148
(6,0)	106
(-6,0)	128
(0,2)	222
(2,2)	200
(-2, 2)	210
(4,2)	160
(-4,2)	180
(6,2)	120
(-6,2)	124

(0,4)	208
(2,4)	184
(-2,4)	200
(4,4)	144
(-4,4)	164
(6,4)	104
(-6,4)	108
(0,6)	188
(2,6)	166
(-2,6)	180
(4,6)	136
(-4,6)	144
(6, 6)	84
(-6,6)	100
(0, -2)	220
(2, -2)	200
(-2, -2)	206
(4, -2)	160
(-4, -2)	176
(6, -2)	116
(-6, -2)	128
(0, -4)	200
(2, -4)	180
(-2, -4)	200
(4, -4)	142
(-4, -4)	164
(6, -4)	108
(-6, -4)	220
(0, -6)	168
(2, -6)	144
(-2, -6)	168
(4, -6)	122
(-4, -6)	144
(6, -6)	88
(-6, -6)	100

Table: B.29 Gas velocity at different points on XY plane situated at Z =40 mm at plenum pressure of 1200 kPa.

(X, Y) coordinates of the points, mm	**Gas Velocity, m/s**
(0,0)	202
(2,0)	184
(-2,0)	196

(4,0)	148
(-4,0)	168
(6,0)	104
(-6,0)	128
(0,2)	200
(2,2)	184
(-2, 2)	194
(4,2)	148
(-4,2)	160
(6,2)	102
(-6,2)	120
(0,4)	184
(2,4)	180
(-2,4)	180
(4,4)	142
(-4,4)	148
(6,4)	89
(-6,4)	116
(0,6)	172
(2,6)	162
(-2,6)	162
(4,6)	138
(-4,6)	120
(6, 6)	88
(-6,6)	80
(0, -2)	196
(2, -2)	168
(-2, -2)	188
(4, -2)	142
(-4, -2)	164
(6, -2)	104
(-6, -2)	122
(0, -4)	184
(2, -4)	162
(-2, -4)	168
(4, -4)	138
(-4, -4)	142
(6, -4)	100
(-6, -4)	108
(0, -6)	158
(2, -6)	120
(-2, -6)	144
(4, -6)	108
(-4, -6)	120
(6, -6)	88

(0, -4)	160
(2, -4)	148
(-2, -4)	160
(4, -4)	120
(-4, -4)	142
(6, -4)	96
(-6, -4)	116
(0, -6)	144
(2, -6)	120
(-2, -6)	140
(4, -6)	100
(-4, -6)	120
(6, -6)	98
(-6, -6)	122

Table: B.31 Gas velocity at different points on XY plane situated at Z =60 mm at plenum pressure of 1200 kPa.

(X, Y) coordinates of the points, mm	**Gas Velocity, m/s**
(0,0)	162
(2,0)	144
(-2,0)	159
(4,0)	128
(-4,0)	140
(6,0)	104
(-6,0)	120
(0,2)	160
(2,2)	152
(-2, 2)	158
(4,2)	132
(-4,2)	140
(6,2)	104
(-6,2)	118
(0,4)	144
(2,4)	140
(-2,4)	144
(4,4)	102
(-4,4)	132
(6,4)	100
(-6,4)	102
(0,6)	140
(2,6)	132
(-2,6)	138

(4,6)	98
(-4,6)	120
(6, 6)	88
(-6,6)	100
(0, -2)	158
(2, -2)	140
(-2, -2)	152
(4, -2)	122
(-4, -2)	141
(6, -2)	96
(-6, -2)	108
(0, -4)	140
(2, -4)	132
(-2, -4)	140
(4, -4)	112
(-4, -4)	132
(6, -4)	88
(-6, -4)	106
(0, -6)	126
(2, -6)	120
(-2, -6)	124
(4, -6)	100
(-4, -6)	120
(6, -6)	80
(-6, -6)	100

Table: B.32 Gas velocity at different points on XY plane situated at Z =70 mm at plenum pressure of 1200 kPa.

(X, Y) coordinates of the points, mm	**Gas Velocity, m/s**
(0,0)	125
(2,0)	120
(-2,0)	120
(4,0)	108
(-4,0)	105
(6,0)	101
(-6,0)	103
(0,2)	124
(2,2)	120
(-2, 2)	120
(4,2)	108
(-4,2)	109
(6,2)	100
(-6,2)	100

(4,6)	98
(-4,6)	120
(6, 6)	88
(-6,6)	100
(0, -2)	158
(2, -2)	140
(-2, -2)	152
(4, -2)	122
(-4, -2)	141
(6, -2)	96
(-6, -2)	108
(0, -4)	140
(2, -4)	132
(-2, -4)	140
(4, -4)	112
(-4, -4)	132
(6, -4)	88
(-6, -4)	106
(0, -6)	126
(2, -6)	120
(-2, -6)	124
(4, -6)	100
(-4, -6)	120
(6, -6)	80
(-6, -6)	100

Table: B.32 Gas velocity at different points on XY plane situated at Z =70 mm at plenum pressure of 1200 kPa.

(X, Y) coordinates of the points, mm	**Gas Velocity, m/s**
(0,0)	125
(2,0)	120
(-2,0)	120
(4,0)	108
(-4,0)	105
(6,0)	101
(-6,0)	103
(0,2)	124
(2,2)	120
(-2, 2)	120
(4,2)	108
(-4,2)	109
(6,2)	100
(-6,2)	100

(4,6)	98
(-4,6)	120
(6, 6)	88
(-6,6)	100
(0, -2)	158
(2, -2)	140
(-2, -2)	152
(4, -2)	122
(-4, -2)	141
(6, -2)	96
(-6, -2)	108
(0, -4)	140
(2, -4)	132
(-2, -4)	140
(4, -4)	112
(-4, -4)	132
(6, -4)	88
(-6, -4)	106
(0, -6)	126
(2, -6)	120
(-2, -6)	124
(4, -6)	100
(-4, -6)	120
(6, -6)	80
(-6, -6)	100

Table: B.32 Gas velocity at different points on XY plane situated at Z =70 mm at plenum pressure of 1200 kPa.

(X, Y) coordinates of the points, mm	**Gas Velocity, m/s**
(0,0)	125
(2,0)	120
(-2,0)	120
(4,0)	108
(-4,0)	105
(6,0)	101
(-6,0)	103
(0,2)	124
(2,2)	120
(-2, 2)	120
(4,2)	108
(-4,2)	
(6,2)	
(-6,2)	

(0,4)	120
(2,4)	120
(-2,4)	108
(4,4)	106
(-4,4)	100
(6,4)	98
(-6,4)	88
(0,6)	108
(2,6)	112
(-2,6)	108
(4,6)	102
(-4,6)	100
(6, 6)	84
(-6,6)	82
(0, -2)	124
(2, -2)	120
(-2, -2)	120
(4, -2)	102
(-4, -2)	108
(6, -2)	98
(-6, -2)	100
(0, -4)	120
(2, -4)	104
(-2, -4)	108
(4, -4)	100
(-4, -4)	100
(6, -4)	88
(-6, -4)	84
(0, -6)	112
(2, -6)	102
(-2, -6)	104
(4, -6)	96
(-4, -6)	100
(6, -6)	81
(-6, -6)	84

Table: B.33 Gas velocity at different points on XY plane situated at Z =80 mm at plenum pressure of 1200 kPa.

(X, Y) coordinates of the points, mm	**Gas Velocity, m/s**
(0,0)	115
(2,0)	110
(-2,0)	108
(4,0)	102

(-4,0)	104
(6,0)	96
(-6,0)	100
(0,2	112
(2,2)	108
(-2, 2)	108
(4,2)	100
(-4,2)	100
(6,2)	88
(-6,2)	92
(0,4)	108
(2,4)	104
(-2,4)	100
(4,4)	100
(-4,4)	96
(6,4)	92
(-6,4)	88
(0,6)	100
(2,6)	100
(-2,6)	96
(4,6)	92
(-4,6)	88
(6, 6)	84
(-6,6)	80
(0, -2)	112
(2, -2)	108
(-2, -2)	108
(4, -2)	100
(-4, -2)	102
(6, -2)	92
(-6, -2)	100
(0, -4)	108
(2, -4)	100
(-2, -4)	102
(4, -4)	92
(-4, -4)	96
(6, -4)	82
(-6, -4)	86
(0, -6)	100
(2, -6)	100
(-2, -6)	100
(4, -6)	88
(-4, -6)	86
(6, -6)	80
(-6, -6)	80

Table: B.34 Gas velocity at different points on XY plane situated at Z =90 mm at plenum pressure of 1200 kPa.

(X, Y) coordinates of the points, mm	Gas Velocity, m/s
(0,0)	104
(2,0)	100
(-2,0)	100
(4,0)	98
(-4,0)	96
(6,0)	88
(-6,0)	89
(0,2	104
(2,2)	100
(-2, 2)	102
(4,2)	100
(-4,2)	100
(6,2)	88
(-6,2)	88
(0,4)	100
(2,4)	96
(-2,4)	96
(4,4)	88
(-4,4)	86
(6,4)	82
(-6,4)	82
(0,6)	92
(2,6)	88
(-2,6)	98
(4,6)	84
(-4,6)	88
(6, 6)	80
(-6,6)	80
(0, -2)	102
(2, -2)	100
(-2, -2)	100
(4, -2)	92
(-4, -2)	92
(6, -2)	86
(-6, -2)	86
(0, -4)	100
(2, -4)	92
(-2, -4)	92

(4, -4)	84
(-4, -4)	88
(6, -4)	80
(-6, -4)	80
(0, -6)	96
(2, -6)	88
(-2, -6)	92
(4, -6)	84
(-4, -6)	88
(6, -6)	80
(-6, -6)	80

Table: B.35 Gas velocity at different points on XY plane situated at Z =100 mm at plenum pressure of 1200 kPa.

(X, Y) coordinates of the points, mm	**Gas Velocity, m/s**
(0,0)	100
(2,0)	100
(-2,0)	100
(4,0)	96
(-4,0)	96
(6,0)	84
(-6,0)	86
(0,2	100
(2,2)	100
(-2, 2)	100
(4,2)	96
(-4,2)	95
(6,2)	84
(-6,2)	84
(0,4)	92
(2,4)	92
(-2,4)	92
(4,4)	88
(-4,4)	88
(6,4)	80
(-6,4)	80
(0,6)	89
(2,6)	89
(-2,6)	89
(4,6)	80

(0,4)	240
(2,4)	224
(-2,4)	232
(4,4)	180
(-4,4)	176
(6,4)	140
(-6,4)	102
(0,6)	176
(2,6)	168
(-2,6)	160
(4,6)	144
(-4,6)	140
(6, 6)	100
(-6,6)	98
(0, -2)	240
(2, -2)	232
(-2, -2)	220
(4, -2)	180
(-4, -2)	200
(6, -2)	120
(-6, -2)	140
(0, -4)	220
(2, -4)	180
(-2, -4)	204
(4, -4)	160
(-4, -4)	162
(6, -4)	102
(-6, -4)	120
(0, -6)	176
(2, -6)	164
(-2, -6)	164
(4, -6)	136
(-4, -6)	122
(6, -6)	96
(-6, -6)	92